Estimating future coastline changes along Holland coast, under different sea level rise scenarios, using a probabilistic approach

Argyro Bitaki

Estimating future coastline changes along Holland coast, under different sea level rise scenarios, using a probabilistic approach

By

A. Bitaki

in partial fulfilment of the requirements for the degree of

Master of Science

in Offshore and Dredging Engineering

at the Delft University of Technology,

to be defended publicly on Friday November 15, 2019 at 14:00.

Thesis committee:	Prof. dr. A.V. Metrikine,	TU Delft
	Dr. ir. S. de Vries,	TU Delft
	Ir. W.P. de Boer,	Deltares/TU Delft
	Ir. F. Scheel,	Deltares
	Prof. dr. R. Ranasinghe,	IHE Delft Institute for Water Education
	Dr. ir. A. Dastgheib,	IHE Delft Institute for Water Education

An electronic version of this thesis is available at http://repository.tudelft.nl/.

Abstract

Due to climate change and sea level rise the coastal zones are getting exposed to increasing risks like coastal recession, putting in risk human lives and coastal infrastructure being worth billions of dollars. Low lying countries like the Netherlands are considered more vulnerable to the effects of sea level rise. Large parts of the Dutch coast have been eroding for centuries and nourishments schemes of approximately 12 million m^3 have been implemented annually in order to maintain the coastline as it was in 1990. However, the future dune erosion will further increase due to the impacts of climate change and hence the adaptation strategies should be in line with the accelerated sea level rise and the possible effects that may bring.

The most commonly used method to assess sea level rise impacts on shorelines is the Bruun rule. However, Bruun rule's deterministic nature cannot align with the risk-based framework that coastal zone management requires nowadays. This necessity initiated the development of a process-based model, the Probabilistic Coastline Recession (PCR) model, estimating the future coastal recessions in a probabilistic approach.

In this research, the PCR framework was applied at eleven locations along the Holland coast, in the Netherlands, under three different SLR scenarios, the RCP4.5, RCP8.5 and Deltascenario. The availability of coastal profile data (from 1965 until now) and coastline position data (from 1843 till 1980) made the Holland coast an ideal location to explore and extend the applicability of the PCR framework. The most relevant assumptions for this coast were identified and explored. The recovery rate of the dune was a weak point of the PCR model and Holland coast was an interesting area to be tested. Three approaches of calibrating the natural recovery rate of the dunes were followed. In addition, the alongshore sediment transport which was assumed negligible to the previous case studies, in this work it was integrated into the PCR model and pointed out that its contribution is important to the PCR.

For the eleven selected coastal profiles, 20,000 simulations of 81 years (2020-2100) have been conducted and for every simulation the most landward position of the coastline in every calendar year has been recorded. Hence, an empirical distribution of coastline recession for every future year has been constructed. The ranges of the expected retreats in 2100 (relative to 2020) for the different SLR scenarios are: 0.5 m-155 m (for RCP4.5), 6 m-194 m (for RCP8.5) and 18 m-272 m (for Deltascenario), corresponding to the 50 % exceedance probability values of the cumulative distribution function of the coastline retreat. The average values of the coastal retreat for 2100 are 61 m, 73 m and 97 m for RCP4.5, RCP 8.5, and Deltascenario respectively. The relevant average erosion volume by 2100 are 1664 m^3/m, 2005 m^3/m and 2665 m^3/m. According to the findings, in 2100 the relative increase in volume loss along the entire the Holland coast is expected to be 95 %, 121 % and 173 % respectively for RCP4.5, 138 % for RCP8.5 and 195 % for Deltascenario. Finally, the results were compared to those raised from the Bruun rule method. According to the findings, the majority of the profiles showing an erosive trend in the past (before the 'hold-the-line' policy) raised slightly more conservative results when implementing the PCR model rather than when applying the Bruun rule method- especially under the Deltascenario. On the other hand, the Bruun rule method is more conservative than PCR model for most of the accretive profiles.

The PCR model can now be explored to locations where the longshore sediment transport is not negligible. The approach followed in this study allows investigating the ability of the model for future coastal retreat estimates when a construction of a hard defence structure or a port may change abruptly the longshore sediment transport. Last, this study advances the PCR framework and can be a valuable assistance in the course of further improving the model.

Preface

The present thesis marks the completion of my Master of Science in Offshore and Dredging Engineering at Delft University of Technology. The study was carried out in Deltares from November 2018 to November 2019.

To start, I would like to thank my thesis committee members for their contributions to this study. Your experience and insightful comments were always valuable for the progress of my work. Sierd, I would like to thank you for your critical eye, your advice and your positive attitude during the meetings. Rosh, it is because of you and your beautiful research the existence of this thesis. Wiebe, thank you for your constructive feedback and your patience -especially the times you had to repeat things that I couldn't understand. Ali, thank you for your help and for always being available for a meeting to discuss about any questions I had. Lastly, Freek, thank you for being such a good supervisor, for your support and the time you invested on me.

I would like to thank my friends for always being there, supporting me and being my source of stress relief. Special thanks to Vassia for her help and the conversations during our "ice-cream" meetings.

Lastly, I would like to thank my family. The completion of my master would not have been possible without their unconditional love and support. This thesis is dedicated to them.

A. Bitaki

Delft, November 2019

Table of Contents

List of Figures

List of Tables

List of Symbols

Latin Symbols

Symbol	Units	Description
$b_1 \sim b_4$	-	exponents
B	m	The berm or dune elevation estimate for the eroded area
c_1, c_2	-	Coefficients defining the transport rate as a function of the actual coastline orientation
dur	hours	Storm duration
d_{50}	m	Median sediment diameter
H_s	m	Significant wave height
$H_{s,0}$	m	Offshore significant wave height
h_d	m	Height of dune crest above mean sea level
h_{max}	m	Maximum (positive) water level
h_*	m	Depth of closure
L	m	The horizontal distance from the shoreline to depth h_*
LSTR	m³/m /yr *or m/yr*	Longshore sediment transport rate
S	Mm³/yr	Longshore sediment transport rate
R	m	Average horizontal dune recession
RR	m³/m /yr	Recovery rate in cross-shore direction
T_p	sec	Peak wave period
t	hours	time
tanβ	-	Coastal slope gradient defined as the slope between the -3 m depth contour (below MSL) and the dune toe (+3 m)
$V_{d,t}$	m³/m	Dune erosion area above storm surge level after t hours

Greek Symbols

Symbol	Units	Description
$\alpha_1 \sim \alpha_7$	-	exponents
ΔCL	m	Coastline change (retreat/accretion)
ΔCL_rate	m/yr	Rate of coastline accretion or recession
δx_{DF}	m/yr	Rate of accretion/recession of dunefoot indicator
δx_{MHW}	m/yr	Rate of accretion/recession of MHW indicator
δx_{MLW}	m/yr	Rate of accretion/recession of MLW indicator
φ	degrees (°)	Coastline orientation (nautical convention)
θ	degrees (°)	Wave direction (from North)
θ_0	degrees (°)	Offshore wave incidence angle to coast normal
θ_c	degrees (°)	Coast angle
θ_e	degrees (°)	The equilibrium angle
θ_R	degrees (°)	The angle between the actual coast orientation and the equilibrium angle

List of Abbreviations

Abbreviation	Description
BCL	Basal Coast Line
CDF	Cumulative Distribution Function
DF	Dunefoot
DoC	Depth of Closure
JarKus	Jaarlijkse Kustlodingen (Yearly coastal measurements)
IPCC	Intergovernmental Panel on Climate Change
LST	Longshore Sediment Transport
MHW	Mean High Water
MLW	Mean Low Water
MSL	Mean Sea Level
PCR	Probabilistic Coastline Recession (model)
RCP	Representative Concentration Pathway
RR	Recovery Rate
SLR	Sea Level Rise
SSTS	Synthetic Storm Time Series
UB	UNIBEST

1 Introduction

This chapter presents the topic of this study, the problem statement, the research objective and questions, and the outline of the report.

1.1 Sea level rise and coastal erosion

Climate change driven sea level rise (SLR) is an important issue for many countries around the globe. A subsequent impact of SLR on coasts is coastal erosion. For decades, low-lying countries have invested a lot of time, in terms of research, as well as a great amount of money for coastal infrastructure and developments in order to protect themselves from coastal hazards. However, nowadays, coastal managers must face new challenges raised by the accelerated SLR; a potential increase in storm frequency and intensity threatens the coastal zones. Therefore, it is urgent now more than ever to be able to make reliable and accurate estimates of the future coastal recession in order to adjust accordingly the coastal planning. The process of predicting accurately the coastline retreat is far from trivial.

One simple method, which has been widely used, for the estimation of coastal recession, in response to SLR, is the so-called **Bruun rule** (Bruun, 1962). The basic assumption in this concept is that the shoreface has a profile, which is in equilibrium with the hydrodynamic forcing (Bosboom and Stive, 2012). Bruun was the first who introduced the relationship between the response of this equilibrium profile to the climate change driven SLR (Bruun, 1962, 1988). Even though this method has been used for more than a half century, nowadays it is receiving a lot of criticism due to the questioning legitimacy of the assumptions behind the method (Passeri et al., 2015). Moreover, its deterministic nature cannot align with the emergence of risk management style coastal planning framework, the main requirement of which is not just a single value, but a probabilistic estimation of coastal recession (Ranasinghe et al.,2012).

In the scope of a new approach based on a **probabilistic framework**, a process-based model is developed by Ranasinghe et al. (2012) to provide probabilistic estimates of SLR driven coastal recession. The **Probabilistic Coastline Recession** (PCR) model takes as input statistical parameters of the wave climate and storm gaps (generated by fitting distributions and dependency structures). Using Monte Carlo simulations, it generates multiple realistic long time-series of beach erosion and recovery. Next, statistical analysis is performed, and exceedance probability curves for future coastal recession can be retrieved (Dastgheib et al., 2018; Da Cruz, 2018). Having these estimates for the future years, coastal managers can make a better and more reliable planning on their land-use strategies in order to protect the coastal zone.

1.2 Problem description of the case study

Although the PCR model has been applied successfully to cases such as in Japan, Australia and Sri Lanka, its suitability for coastline dominated by longshore sediment transport and beach nourishment is not well-understood.

In this study, the PCR framework will be applied to the Holland coast, in the Netherlands and the most relevant assumptions for this region will be identified and explored. The recovery rate of the dune is a weak point of the PCR model and therefore the Dutch coast is an interesting and challenging area for the model to be tested, because nourishment schemes are part of the coastal management planning since 1990. In addition, the alongshore sediment transport is dominant, with the latter never considered for the regions where PCR has so far been applied.

The Holland coast is one of the three parts of the Dutch coast (Figure 1.1). It is one of the most data-rich environments globally (Giardino et al., 2019), with JarKus dataset providing yearly beach profile data since 1965, with an alongshore spacing of 250 m (Wang et al., 2011), and Rijkswaterstaat and KNMI providing abundant wave climate data. Therefore, the Holland coast consists an ideal location to explore and extend the applicability of the PCR framework.

Figure 1.1: The three regions of Dutch coast, the Wadden Islands, the coastline of the provinces North-Holland and South-Holland, and Zeeland[1]

1.3   Research objective and research questions

Climate change driven SLR can deteriorate the storm-induced as well as structural erosion of dunes in the Netherlands, putting people's lives and the economy of the country at risk. Since 1990, the coastal management in the Netherlands has followed a coastline maintenance policy by using yearly nourishments. The objective of this thesis is to explore and improve the applicability of the PCR model for the Holland coast to estimate the shoreline retreat due to SLR as well as the required nourishment volumes to maintain the hold-the-line policy.

The research questions that motivate this study are the following:

1. What are the relevant physical processes for the long-term coastline evolution of the Holland coast and to what extent does the current PCR model includes them? Which methodologies can be applied to improve the PCR model for the Holland coast?
2. What is the predicted coastline recession and required nourishment volumes for different SLR scenarios using the (updated) PCR model?
3. How do the results obtained from the (updated) PCR model compare to the estimates of the Bruun rule?

1.4   Report Outline

Chapter 1 – Introduction: the reader is introduced to the field of interest, the research gap, the objective and research questions.

Chapter 2 – Literature review: provides the literature study which consists of the relevant topics motivating this research. It is composed by two broad thematical sections. The first section includes topics about climate change induced SLR and coastal erosion in global coasts, the models

---

[1] https://en.wikipedia.org/wiki/List_of_islands_of_the_Netherlands#/media/File:Map_provinces_Netherlands-en.svg

used for estimating coastal retreat and the PCR model. The second thematical section is devoted to PCR model. Background information of how it works, where it has been already applied and under which assumptions. Last, there is case study description.

Chapter 3 –Methods: presents the methods followed to achieve the objective of this study and answer the research questions.

Chapter 4 – Results: presents the results raised from the PCR implementation and the Bruun rule method.

Chapter 5 – Discussion: provides a discussion over the decisions and assumptions which were used in the study.

Chapter 6 – Conclusion and recommendations: presents the main conclusions derived from this study and provides recommendations for further research.

Appendix A – Includes information about the erosion function.

Appendix B – Presents the analyses performed based on the methods described in Chapter 3.

Appendix C – Includes information of the profiles where the PCR is applied.

Appendix D – Includes results of the profiles where the PCR is applied.

Figure 1.2: Outline of the report

2 Literature Review

This chapter consists of the relevant topics motivating this research. It is composed by two broad thematical sections. The first section includes topics about climate change induced SLR and coastal erosion in global coasts and the models used for estimating coastal retreat. The second thematical section is devoted to PCR model. Background information of how it works, where it has been already applied and under which assumptions, are provided in this section. Furthermore, it is presented the description of the case study.

2.1 Coastal (morpho)dynamics and evolution of coastal systems

Due to the economic benefits and amenity that coastal zones provide, these areas have always attracted people thus, they are densely populated (Luijendijk et al.,2018). A great amount of money and many infrastructures have been invested on these zones around the globe either because of their strategic location (i.e. ports) but also for protecting the population living and working in the coastal area. One of the most classical coastal hazards threatening the coastal zones is coastal erosion, existing until now, despite the development of coastal engineering and the science of coastal processes.

Coastal erosion is a natural phenomenon which has always been present, influencing and shaping the coastal morphology and it results from higher sediment demand and insufficient available sediment supply (Salman et al., 2004). According to van Rijn (2011) the coastal erosion is described as the permanent loss of sand from the beach-dune system, with the amount of erosion and erosion rate being strongly influenced by the type of coast, in terms of exposure, wave environment, surge level ranges, sediment deposit composition and beach slope.

The coastal erosion can be distinguished in two types based on its **temporal** description; the **episodic (storm-induced) erosion** (time scale: year - decade) and the **structural erosion** (**long-term** recession) (time scale: decades- century) of the coasts (Ranasinghe, 2016). A storm-induced dune erosion is an episodic phenomenon, happening in a short-time scale, during which the water level at sea is higher than the usual (storm surge) and is accompanied with also much higher waves than usual. After the storm, and if the pre-storm beach profile was in morphological equilibrium before the event, a **recovery process** towards the original situation will take place. On the other hand, structural erosion is a permanent phenomenon induced by sea level rise and gradients in alongshore sediment transport. As illustrated by Bosboom et al., the public is unaware of the structural erosion, and mistakenly believe that the extreme weather events, like storms, are the reason causing the (permanent) beach and dune erosion problem, whereas in fact it is the gradient in longshore sediment transport rates. The storm event just initiates the procedure by providing sediment from the upper part of the beach to the active littoral zone (Bosboom et al., 2015).

Coastal erosion can be caused either by **natural** factors or **human-induced** (Figure 2.1). According to Salman et al. (2004) as natural factors driving the coastal erosion are considered the action of waves, wind, tides and near-shore currents, the occurrence of storm events, SLR, vertical land movements (including isostatic rebound, tectonic movement, or sediment settlement) and mass wasting processes on slopes. As anthropogenic causes can be regarded the human interventions like the construction of engineering structures for coastal defences (e.g. seawalls, groynes, nourishments), ports and river dams, land reclamation projects, dredging processes, gas mining or water extraction works (Salman et al., 2004; Giardino et al.,2018).
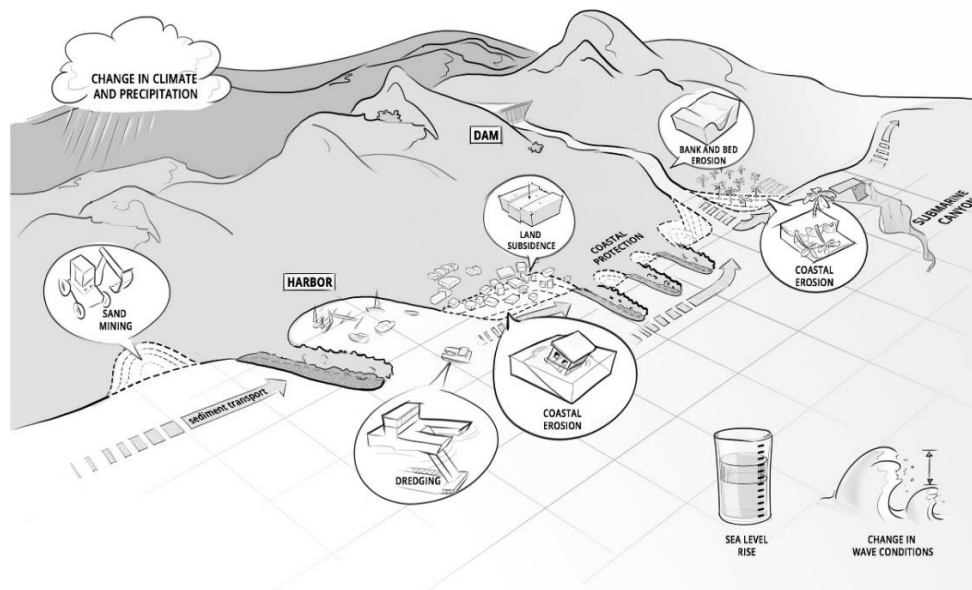
Figure 2.1: Factors affecting the morphodynamic equilibrium in coastal areas (Giardino et al.,2018)

2.2   Sandy coasts, climate change and SLR

There are several types of coastal zones depending on the influence of the tectonics and the exposure to wave climate (Inman, 1994). In literature study, focus is made on **sandy coasts**, which constitutes a 40% of coastline globally. Sandy coasts are complex and highly dynamic systems, therefore, very susceptible to changes in a range of time and space (Miller & Dean, 2004; Bird, 1996, as cited in Luijendijk et al., 2018; Ranasinghe, 2016). Sand dunes constitute a first line of defence against flooding, storms and coastal erosion for many coastal regions. Sand bars, beaches and dunes, have always been appreciated, not only for their significance as coastal defences, but also for their contribution to a number of biological processes, ecological services, nature conservation and recreation uses (Doody, 2012; Hanley et al.,2014).

The major threat to coastal sandy environments is posed by **climate change** effects. Since 1990, it has been estimated that a 25% of dunes have been lost only in Europe and that approximately 85% is under threat (Heslenfeld et al., 2004; Hanley et al.,2014). Based on satellite derived shoreline data from the 1984 till 2016, Luijendijk et al., (2018) showed that 24% of the world's sandy beaches are persistently eroding at a rate exceeding 0.5 m/yr, 28% are accreting and almost the half are stable, and especially for the marine protective areas, it is said that most of them appear an erosive trend. However, the impacts of climate change will aggravate the situation on the erosive sandy coasts, threatening the coastal community and its socio-economic activities globally (Ranasinghe, 2016).

The climate change has influenced wave actions, mean sea level, storm surge and riverflows, which are the main factors shaping the coastlines around the world (Ranasinghe 2016). Any climate change driven variation of these factors will have a serious effect on the evolution of the coastal systems. One major impact of climate change is the **sea level rise** (SLR) which results in an increase of sediment demand, amplifying the phenomenon of coastal erosion (Toimil et al.,2017). The rising sea levels coupled with powerful storm events, have allowed wave breaking closer to near-shore and attacking the dune at a higher level and more landward and thus the

erosion volumes have been greater (de Winter et al., 2017). Additionally, the frequency of storm events has also increased, leaving not enough time for the coast to recover. So, the episodic erosion from storms has been exacerbated due to SLR, and in long term there is going to be an aggravation in structural erosion, since the coast does not recover fully after the storm events, and this puts the livelihoods and sustainability of many coastal communities in great danger (Ranasinghe et al., 2012).

SLR scenarios

One of the key factors contributing to the ongoing global warming is the amount of the upcoming greenhouse gas emissions (Figure 2.2). At the Intergovernmental Panel on Climate Change (IPCC) Fifth Assessment Report (AR5) a set of four scenarios was built, following certain criteria, called Representative Concentration Pathways (RCPs), and each having a certain level of radiative forcing set as target for 2100. Four scenarios are designed to assist in research on the expected impacts of and potential policy responses to climate change (Riahi et al. 2011) and each one is described shortly below:

- RCP 2.6: It is the best-case scenario which reflects aggressive greenhouse gas reduction. Its radiative forcing level first reaches a peak value of approximately 3.1 W/m² by mid-century, and then it reduces by 0.5 6 W/m² reaching 2.6 W/m² by 2100 (Van Vuuren et al.,2011).
- RCP 4.5: A medium stabilization scenario in which greenhouse gas emissions is stabilized shortly after 2100, without overshooting the long-run radiative forcing target level (Van Vuuren et al.,2011).
- RCP 6.0: A medium scenario in which total radiative forcing is stabilized shortly after 2100 using several strategies and technologies in order to reduce greenhouse gas emissions (Van Vuuren et al.,2011).
- RCP 8.5: A very high baseline emission scenario in which the pathway represents the trajectory with the highest greenhouse gas concentration levels and in this case and it is not considered any specific climate mitigation target (Riahi et al. 2011).
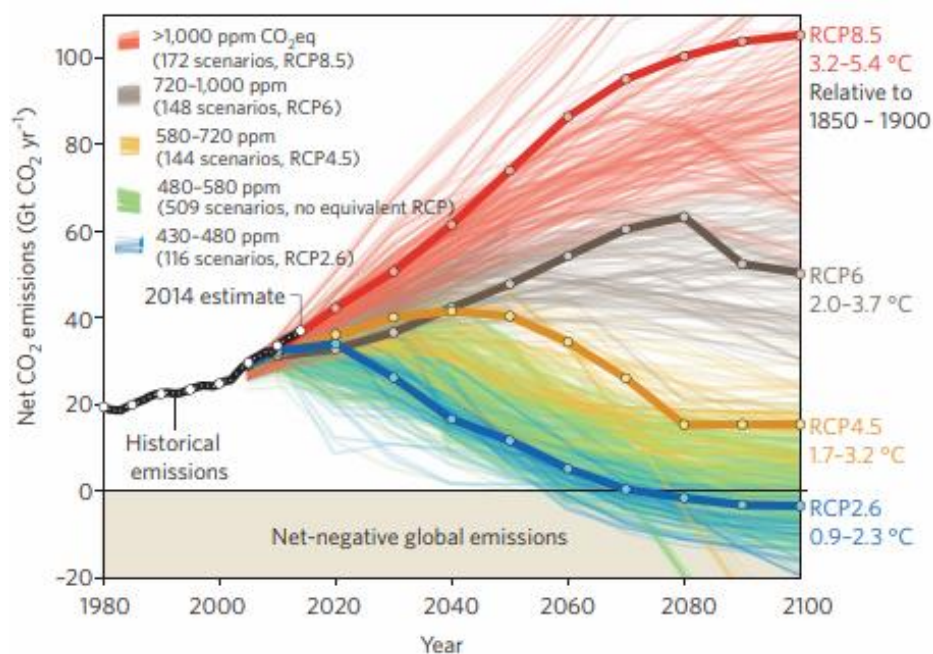
Figure 2.2 : Carbon dioxide emission pathways until 2100. Right of panel is the temperature increase referring to the warming in the late twenty-first century (2081–2100 average) relative to the 1850–1900 average (Fuss et al., 2014)

The next table (Table 2.1) shows the for projections of global mean sea level (GMSL) rise and its contributions in metres in 2046–2065, in 2081–2100 and in 2100 relative to 1986–2005 for the four RCP scenarios.

Table 2.1: Median values and likely ranges for projections of global mean sea level (GMSL) rise and its contributions in metres in 2046–2065, in 2081–2100 and in 2100 relative to 1986–2005 for the four RCP scenarios (Church et al., 2013)

	RCP2.6	RCP4.5	RCP6.0	RCP8.5
Global mean sea level rise in 2046–2065	0.24 [0.17 to 0.32]	0.26 [0.19 to 0.33]	0.25 [0.18 to 0.32]	0.30 [0.22 to 0.38]
Global mean sea level rise in 2081–2100	0.40 [0.26 to 0.55]	0.47 [0.32 to 0.63]	0.48 [0.33 to 0.63]	0.63 [0.45 to 0.82]
Global mean sea level rise in 2100	0.44 [0.28 to 0.61]	0.53 [0.36 to 0.71]	0.55 [0.38 to 0.73]	0.74 [0.52 to 0.98]

2.3   Coastal management

In many cases, sustainable planning was absent and, therefore, urbanization and infrastructures has been invested near erosive coastal zones deteriorating the consequences of structural erosion and resulting in coastal squeeze (Doody, 2012; Pontee,2013). This development pressure on land combined with the ongoing coastal erosion has led to requirements for coastal protection and sustainable coastal planning (Mangor et al., 2017). **Integrated coastal zone management** (ICZM) requires a fully understanding and assessment of the physical processes which take place and shape the morphology of coasts. Specifically, the phenomenon of accelerated coastal erosion has gained a lot of attention the last years. To be protected from coastal erosion, the coastal management has addressed to hard and soft protection measurements, accommodation and managed retreat strategies (Williams et al., 2017).

The concept of setback lines is used as a sustainable means of retreat adaption strategy, in order to protect the coastal zone from both coastal erosion and uncontrolled infrastructure activities. According to Camber "A coastal development setback may be defined as a prescribed distance to a coastal feature, such as the line of permanent vegetation, within which all or certain types of development are prohibited" (Cambers, 1997). A setback line reserves a zone between the shoreline and the infrastructure, which acts as buffer between a coastal hazard, (i.e. flooding and erosion) and certain development activities (Fenster, 2005). There are two types of setback lines; the elevation setbacks and the lateral setbacks, providing protection from flooding and erosion respectively (Linham and Nicholls, 2010). Setback lines contribute in maintaining the natural appearance of the coastline and this is one of the main tasks of Integrated Coastal management for the broader scope of sustainable coastal systems. Dastgheib et al. (2018) has shown that a probabilistic approach of coastal recession can be combined with the concept of economically optimal set-back lines in order to have a balance between the gains from investments in the coastal zone and the risk due to coastal erosion (Jongejan et al.,2016, Wainwright et al., 2014, as cited by Dastgheib et al., 2018). The concept of setback lines should be incorporated into ICZM implementation, since their definition should be based on an integrated approach with embedded aspects such as the understanding and control of physical processes, the ecosystem efficiency, coastal safety for economic and recreational activities and landscape protection from a natural and cultural heritage perspective (Sanò et al., 2009).

Sand nourishments have also become common practice in coastal management, since they have successfully limited erosion without raising the side effects other methods trigger (e.g. a construction of a 'hard engineering' structure). On the contrary, nourishment interventions do not interfere on the natural processes of the coastal system and are in line with the principles of

ICMZ for sustainability and resilience. It is a flexible approach to deal with climate adaptation and it is reversible letting the widest range of coastal management options to be passed to the next generation (Harman et al., 2013). Beach nourishments are also combined with hard engineering solutions such as seawalls that can be still used as a last line of defence. A wide and sandy beach in front of such structures may provide additional protection to such structures by reducing considerably the wave energy reaching them (Zhu et al., 2010).

To sum up, the type of protection of every coastal area is assigned on coastal managers who take decisions that impact the social, political, and economic well-being of their communities. As indicated by Tribbia & Moser (2008), policy makers and local managers and planners, prefer certain types of information to support them in confronting the growing risks from climate change. Having a better insight in the estimates of the shoreline retreat under the impact of SLR is one of them and is further described in the next section.

2.4 Methods to estimate shoreline retreat

2.4.1 From deterministic to probabilistic

Accelerated sea level rise will exacerbate the existing coastal erosion and will trigger erosion processes on many beaches that are now stable or growing, having detrimental socioeconomic effects on the coastal zone community (Bird, 1996). Predictions of shoreline retreat due to the projected, ongoing SLR should be incorporated into the coastal planning and management and they must be robust and reliable.

Coastal managers and policy-makers have used the Bruun rule method (Bruun, 1962) for predicting the SLR driven coastal recession and taking proactive mitigation measures for many years. The Bruun rule is a widespread deterministic approach. However, due to the limitations and drawbacks of Bruun rule, other methods have been developed. The need of coastal planning to integrate the range of uncertainties of wave climate and stochastic forcing into the coastal management framework has led to the development of approaches that yield estimates of coastal recession in probabilistic terms.

2.4.2 Erosion models

There have been developed several models and structural functions estimating coastal erosion and shoreline retreat over the last 50 years. These methods range from approaches based on basic geometric principles (e.g. the Bruun rule (Bruun, 1962)) to more complex process-based assessment (e.g. XBeach) (Shand et al. 2013).

Bruun Rule
The Bruun rule (Bruun 1962) is one of the most widely used methods to determine shoreline retreat due to sea level rise. It is a simple two-dimensional model which estimates the horizontal extent of coastal recession (R) of a cross-shore profile in response to a SLR, expressed as:

Equation 2.1

$$R = \frac{L \cdot SLR}{B + h}$$

where,
    h: the maximum depth until which there is exchange of material between nearshore and offshore,
    L: horizontal distance from the shoreline to depth h,
    B: berm or dune elevation estimate for the eroded area (see Figure 2.3, Ranasinghe et al. 2012).
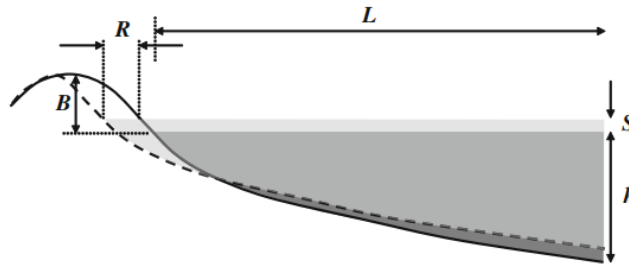
Figure 2.3:Shoreline retreat based on the Bruun rule (Ranasinghe et al. 2012)

Besides its simplicity and easy-to-use advantage, there are critical reviews against this method regarding this tool unreliable and inappropriate for using it to make accurate and robust estimates with many shortcomings and uncertainties (i.e. a major one is about the depth of closure employed in the estimation of the active profile's slope) (Cooper and Pilkey 2004; Ranasinghe and Stive 2009; Stive et al. 2009, as cited in Ranasinghe et al. 2012; Shand et al. 2013).

SBEACH

The SBEACH (**S**torm-induced **BEA**ch **Ch**ange) is an empirically based numerical simulation model, designed to estimate beach profile and dune erosion changes caused by storm events and wave action, and developed by the U.S. Army corps of Engineers. It is a cross-shore sediment transport model, considering that there is not any longshore sediment transport gradient. The model was initially developed using data from large wave tanks and afterwards verified based on field measurements. It is a cross-shore sediment transport model, considering that there is no longshore sediment transport gradient (Larson and Kraus, 1989). However, when there is a non-trivial longshore sediment component, its use is regarded controversial because the model underestimates storm erosion demand (Woodroffe et al., 2012).

XBeach

XBeach is a fully process-based coastal morphodynamic, numerical model and has been developed collaboratively by the US Army Corps of Engineers, Rijkswaterstaat and the EU, UNESCO-IHE, Deltares (formerly WL|Delft Hydraulics), Delft University of Technology and the University of Miami. This time-dependent 2DH model can solve coupled equations for cross-shore and longshore hydrodynamics and morphodynamics (Williams et al.,2012).

XBeach, as a tool for modelling coastal change, has been extensively validated against numerous flume experiments (1D) and some field case studies (2DH) (Roelvink et al., 2009). The model has then been successfully applied to simulate storm response of sandy beaches at Assateague Island, Maryland (Roelvink et al., 2009), Santa Rosa Island, Florida (McCall et al., 2010) and Ostend Beach, Belgium (Bolle et al., 2010). More recently, the use of XBeach has been extended to the modelling of gravel beach variability (de Alegria-Arzaburu et al., 2010; Jamal et al., 2010; Williams et al., 2012). Until now its use has been curtailed at the storm event timescale (hours to days). Pender & Karunarathna (2013) indicate that although XBeach has been validated and used extensively for erosive conditions, it has not been successfully validated or used to simulate post-storm beach accretion and recovery.

Kriebel and Dean

The Kriebel and Dean (1993) method, which is a simple analytical solution for approximating the time-dependent beach-profile response to severe storms. It is based on an equilibrium profile and if it is used as recommended by its authors then calibration is not needed.

Wave impact erosion model by Larson et al. (2004)

The wave impact erosion model by Larson et al. (2004), a process based analytical model relating the impact force applied to the dune from the swash zone motion to the volume of dune erosion during severe storms. The fundamental assumption of this method is that there is a linear relationship between the wave impact and the weight of sand eroded from the dune.

Structural function by Mendoza & Jiménez

The structural function presented by Mendoza & Jiménez, (2006), which predicts the eroded volume in the inner part of the beach by relating the storm-induced eroded volumes simulated using the semi-empirical model SBEACH (Larson and Kraus 1989) with a coastal morpho-dynamic parameter.

DUROS+

DUROS+ is a deterministic, cross-shore dune erosion model. Taking as input hydraulic loads (significant wave height, wave period and water level) and dune characteristics, it predicts the post-storm equilibrium profile. The actual erosion profile and the dune retreat are computed based on the shape of an equilibrium profile and a cross-shore balance between erosion and sedimentation (Ruessink et al. 2012).

DUNERULE

DUNERULE-model by van Rijn (2013). The results of the sensitivity study based on the process-based profile CROSMOR-model runs have been used to develop this empirical model. Experimental results based on flume model tests performed by Vellinga (1986) and Delft Hydraulics (2004, 2006a,b, 2007) have been used to verify it.

PCR model

The Probabilistic Coastline Recession (PCR) model provides coastal erosion estimates into a probabilistic framework, integrating the component of SLR. This model is further described in the next section.

2.5 Description of PCR framework

The probabilistic coastline recession (PCR) framework has been developed by Ranasinghe et al. (2012) and overcomes the Bruun rule's (Bruun 1962) limitations. In contrast to Bruun rule method, this framework includes the physical processes which take place during a SLR-driven coastal retreat and it departs from the deterministic approach by making robust estimates of coastal recession within a probabilistic scheme (Ranasinghe & Stive, 2009). This method deviates from the benchmark event (usually one of the maximum historical records) approach, which does not align with the probabilistic framework that the coastal zone managers are nowadays require (Callaghan et al. 2008).

The method is based on the fundamental argument that any net long-term recession of the coastal dune is owned to the combined effect of storm erosion and SLR. It is applicable to pocket beaches where the alongshore rate is negligible.

The basic procedure of the PCR model is summarized below in 6 steps (Ranasinghe et al., 2012):

1. Generate a long time series of storms (e.g. 1990–2100) using data derived from joint probability distributions of storm characteristics within a Monte Carlo simulation.
2. Estimate the sea level rise the moment each storm event occurs, by using IPCC projections.
3. Estimate the dune recession (or erosion volume) for each storm event, using an erosion model function while allowing for dune recovery between storms.

4. Estimate the final coastline position having as indicator the dune toe.
5. Estimate the dune recession by subtracting the initial dune toe position from the final dune toe position.
6. Repeat steps 1 to 5 until exceedance probabilities greater than 0.01% converge (i.e. bootstrapping).

The PCR framework is composed of four main modules:
- The synthetic storm time series
- Erosion function
- Recovery rate
- SLR

2.5.1 Synthetic storm time series

The generation of a long time series of storms is the first step of the PCR model. For this scope, the **Joint Probability Method** (JPM) model is employed which was developed by Callaghan et al. (2008). First, marginal, dependency and conditional distributions are fitted to long time series of forcing parameters through the JPM model and then are used as an input within a Monte Carlo simulation to derive a time series of storms and their characteristics (Ranasinghe et al., 2012).

The JPM is implemented in steps as follows (Ranasinghe et al., 2012):

1. Gather the available data and identify meteorologically independent storm events.
2. Fit extreme value (marginal) distributions to offshore wave height and storm duration.
3. Fit the dependency distributions between offshore wave height and storm duration and between offshore wave height and storm surge.
4. Fit the offshore wave height and wave period conditional distribution.
5. Determine the empirical distribution for offshore wave direction.
6. Fit a non-homogenous Poisson distribution to the storm spacing.
7. Finally, simulate the offshore wave climate using the fitted distributions to obtain storm time series.

2.5.2 Erosion function

The PCR model needs a structural function to estimate the storm-induced dune erosion. Once the storm time series are generated, then the associated eroded volume and the recession distance need to be calculated. Several models have been developed to calculate storm induced erosion (section 2.4.2). Increasing the level of sophistication of the structural function does not necessarily ensures better results; on the contrary, in some cases can be counter-productive. Applying XBeach or SBEACH within the JPM function requires a lot of computational time therefore a simpler model is considered a more efficient erosion function for PCR (Ranasinghe et al. 2013).

2.5.3 Recovery rate

The recovery process of a dune/beach takes place during the inter-storm periods. It is the process of 'dune healing' in terms of redistributing the sediment in the cross-shore direction after the impact of a storm event. It is an important parameter in the PCR framework and defining the natural recovery rate is not an easy task.

2.5.4 Study Cases of PCR implementation

So far, the PCR has been implemented in the following four countries: Australia, the Netherlands, Sri Lanka and Japan. The assumptions made in each case study concern: the storm event definition, the erosion function, the fitting distributions, the seasonality, SLR scenarios and the recovery rate. It should be noted that in all these cases the alongshore sediment transport was assumed negligible.

2.6 Case study analysis: Holland Coast, the Netherlands

The Netherlands is located Northwest of Europe and is bordered by the North Sea on its left. The history of Dutch people is highly interwoven with their struggle to dominate sea, to protect their land and when possible, by land reclamation to gain even more space. The coastal zone largely consists of vegetated dunes, multi-barred beaches and can be identified as a wave-dominated coast (Sistermans & Nieuwenhuis, 2004). In the Netherlands, the first line of coastal defence against flooding and storm erosion is constituted by natural dunes, situated along the sandy shorelines with the dune regions accounting for around 255 km of the Dutch coast (van Vessem & Stolk, 1991). Furthermore, a 15 % of the Dutch coast stands for the sea dikes and man-made sea barriers, and an amount of 10 % represents the beach flats along the tips of the northern Wadden islands (van Koningsveld et al., 2007). The length of the Dutch coastline along the southeast part of the North Sea is about 350 km and including all estuaries, is approximately 1000 km (De Ronde et al., 2003). Specifically, the Dutch coastal zone consists of three parts the Delta coast, the Holland coast and the Wadden coast (see Figure 2.4).
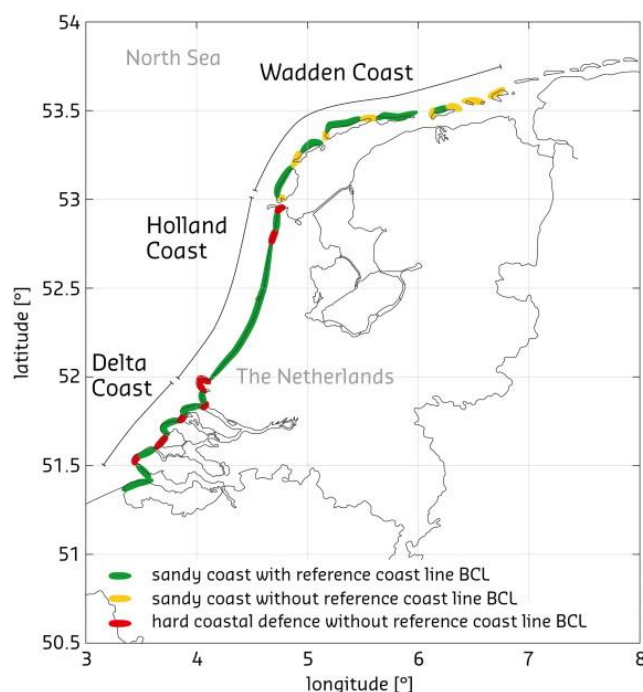
Figure 2.4: The three sub-regions of Dutch coast (Mulder et al.,2011)

The coastal zone is densely populated (half the population is located there) and it is the most valuable part of the Netherlands, since most of the national gross product of the country comes from companies and infrastructure located in coastal areas (Den Heijer et al., 2012). The main function of the coast it to protect the low-lying hinterland from inundation. However, also other functions such drinking water supply, ecological values, recreation and industrial functions are in danger due to accelerated coastal erosion (Mulder et al, 2011).

In this study, the PCR framework will be applied to the Holland coast which forms the middle part of the Dutch coast. It is bordered on the west by the North Sea, bounded on the north by a tidal inlet called Marsdiep next to Den Helder and on south by a long jetty close to Hook of Holland, and it consists of three subregions: Delfland, Rijnland and Noord-Holland (Giardino et al., 2019) (Figure 2.5). The Holland coast is a sandy, microtidal, wave-dominated coast (Giardino et al., 2012) and its width from the low water line to the dune foot ranges from 100 m to 200 m. The sediment at the Holland coast is well sorted, composed by fine to medium sand with an average size of the beach sediment d_{50} varying from 200 to 350 μm (Sistermans & Nieuwenhuis, 2004; Brière & van den Boogaard, 2009). The coastline is stretched in a length of approximately 120 km, it is slightly concave and shows an erosive trend (Sistermans & Nieuwenhuis, 2004.; Giardino et al., 2019) which is compensated by applying sand nourishments schemes after the Dynamic Preservation policy.
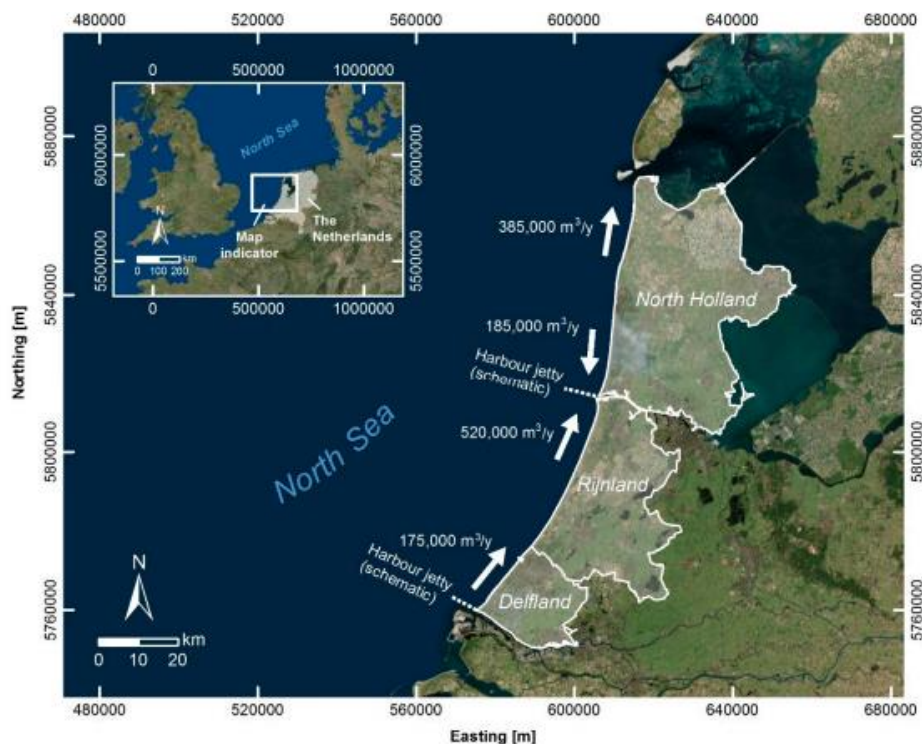
Figure 2.5: The three subregions of Holland coast: Delfland, Rijnland, and North Holland and net annual alongshore sediment transport rate (Giardino et al., 2019)

Gradients in longshore sediment transport are of utmost importance in erosion and accretion processes and along the Holland coast, sediment transport is dominated by wave related longshore transport processes (Bosboom & Stive, 2015). De Vries et al., (2014) report that derived gradients in alongshore sediment transport show significant differences depending on the alongshore location and the temporally varying forcing conditions. During stormy periods gradients are of higher order than during mild wave forcing.

This coast is one of the most data-rich environments globally (Giardino et al., 2019), with JarKus dataset providing yearly beach profile data since 1965, with an alongshore spacing of 250 m (Rosati et al., 2011; Wang et al., 2011), and Rijkswaterstaat and KNMI providing abundant wave climate data. Therefore, the Holland coast consists an ideal location to explore and extend the applicability of the PCR framework.

2.6.1 Hold-the-line policy

A history of catastrophic floods as well as the continuous fight to dominate over the sea hazards, has led to a sound coastal planning and management. Even though, the Dutch are known for their innovative projects of hard structured flood defences, there is a 75% of the Dutch coast consisting of dune areas (Van Koningsveld et al.,2007). Thus, there many policies developed during the years in the Netherlands related to sandy coasts. Moreover, the nature of coastal management in the Netherlands demands a dynamic framework, since the system that needs to be framed is also dynamic. In the view of sustainable coastal management, integration into values describing social, cultural, ecological and economically productive dimensions of the coast are of utmost importance (Stocker et al. 2012).

There are three scales constituting the basic frame of coastal policy in the Netherlands; the smallest scale (1 year) comes under the "**Coastal Safety**" context aiming for the preservation against flooding by maintaining a minimum threshold of dune strength whereas the middle (5-10 years) and large scale (50-200 years) consist the "**Dynamic Preservation**" policy (or *'hold-the-line'* policy) focusing on the sustainable coastal management in order to guarantee sustainable preservation of functions and values of the dune area, as stated by van Koningsveld et al. (2007). The last two scales aim at preservation of sustainable safety and the functions in coastal zone which are in risk, by using nourishments to maintain the coast line and the sand volume in coastal foundation (Mulder et al, 2011). Table 2.2 summarizes the Dutch coastal management strategies.

The idea of the "Dynamic Preservation" has been to maintain the entire coastline as it was in 1990 (referred to as Basal Coast Line- BCL) by counteracting the further erosion with sand nourishment, which is a measurement used in the Netherlands in the late 70's (De Ronde et al. 2003). This policy aims for the sustainable preservation of safety against flooding and of the functions at risk in the dune region by maintaining a minimum dune strength (Mulder et al, 2011). Later on, in 2000, the policy had to be updated and thus extended into a larger scale in order to achieve a sustainable preservation plan. Therefore, besides the main tactical objective to maintain the coastline, it was then induced another objective; maintaining the sand volume in the coastal foundation which is the area between the landward boundary and the depth contour of -20 m. A yearly nourishment volume of 6 M m^3 since 1990, was updated to 12 M m^3 in 2001 (Van Koningsveld and Mulder, 2004), and there is also indication of need for even more higher annual nourishment rate (Mulder et al, 2011).

To sum up, the strategic objective (Figure 2.6) which have been interpreted into tactical management objectives at the three scales (small, middle and large) are:

1. Residual dune strength assurance
2. Maintenance of 1990's coastline position
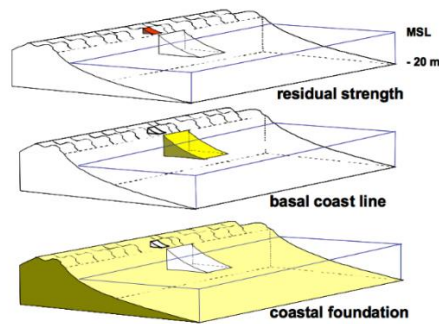3. Preservation and development of coastal foundation

Figure 2.6: Coastal management in the Netherlands in three scales: dune residual strength (days- meters); BCL (years-kilometres); Coastal Foundation (decades to centuries-10s to 100s of kilometres) (Mulder et al., 2011)

Table 2.2: The 'basic' frame of reference for Dutch coastal management strategies (Van Koningsveld et al.,2007)

Management context:	Coastal safety Small scale (< ~ 1 years)	Dynamic Preservation	
		Medium scale (~ 10 years)	Large scale (~ 50-100 years)
Strategic objective:	Guarantee safety levels provided by the dunes	Guarantee a sustainable safety level and sustainable preservation of functions and values of the dune area	Guarantee safety against flooding and preserve spatial quality of the coastal zone
Operational objective:	Dunes should be kept at sufficient strength to withstand hydraulic boundary conditions with a predetermined probability of occurrence.	To maintain the coastline not landward of its position of 01/01/1990	Preserve and improve the coastal foundation
Quantitative State Concept (CSI):	The dune erosion point (DEP): developed to unambiguously quantify the effects of dune erosion under design conditions per profile	The momentane coastline (MCL): developed to unambiguously quantify the position of the coastline per profile	The coastal foundation: the area between the inner dune edge and the (modified) NAP -20 m depth contour.
Benchmarking:	**Current state:** Extrapolation of a linear regression of all erosion points results in the testing dune erosion point **Reference State:** The reference state is a predefined critical position of the erosion point at which the dunes are assumed to have a sufficient rest strength.	**Current state:** Extrapolation of a linear regression of 10 previous MCL positions estimates the testing coastline position (TCL) **Reference State:** The TCL for 1990 is the Basal Coastline (BCL) and the reference state.	**Current state:** No procedure available yet **Reference State:** The TCL No procedure available yet
Intervention	**Procedure:** If the dune test returns 'unsafe', strengthen dune according to the measured shortfall (design life 5 years)	**Procedure:** If TCL exceeds the BCL position replenish according to the measured shortfall in volume (design life 5 years)	**Procedure:** Preferred intervention method is sand nourishment. No procedure available yet.
Evaluation	**Procedure:** Review strategy effectiveness by repeat benchmarking process	**Procedure:** Review strategy effectiveness by repeat benchmarking process	**Procedure:** No procedure available yet

Periodic sand nourishment is distinguished by the other coastal protection measures against storm-induced erosion or structural erosion and relative sea level rise, because it is an environmentally acceptable method of coastal management (Hanson et al., 2002; Pit et al., 2017). On the contrary, using hard structures on dune areas may decrease its recreational value (Marchand, 2010). Building hard structures may help in the short-term but their long-term effects may deteriorate the situation. Therefore, the Netherlands choosing for a solution 'working with Nature' like the sand nourishments, is one of the countries in Europe with the largest volumes of

sand nourishment (Hamm et al., 2002). Figure 2.7 shows the volume of sand nourishment along the Dutch coast for the period 2001-2011.
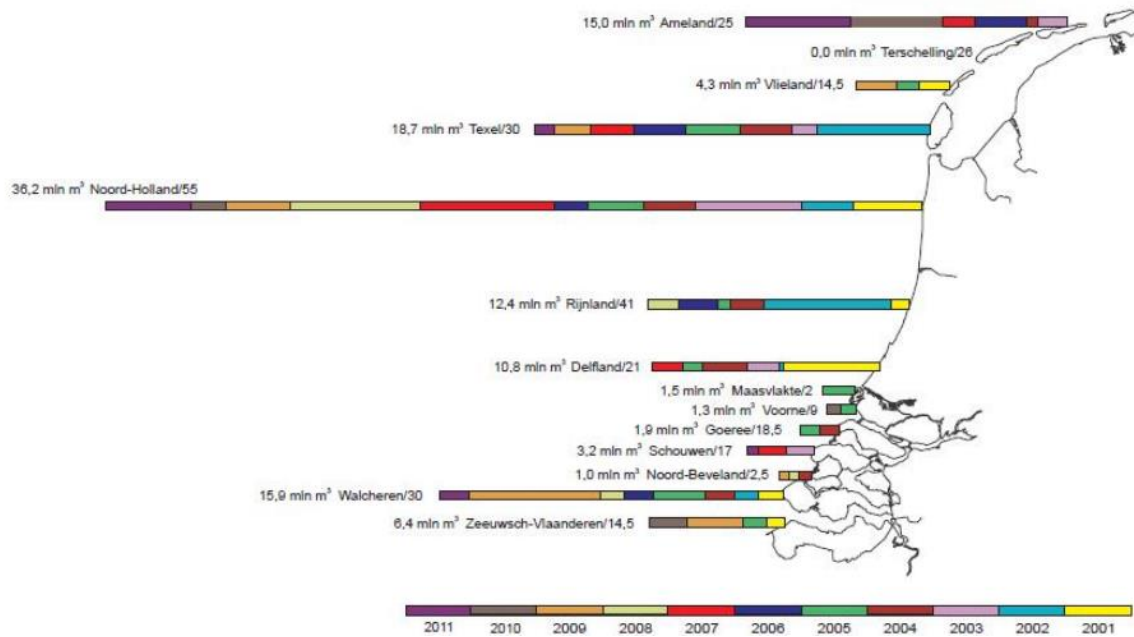

Figure 2.7: Sand nourishments 2001-2011 along the Dutch coast (Source: Rijkswaterstaat nourishment statistics dated from 2011)

3 Methods

This chapter describes the methods applied in this thesis. It includes the data collection and analysis, the formation of the synthetic storm time series and the description of the erosion function used for the Holland coast. It describes three approaches of calibrating the recovery rate and it provides the setup of the PCR model used for estimating the future erosion volumes and future coastline.

3.1 Overall approach

The scope of this thesis is to explore the applicability of the PCR framework, to estimate the coastline retreat due to SLR along the Holland coast and compare the results in terms of coastline retreat and erosion volumes with the Bruun rule application. The methodology performed for this thesis can be distinguished in three phases; it includes the data collection, the setup of PCR for the Holland coast and finally the outputs from the application both of PCR model and Bruun rule (Figure 3.1).
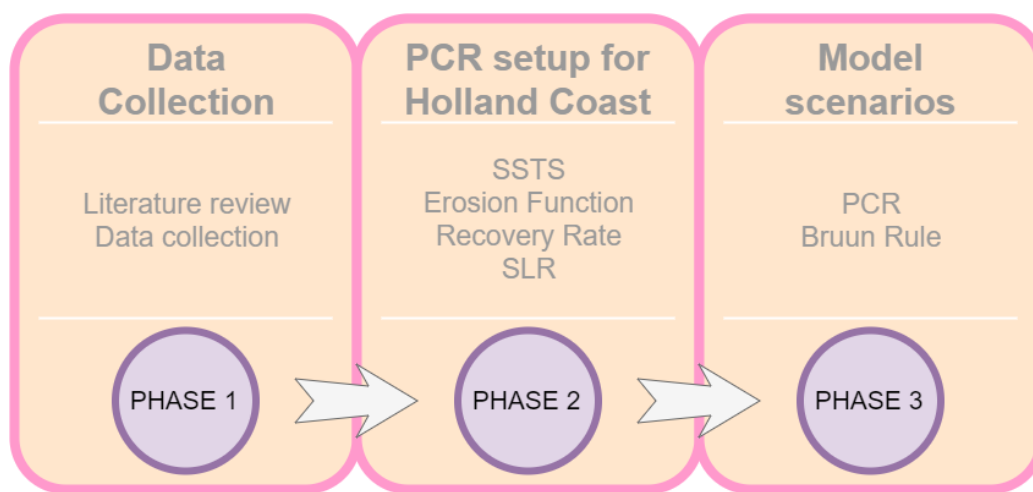
Figure 3.1: The three phases of methodology

The literature study helps to get familiar with the topic, understand the underlying challenges, set the approach of dealing with them and filling the knowledge gaps. Previous applications of the PCR model in other locations have already shown the sensitivities of this model and have given recommendation for further research. So, the first phase includes the literature study and the data collection required. The second phase includes the data analysis and the synthesis of the model, which includes the generation of the synthetic storm time series (SSTS), the erosion function, the calibration of the recovery rate and the SLR scenarios. Finally, the last phase regards the implementation of the PCR framework. Starting with a single profile and then applied for ten more locations. The projected coastal recessions generated from PCR model are compared to those of Bruun rule and conclusions are retrieved for the updated PCR model.

According to literature review and the previous case studies, it is pointed out that the **recovery rate** (RR) and the **longshore sediment transport** (LST) are two basic factors that may need further research and development. At the Holland coast the alongshore sediment rates are not negligible and therefore need to be integrated into the PCR framework. Moreover, further adjustments are required specifically for the Holland coast due to the Dynamic preservation policy. Since 1990, nourishments schemes have been implemented and if these actions are not considered, the calibrated RR values will not be realistic. The RR is a sensitive and important factor for the PCR model, thus, depending on how it is calibrated, it yields different results.

The PCR model and its basic components are described in detail in section 2.5. In order to have a better understanding of how the PCR model is implemented, this chapter shows the approach of "constructing" the basic modules that will finally form the PCR model (Figure 3.2, Figure 3.3). These are:

1. Synthetic Storm Time Series (SSTS)
2. Erosion Function
3. Recovery Rate
4. Sea Level Rise (SLR)
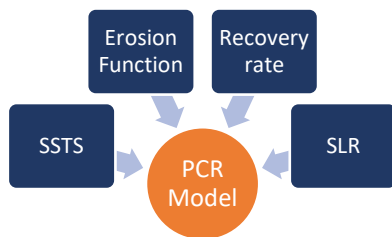
Figure 3.2: The basic components of PCR
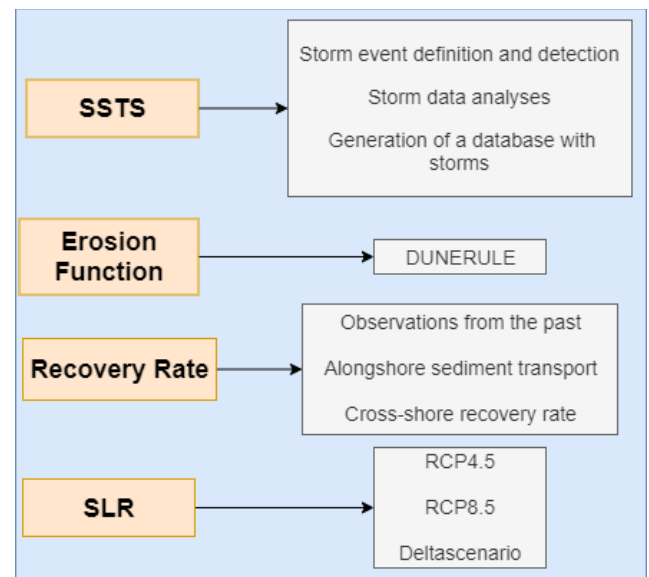
Figure 3.3: Building the basic components of PCR

3.2 Physical description of Holland coast

In this study, the data required for the generation of the synthetic storm time series are the **beach profiles transects** and the **wave recordings** describing the wave conditions along the Holland coast (wave height, mean wave period, wave direction and water level).

3.2.1 Beach Profiles

The JarKus dataset (an acronym for annual soundings-'Jaarlijkse Kustlodingen'), accessed through OpenEarth[2], provides cross-shore bathymetric profile data since 1965, and it is composed of coastal transects perpendicular to coastline, spaced by alongshore intervals of 250 m (see Figure 3.4). Each cross-shore profile corresponds to a pole located on the beach and numbered according to its distance from Den Helder. This permanent base of beach poles is known as RSP reference line ('Rijks Strand Palen lijn') (Collins and Balson, 2007). Since 1965, the JarKus survey has been conducted annually between April and September for each profile and the measurements are performed from the foredune to roughly 1 km seaward (Minneboo, 1995). However, due to the annual time interval between successive measurements, it is not possible to monitor an after-storm event.

Rijkswaterstaat collects and stores the JarKus data in a raw form; then, Deltares processes it by reformatting it to a standardized format (NetCDF) and finally the data is stored in the OpenEarth database so they can be accessed by the users (Elias, 2017). In this thesis, the data of the JarKus survey is retrieved from OpenEarth and it is processed with Matlab[3] scripts.

---

[2] https://www.openearth.nl
[3] MATLAB Version: 9.4.0.813654 (R2018a)
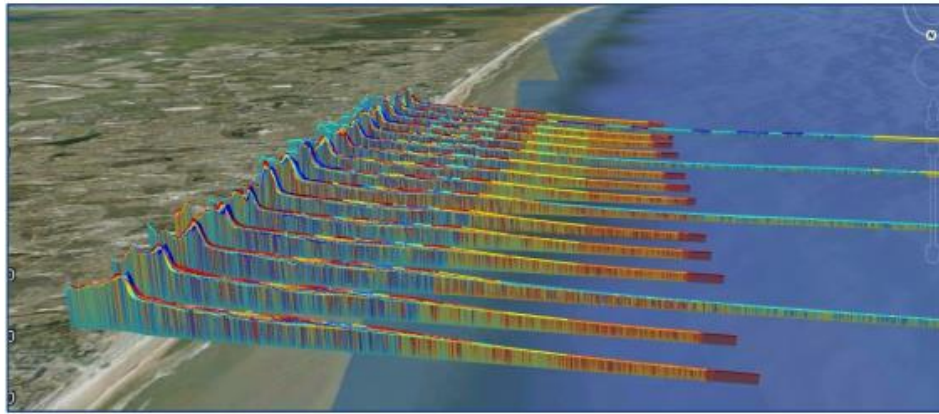
Figure 3.4: JarKus profiles in Google Earth (Pot, 2011)

3.2.2 Wave data and water level

The data required in this thesis is the time series of the significant wave height, the wave period, the wave direction and the water level. These measurements are retrieved from MATROOS and DONAR dataset, accessed through OpenEarth and processed with the Wave Transformation Tool developed by Deltares (Fockert & Luijendijk, 2011). The length record of the available data, for the wave height, the wave period and wave direction, is 39 years (January 1979- December 2018) and for the water level is 29 years (April 1989-December 2018).

Wave Transformation Tool

Deltares developed a wave look-up table for the purposes of Building with Nature project, in a Matlab script. The wave look-up table collects the wave time series from the waverider stations and then transforms them to any nearshore location. In more detail, the wave transformation matrix is built by applying the following procedure (Fockert & Luijendijk, 2011):

1. Determine the existing wave conditions by collecting the wave data from the wave rider buoys.
2. Smooth the wave binned-classification matrices. Then, the wave conditions generated from the smoothed classification matrices are forced in a SWAN model in stationary mode to obtain the nearshore wave climate.
3. After, the transformation matrix is composed by the offshore wave climate and the generated nearfield wave conditions. Depending on the direction of the waves, there is a specification of the dominant wave station, used for the generation of the offshore wave data (Figure 3.5).
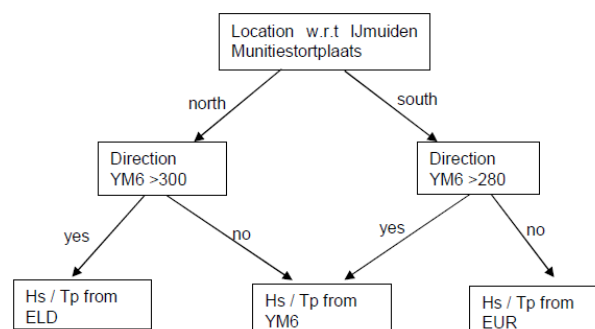
Figure 3.5: Decision diagram for wave height and wave period (Fockert & Luijendijk, 2011)

4. MATROOS and DONAR data are collected from the wave transformation tool for all the offshore stations (Figure 3.6).
5. Based on the measured data the validation of the transformation matrices is done for the nearshore wave stations.
6. Finally, the transformation tool is refined by interpolating the SWAN results.

Data collection using the Wave Transformation tool

Using the Wave Transformation tool, the measurements are collected from the following four stations, the location of which can be seen in Figure 3.6. Depending on the nearshore coordinates of the transect in interest, the Wave Transformation tool transforms the wave data for this location. The wave stations, where the measurements are taken, are listed below:

- Schiermonnikoog noord, located at 53° 35' 37.00''N, 6° 10' 5.00''E;
- IJmuiden munitiestortplaats, located at 52° 33' 00''N, 4° 03' 45''E;
- Euro platform, located at 51° 59' 55.00''N, 3° 16'19.50''E;
- Eierlandse Gat, located at 53° 16' 47.50''N, 4° 40' 38.00''E.
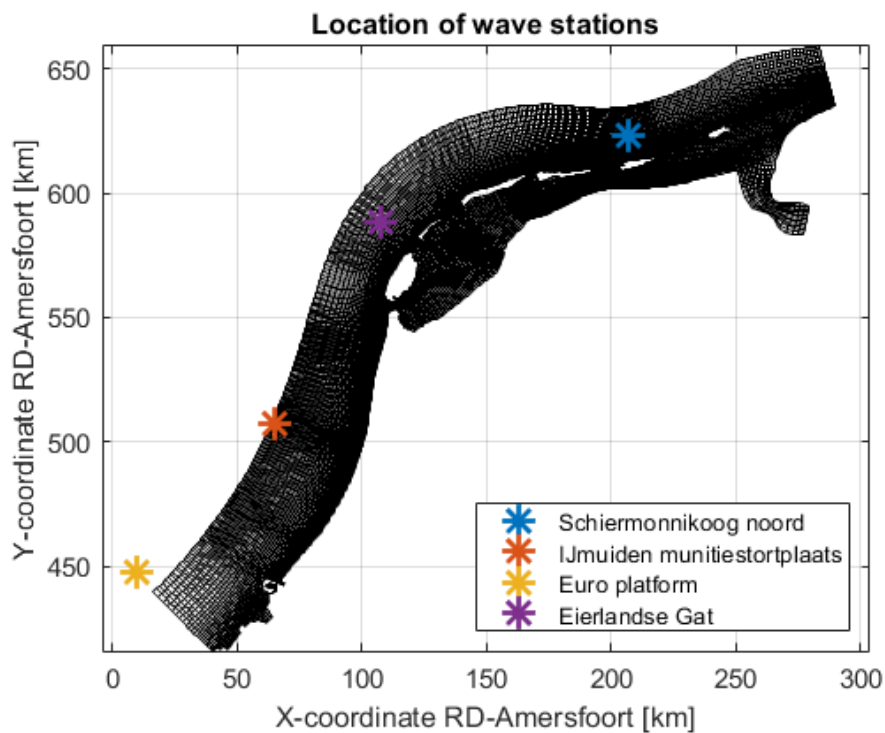
Figure 3.6: Location of wave stations along the Holland coast

3.3 Synthetic Storm Time Series

One main function of the PCR model is the generation of storm time series which are based on historical data and keep the statistical character of the storm variables. This component requires the following steps:

1. Storm event definition and detection
2. Fitting of the main variables to theoretical or empirical distributions

3. Setting the dependencies between different storm characteristics
4. Generation of storm time series

3.3.1 Storm definition and detection

In order to generate the long and realistic time series of storms needed for the PCR implementation, first it is required to define and detect the storms and their characteristics from the available data for the period 1979 until 2018. In this study, as a **storm event** is defined the period within which the significant wave height H_s exceeds a specific threshold. In order to establish a meteorogical independence among the storm events, an opening of 3 hrs is set. So, when two storm events lie within a time interval lower than this limit then these two storms are merged and grouped as one (**storm grouping**). Moreover, if the duration of a storm event is less than 6 hours then this event is not taken into consideration as a storm, see Figure 3.7. Clearly the definition of a storm event is subjected to sensitivities and maybe small changes can lead to different results (e.g. influence the number of events detected during the period of interest).
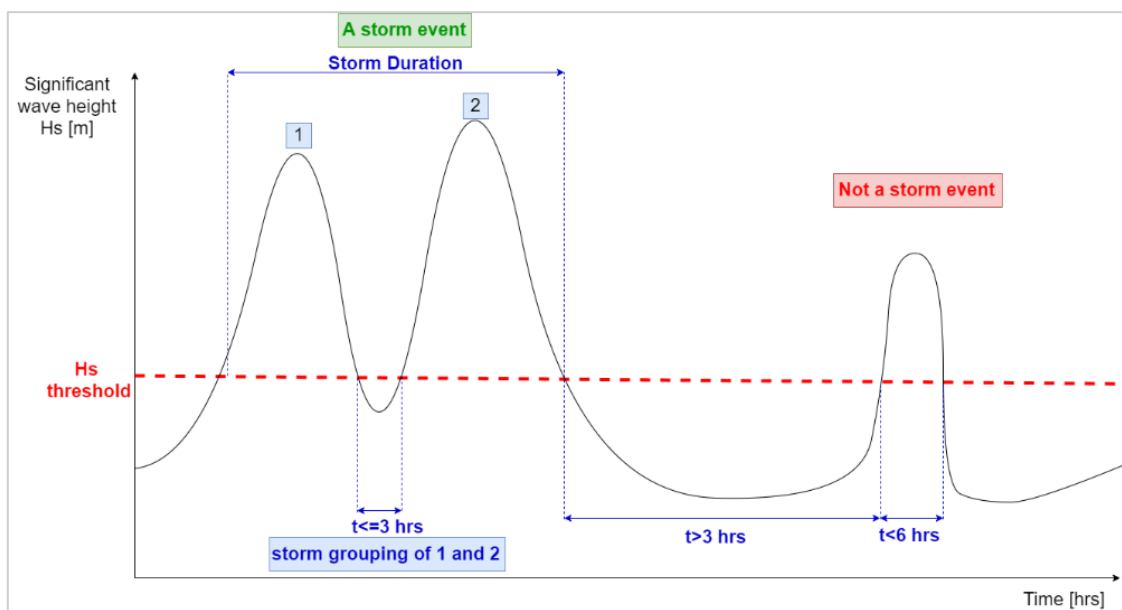
Figure 3.7: Storm definition, storm grouping, minimum storm duration

For each of the selected coastal profiles the storm event characteristics are extracted from the time series of wave conditions. The event characteristics consist:

- the maximum significant wave height event (**H_s**),
- the average peak period of waves (**T_p**),
- the maximum (positive) water level (**h_{max}**),
- the mean wave direction (**θ**),
- the storm duration of each event (**dur**).

3.3.2 Storm Data analysis

The next step for the generation of the SSTS that preserve the statistical characteristics of the storm variables, is statistical analysis by fitting the storm characteristics (derived in the previous step) to theoretical or empirical distributions and also fit dependency distributions between different storm characteristics.

Data fitting of Hs, dur and h$_{max}$ to theoretical distributions

First, the detected data for the maximum significant wave height event **H$_s$**, the storm duration **dur** and the maximum water level **h$_{max}$** are fitted to theoretical probability distribution functions. This is accomplished in two steps; first, the parameters describing best the data should be estimated for a range of theoretical probability distributions and then the family of the theoretical distribution depicting best the data is chosen.

For the estimation of the parameters, several distributions functions are tested and then through the **maximum likelihood estimation** (MLE) method the definition of the parameters is accomplished. The scope of MLE method is to find the parameter values (the shape parameter, scale parameter etc. depending on the probability distribution function) that describe the distribution in a way that maximizes the probability of observing the historical data.

In software like Matlab, optimizers of statistical packages prefer to optimize their result by minimizing a function. In this case, for the MLE method, it is used the negative loglikelihood (**NLL**) function (Equation 3.1).

Equation 3.1

$$NLL = -log(\hat{L}) \text{ where, } \hat{L} = p(x|\bar{\theta}, M)$$

- x is the dataset of the observations
- $\bar{\theta}$ the maximized value of the likelihood function of the model M

Loglikelihood has been regarded analytically more convenient and numerically more efficient because the multiplications (hidden in the joint probability $p(x|\bar{\theta}, M)$) convert to sums (Frank,2013). The logarithm is monotonic; thus, the minimum of NLL coincides with the maximum of $\hat{L}$ (Kane, 1948).

For better understanding an example can be seen in Figure 3.8. It shows the likelihood surface generated by the several combinations of the two parameters A and B, describing a Gamma distribution for a set of data X. The red point corresponds to the pair of parameters A and B that give the minimum likelihood surface.
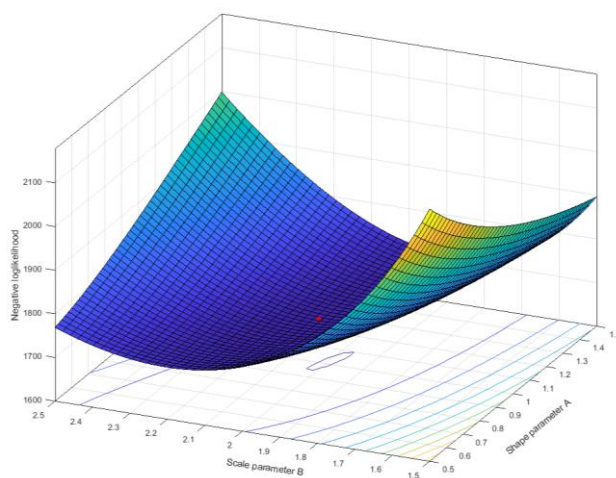
Figure 3.8: Likelihood surface for a set of data X

For the family definition of the storm variables, the **Bayesian information criterion** (BIC) and the **Akaike information criterion** (AIC) are used. Both criteria are similar and are based on the likelihood function. In model fitting, the likelihood may increase by adding parameters, but this can lead to overfitting. To overcome the problem of overfitting and underfitting, the two criteria take into consideration the number of parameters (Burnham and Anderson, 2004).

The formula for the BIC criterion is (Wit et al., 2012):

$$BIC = \ln(n) \cdot k - 2 \cdot \ln(\hat{L})$$

- n is the number of observations,
- k is the number of parameters estimated by the model
- $\hat{L}$ is the maximized value of the likelihood function of the model M,

Similarly, the formula of the AIC criterion is:

Equation 3.2

$$AIC = 2 \cdot k - 2 \cdot \ln(\hat{L})$$

The model (i.e. theoretical distribution family) that corresponds to the minimum value of the BIC or AIC, can be regarded as the best choice for the observed data (Wit et al., 2012).

Dependency structure

It is observed that among maximum significant wave height, storm duration and maximum (positive) water level there is a dependency. Using a dependency structure, e.g. employing a copula method, we generate a dependency distribution for the synthetic storm characteristics. Copulas are basically a family of multivariate cumulative distribution functions for which the marginal distribution of each variable is uniform (Gao, 2018), see Figure 3.9. Specifically, the main variable H_s is correlated with the other two variables and this is achieved by employing two copulas for describing the relations between the two pairs of H_s with the other two storm event characteristics (i.e. H_s-dur, H_s- h_{max}).

Figure 3.9: Joint probability model of maximum significant wave height and storm duration (Dastgheib et al., 2018)

The wave height is linked with the wave period with the use of a linear function whereas the wave direction and the gaps are not related with any variable.
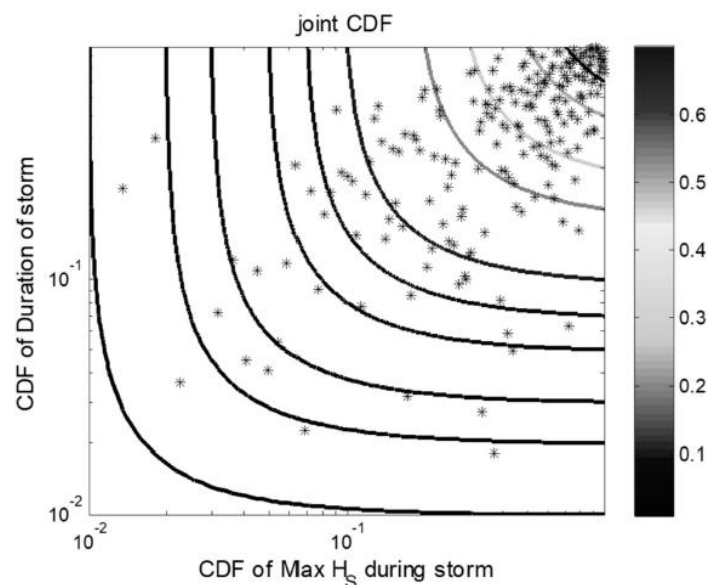
The choice of copula family for each pair of variables is made using as a criterion the comparison of the correlation coefficient of the initial pair of datasets with the correlation coefficient of the generated samples. Different copula families (such as Gumbel, Frank, Gaussian, Clayton) are tested and, finally, the family that generates a sample with a correlation coefficient close to the initial correlation coefficient, is selected.

The correlation coefficient is a measure of the linear dependence between two random variables. If A and B are the vectors of observations of two random variables, then the formula used to calculate the correlation coefficient is the following:

Equation 3.3

$$\rho(A, B) = \frac{\text{cov}(A, B)}{\sigma_A \cdot \sigma_B}$$

where, $\text{cov}(A, B)$ is the covariance of the two vectors and σ_A, σ_B the standard deviation of A and B respectively.

3.3.3 Generation of storm time series

In summary, to generate N number of storms, the following information is required:

- Fitting of the maxima of wave heights (H_s), the storm duration (dur) and the maxima of the peak water levels (h_{max}) to theoretical distributions;
- Fitting the pairs of H_s - dur and H_s - h_{max} to copulas;
- Linear fit of the wave period (T_p) to H_s;
- Empirical distributions for wave direction (θ) and storm gaps.

Having the aforementioned requirements, a number (N) of storms can be randomly generated by following the next steps:

1. Generate N uniformly distributed random numbers and use the inverse theoretical cdf of H_s, to generate a vector with **N maximum significant wave heights** for N the storm events;
2. Generate N uniformly distributed random numbers using the linear correlation rho of the copula describing the pair H_s – dur; then use the inverse theoretical cdf of dur, to generate a vector with **N storm durations** for the N storm events;
3. Repeat step 2, but instead of dur use the **h_{max}**;
4. Generate **N storm wave periods** using the linear fit between H_s and T_p;
5. Generate N uniformly distributed random numbers and use it with the empirical distribution of θ, to generate a vector with **N wave directions** for N the storm events;
6. Generate N uniformly distributed random numbers and use it with the empirical distribution of gaps, to generate a vector with **N storm gaps** for N the storm events;

At this point, a large database of storm characteristics is created (Figure 3.11). A storm event is composed of a maximum significant wave height (H_s), a peak wave period (Tp), a storm duration (dur), a wave direction (θ) and a storm gap (Figure 3.10). For the construction of records of storms, the database is reshaped from 1xN to a form of num_events_per_year x num_years x num_sims, where:

- num_events_per_year is the maximum number of events that can occur within a year
- num_years is the number of years of the record of the storm time series, and
- num_sims is the number of simulations for which the PCR is set.

The initial database shall generate slightly more events than the total number of events that will be used in the end. Since the storm events are considered statistically independent, the approach of generating in advance the events, saves a lot of computational time when using Matlab, because it omits the time-consuming loop functions.
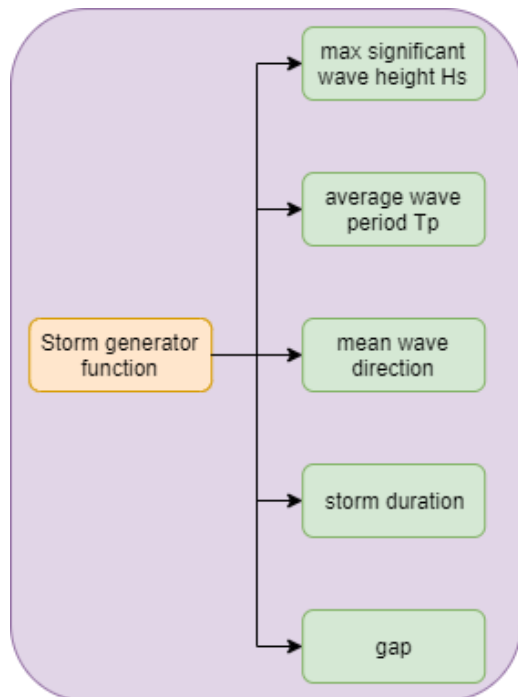
Figure 3.10: Storm event generation
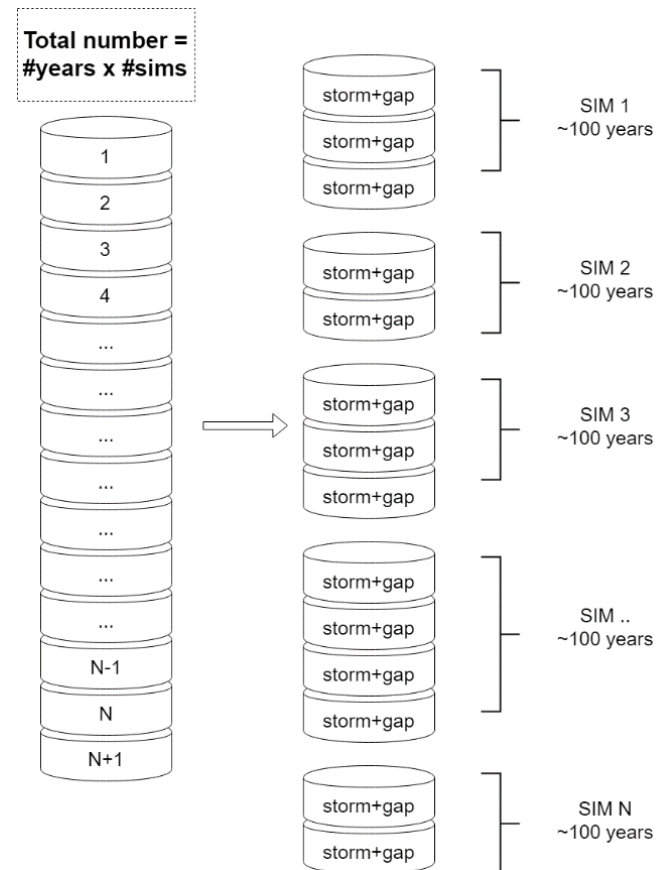
Figure 3.11: Database of storms

3.4 Erosion function

Once the storm record is generated, the use of an erosion function is needed for the estimation of the eroded volume related to each storm event, which can be also converted to coastline retreat. Process-based numerical models (e.g. XBeach) or semi process-based (e.g. SBEACH) would be ideal options for dune erosion calculation; however, due to the Monte Carlo simulations included into the PCR framework, the computational costs would be high and thus such a choice would not be feasible. In contrary, a simpler erosion function is a good fit for the nature of PCR framework.

In this study, as an erosion function for the PCR model is used the adjusted empirical DUNERULE function (Equation 3.4) as calibrated from Li (2004) for all wave directions. The reason for selecting the adjusted DUNERULE formula as an erosion model in this study is that it has been already implemented in a coastal profile of the Holland coast. Thus, Li's study could work as validation process for the results of the current study. The formula will be implemented for the selected coastal profiles for estimating the dune erosion. It should be noted that the coastal slope and the median sediment diameter are constant and have been already merged into the adjusted DUNERULE formula with the values of 0.02 and 200 μm respectively.

Equation 3.4

$$V_{d,t} = 153 \cdot A_{dir} \cdot \left(\frac{h_{max}}{5}\right)^{b1} \cdot \left(\frac{H_{s,0}}{7.6}\right)^{b2} \cdot \left(\frac{t}{5}\right)^{b3} \cdot \left(\frac{T_p}{12}\right)^{b4}$$

With

$$A_{dir} = \begin{cases} 1 - 0.01 \cdot (270 - \theta), for\ \theta \leq 270 \\ 1 - 0.0107 \cdot (26 - |\theta - 298|), for\ 270 < \theta < 326 \\ 1 - 0.01 \cdot (\theta - 326), for\ \theta \geq 326 \end{cases}$$

The exponents *b1, b2, b3 and b4* are defined below:

$$b_1 = \begin{cases} 1.5, for\ h_{max} < 5 \\ 0.2, for\ h_{max} > 5 \end{cases} ; \quad b_2 = \begin{cases} 0.3, for\ H_{s,0} < 7.6 \\ 0.9, for\ H_{s,0} > 7.6 \end{cases} ; \quad b_3 = 0.4 ; \quad b_4 = \begin{cases} 1.3, for\ T_p < 12 \\ 0.9, for\ T_p > 12 \end{cases}.$$

The definition of the rest of the variables and more details about DUNERULE formula are provided in Appendix A.

Once the 'dry' erosion volume induced by a storm is estimated, the translation of this volume into coastline retreat follows. The average horizontal dune recession is estimated using the following equation:

Equation 3.5

$$R = \frac{V_{d,t}}{h_d - h_{max}}$$

Where R is the shoreline retreat [m], V is the dry erosion volume per running meter [m³/m], h_d is the height of dune crest above mean sea level [m] and h_{max} is the maximum water level above MSL.

3.5 Recovery rate

The recovery process of a dune/beach takes place during the inter-storm periods. This process is important for the PCR framework, but the determination of the RR is not a simple task. In this study, three approaches for calibrating the RR are considered.

3.5.1 Approach 1

The previous researches (Sri Lanka, Japan, the Netherlands) followed the following approach for defining the recovery. The RR is determined via trial and error application of the PCR model in absent of SLR (i.e. only storm forcing). It is assumed that the dune would recover in such a way that the coastline would remain in place with an exceedance probability of 50 % (Dastgheib et al., 2018). The alongshore sediment transport is assumed negligible.

First, the PCR model is applied for a period of time (e.g. 100 years). Then the RR is calibrated by satisfying the concept that the accumulated retreat caused by the storm events happened during this period should be counterbalanced by the accumulated accretion due to the periods of recovery process. This is repeated for all the simulations for which the PCR is set up for. Then, the median value of the calibrated recovery rates is used for the future estimates of the coastline retreat or accretion (Figure 3.12).

Figure 3.12: Calibration of the RR based on Approach 1; Future predictions of coastline change using the calibrated RR

3.5.2 Approach 2

The coastal profiles of Holland coast may seem being in equilibrium however this is due to the nourishment schemes that have been implemented along the coast on a regular basis since 1990, according to 'hold-the-line' policy. Therefore, the calibration of the natural RR in the cross-shore direction should be calibrated with observations before 1990 in order to be representative. It is noted that the alongshore sediment transport is assumed to be negligible.

This approach is built on the previous approach (3.5.1). The RR is determined via trial and error application of the PCR model, based on long term field observations of an indicator (e.g. dunefoot, MLW, MHW). The dune/beach recovers in such a way that in the absence of SLR, the coastline would move to a position (defined by the indicator, *ΔCL_rate*) with an exceedance probability of 50 % (Figure 3.13). For example, assume that the dunefoot observations from the past measurements (before 'hold-the-line' policy) show a retreat trend of 0.5 m/year (indicator). By implementing the PCR to make future coastline estimates for 2120 (relevant to 2020), the beach recovers in such a way that in 2120 (in 100 years) the coastline position would retreat by 50 m (= *ΔCL_rate* x 100 years) with an exceedance probability of 50 %.

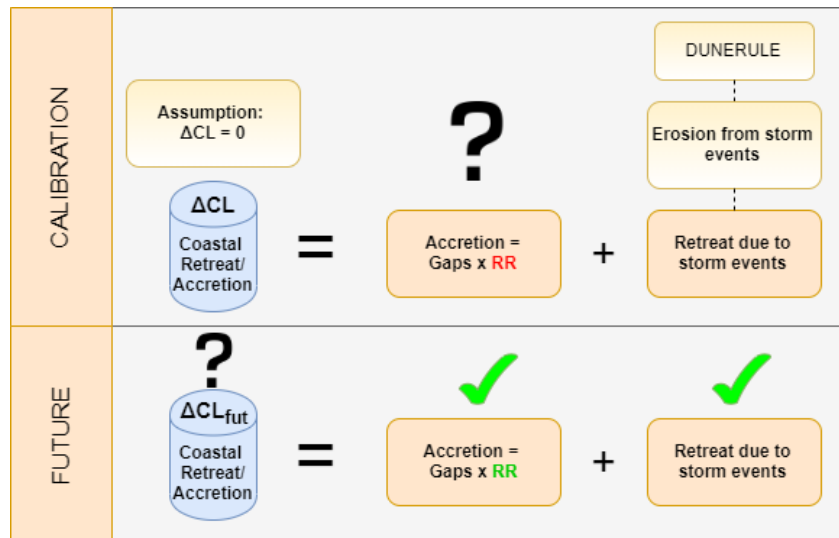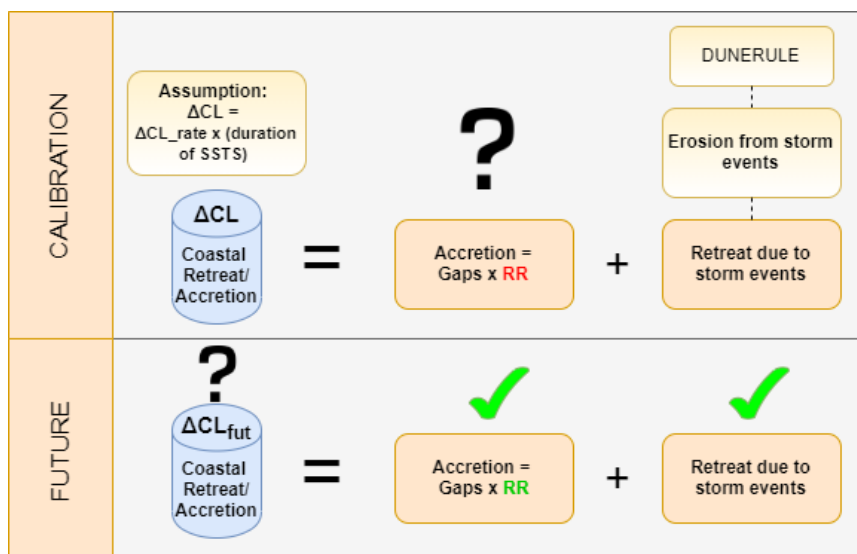*Figure 3.13: Calibration of the RR based on Approach 2; Future predictions of coastline change using the calibrated RR*

Retreat/accretion rate based on field measurements

Since 1990, the coastline of the Dutch coast has not shown major changes. This is due to the decision of the Government and Parliament of Netherlands to maintain the coastline as it was in 1990. However, the coastal profiles can be regarded either erosive or accretive depending on their natural trend noticed before any interventions of nourishment schemes have taken place.
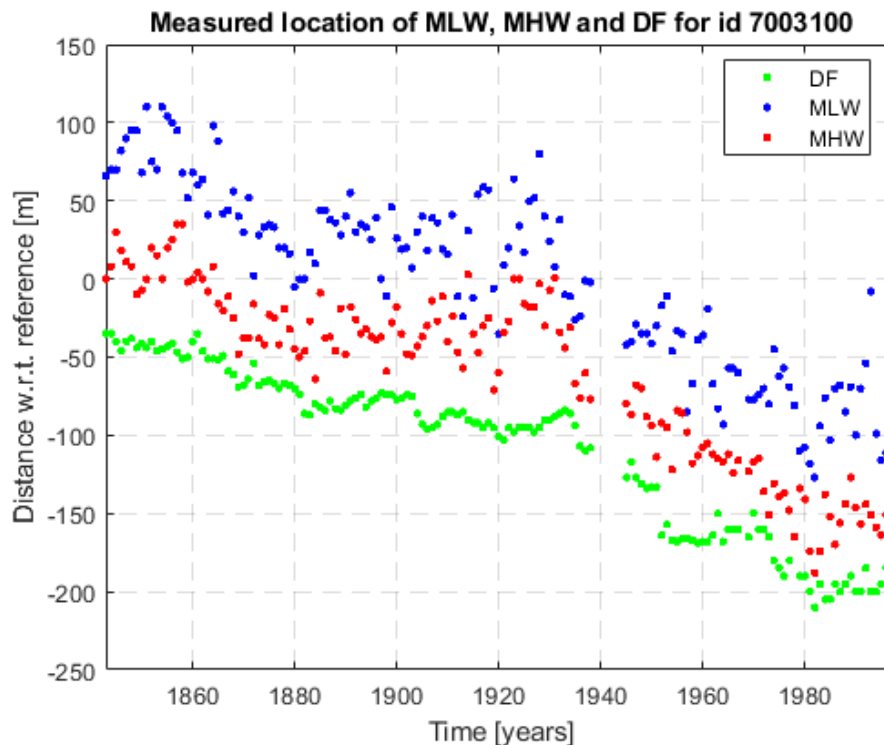
Figure 3.14: Locations of MLW, MHW and DF for a coastal profile in Bergen, id7003100

As seen in Figure 3.14, there are measurements since 1843 of the position of mean low water (MLW), mean high water (MHW) and dunefoot (DF). A first-degree polynomial (linear) fit is performed to the points of each Beach line and the slope of each line shows the rate of retreat/accretion of each of the three Dutch Beach lines. Finally, the mean value of the three slopes is used as the rate of retreat/accretion that it will be used as an indicator for the calibration of the RR in cross-shore direction:

Equation 3.6

$$\Delta CL\_rate = \frac{(\delta x_{DF} + \delta x_{MLW} + \delta x_{MHW})}{3}$$

Where ΔCL_rate: rate of coastline accretion or recession, in m/yr

- If **ΔCL_rate >0**, it means that the specific coastal profile was observed having a natural accretive behaviour for the period before the 'hold-the-line' policy and thus is characterized as accretive;
- If **ΔCL_rate <0**, it means that the specific coastal profile was observed having a natural erosive behaviour for the period before the 'hold-the-line' policy and thus is characterized as erosive.

It should be noted that the wave climate for this period is not available and therefore it is assumed that the wave climate is not changing significantly during the years.

3.5.3 Approach 3

In the two previous approaches the alongshore sediment transport was assumed negligible. However, this assumption is not valid along the whole Holland coast. Thus, in this approach, the alongshore sediment transport is incorporated into the PCR framework and it tunes the RR accordingly. This approach is built on the previous one and considers both the coastline change rate (based on historical data) and the longshore sediment transport for the calibration of the recovery rate. The longshore sediment transport is provided by the coastline model UNIBEST LT for the Holland coast

The RR in cross-shore direction RR is calibrated by assuming that the coastline change keeps the same rate of accretion or recession as the one noticed at the observations of Dutch Beach Lines between 1843 and 1980 - before the 'hold-the-line' policy. This means that after a long period (e.g. 100 years) the beach recovers in such a way that in the absence of SLR, the coastline would be moved by (ΔCL_rate * 100) m, with an exceedance probability of 50 %. Figure 3.15 presents the equilibrium equation used in this work.
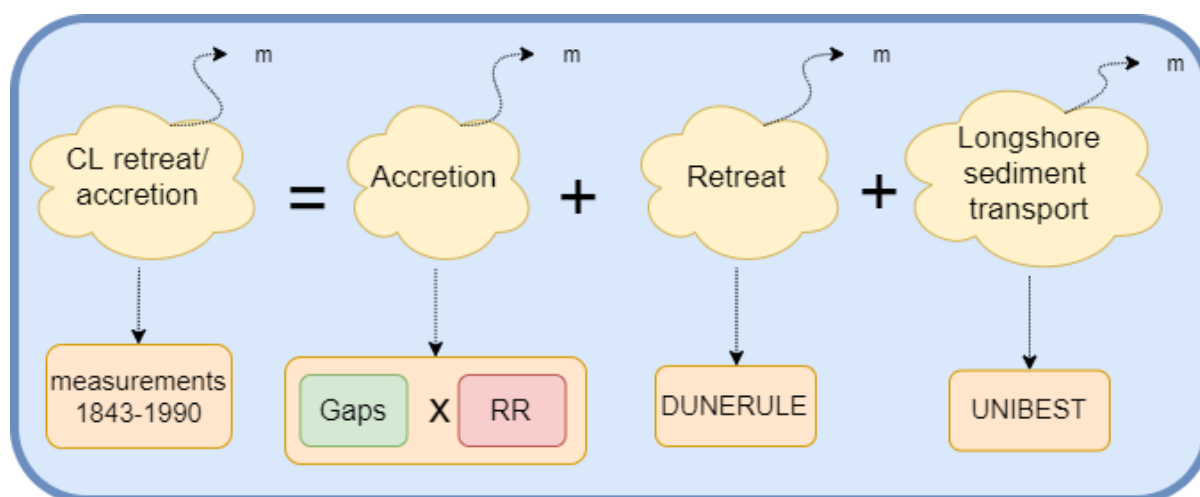
Figure 3.15: Equilibrium equation

Longshore sediment transport

The longshore sediment transport for each of the selected profiles is calculated using the transport rays generated by the coastline model UNIBEST LT for the Holland coast. An important concept in the coastal modelling is the relation between the sediment transport (S) and the coastline orientation (φ) and this model generates the so-called S-φ curves for different rays along the coast.

Figure 3.16 shows the available transport rays generated by the UNIBEST model for the Holland coast. The approach followed first includes the identification of the location of the cross-shore profile between the closest rays. For example, the cross-shore profile 9 is between ray 80 and ray 81 of the UNIBEST model. Each ray file includes the computed transports (S) as a function of the relative coastal angle (Figure 3.17):

$$S = c_1 \cdot \theta_R \cdot e^{[-(c_2 \cdot \theta_R)^2]}, \text{ in Mm}^3/\text{yr}$$

Where, $\boldsymbol{\theta_R} = \theta_c - \theta_e$

$\quad\quad \boldsymbol{\theta_c}$: the coast angle

$\boldsymbol{\theta_e}$: the equilibrium angle, the coast angle for which S = 0

$\boldsymbol{c_1}$ and $\boldsymbol{c_2}$: coefficients defining the transport rate as a function of the actual coastline orientation

Figure 3.16: Transport rays along Holland coast modelled in UNIBEST
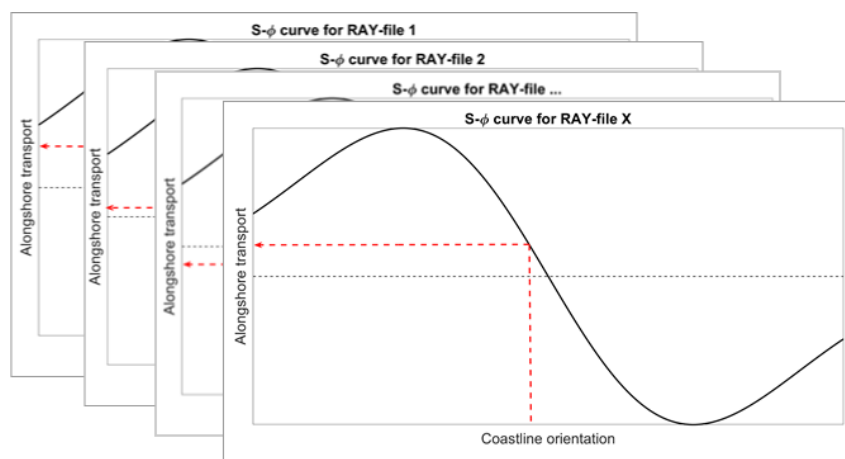
Figure 3.17: S-φ curves output for every transport ray

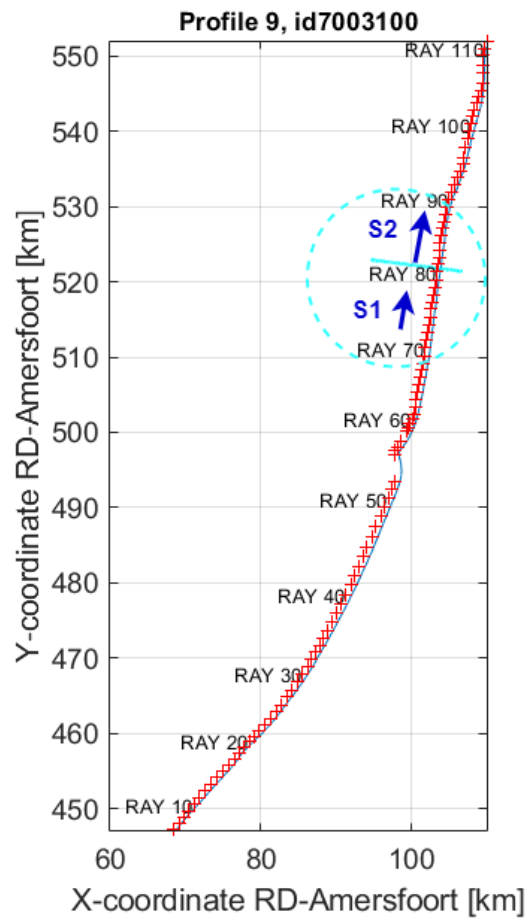Then the coastal orientation for the two rays is estimated and for the given coast orientation the longshore sediment transport rates are found using the look-up tables of S-φ curves. The difference of the two longshore transport rates divided over the distance of the two rays accounts

for the longshore sediment rate for the specific location we are interested in (Figure 3.18). The transport rate in the longshore direction is:

Equation 3.7

$$LSTR = (S_1 - S_2) / d \text{ , in } [\text{Mm}^3/\text{yr/m}]$$

Where,

S$_1$: the alongshore sediment in *ray1* [Mm³/yr]

S$_2$: the alongshore sediment in *ray2* [Mm³/yr]

d: the distance between *ray1 and ray2* [m]
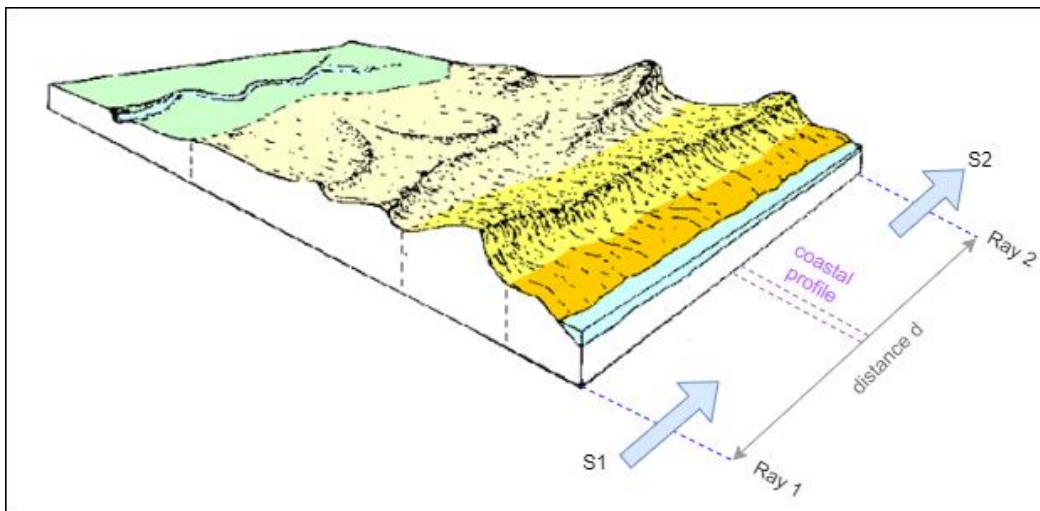
Figure 3.18: Longshore sediment transport rate

A positive value of the LSTR indicates that the longshore sediment transport acts in an accretive way for the profile, whereas a negative induces erosion.

In Figure 3.19 can be seen the methodology of calibrating the RR in cross-shore direction RR. Having as an indicator the field observations of the coastline change from 1843 to 1980, the RR is calibrated using both the rate of longshore sediment transport and the available observations of the coastline change before the Dynamic preservation policy.

Finally, the calibrated RR is used for implementing the PCR model for future estimates of coastline recession.
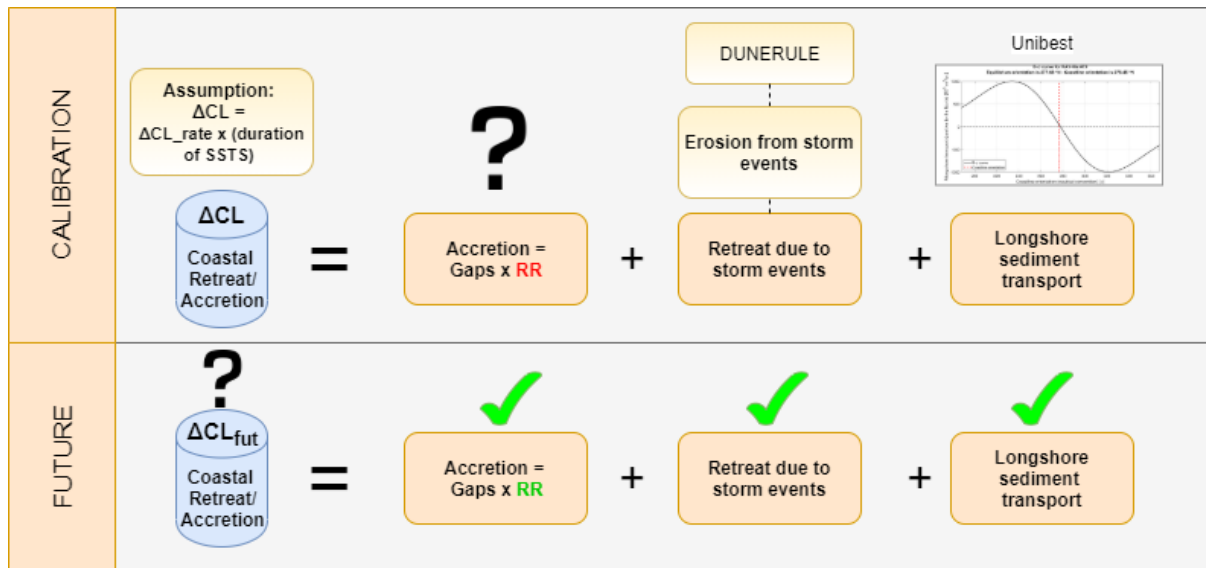
Figure 3.19: Calibration of the RR; Future predictions of coastline change using the calibrated RR

Within the Monte Carlo simulation, the calibration process above is performed for a large number of iterations and a vector with a size equal to the number of iterations is filled with RR values satisfying the equilibrium equation at each simulation. Finally, the median value of this vector is chosen as the constant RR that will be used from the PCR model for the future predictions of the coastline change.

3.6 Sea level rise

The PCR model estimates the SLR at the time each storm occurs. This increase in the sea water level, which results in an extra recession of the coastline, is induced into the PCR framework through the MSL. DUNERULE formula has been hard to be implemented with SLR because it requires water level as an input and by including the SLR the erosion starts increasing sharply (see Fig B.23). This is not realistic because the coastline is also reshaping itself according to SLR. A solution to this complication is to only include the increment in water level into the PCR model implicitly through the maximum water level variable (h_{max}) in the estimation of the average horizontal dune recession (Equation 3.5), but not through the maximum water level variable in the estimation of the dry erosion volume (Equation 3.4). So, the average horizontal dune recession accounting for the SLR is estimated using the following equation:

Equation 3.8

$$R = \frac{V_{d,t}}{h_d - (h_{max} + SLR)}$$

For the purposes of this study, three SLR scenarios are considered, the RCP4.5, the RCP8.5 and the Deltascenario. RCP4.5 is used as a low SLR scenario, RCP8.5 as a medium to high SLR scenario and Deltascenario as a high SLR scenario. For the RCP scenarios the median values and likely ranges for projections of global mean sea level (GMSL) rise and its contributions in metres relative to 1986–2005 can be seen in Table 2.1. The starting date of the simulations in this work is the year 2020, therefore the curves of SLR are fitted setting this year as a reference and considering the SLR equal to zero at that moment (Table 3.1, Figure 3.20, Figure 3.21, Figure 3.22).

Years	SLR [m]		
	RCP4.5	RCP8.5	Deltascenario
2040	0.09	0.10	0.15
2070	0.26	0.32	0.46
2100	0.44	0.65	0.82
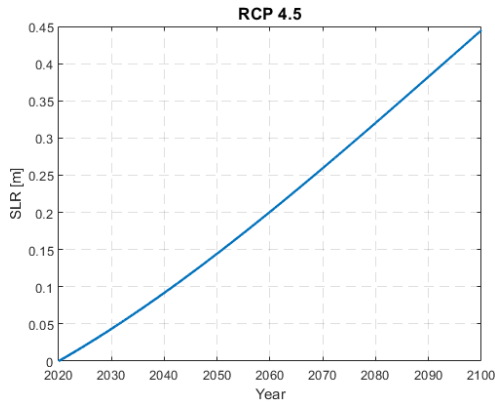
Figure 3.20: SLR for RCP 4.5 by 2100 (relative to 2020)
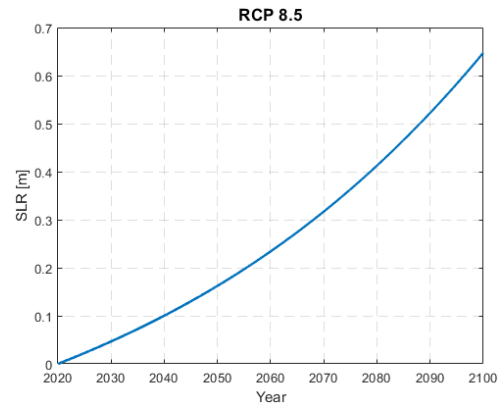
Figure 3.21 SLR for RCP 8.5 by 2100 (relative to 2020)
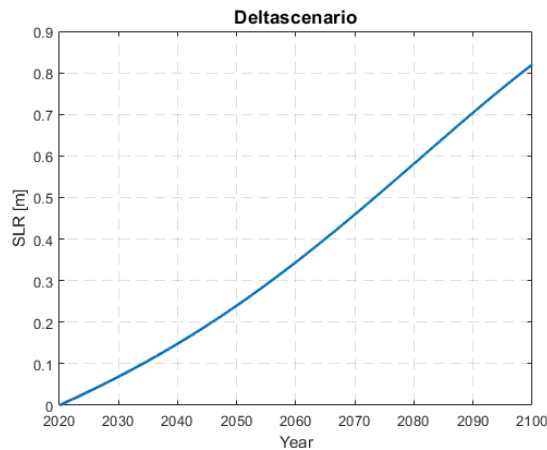
Figure 3.22: SLR for Deltascenario by 2100 (relative to 2020)

3.7 PCR model scenarios

The main functions of the PCR framework include:

- Random generation of long (~ 80 years) time series of storm conditions and the gap between them from pre-determined Joint Probability distributions of storm conditions
- Estimation of coastal erosion and shoreline retreat during the storm
- Estimation of subsequent recovery during the inter-storm periods
- Time series calculation of coastline position stored as output.

This procedure is repeated many times until resulting in the data set required for robust statistical analysis (Ranasinghe et al., 2012).

In this phase, the PCR model is set for implementation and 20,000 PCR simulations are carried out for every selected coastal profile. The duration of the synthetic time series is 81 years (2020-2100) and for every simulation, the location of coastline on the first day of each calendar year is

recorded. Hence, a construction of an empirical distribution of coastline recession for every future year is recorded. Another record is also constructed, this time using the most landward position of the coastline for every future year (Figure 3.23).

Following the methodology presented in this chapter, 20,000 simulations of 81 years (2020-2100) are conducted for eleven profiles along the Holland coast, for each considered scenario of SLR. In this work, RCP4.5 is used as a low SLR scenario, RCP8.5 as a medium to high SLR scenario and Deltascenario as a high SLR scenario. Exceedance probability curves of coastal recession are constructed for all the years and the years 2040, 2070 and 2100 are chosen (arbitrary) for presenting the results. In addition, the model is tested for the three different approaches of calibrating the RR.
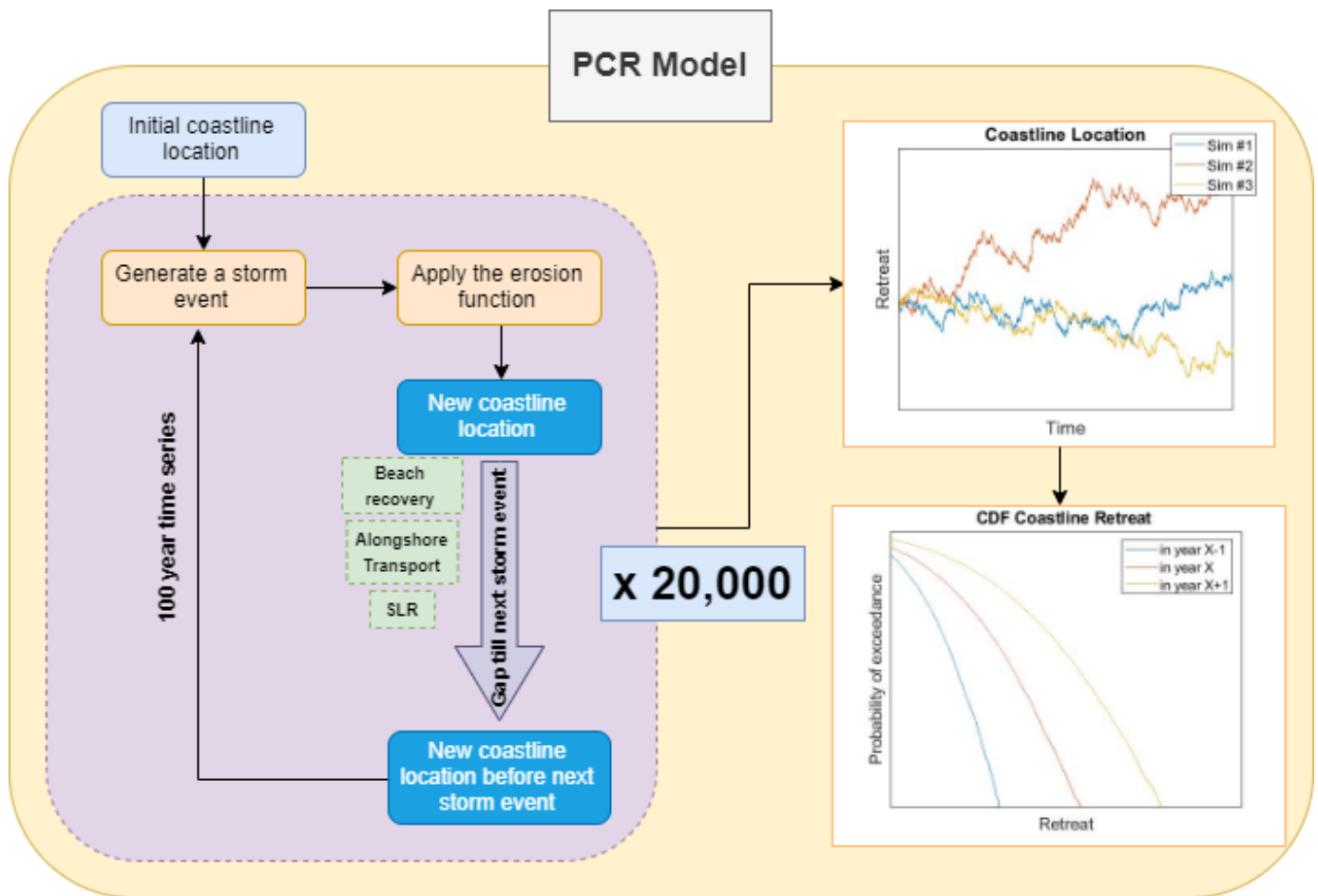
Figure 3.23: PCR concept and output format

3.8 Bruun rule implementation for the Holland coast

The Bruun rule formula is described in section 2.4.2. For the implementation of the formula is needed the maximum depth until which there is exchange of material between nearshore and offshore. In the next section is described the way to estimate the height of the active profile.

The seaward limit of the coast has been introduced by the engineers with the term "**depth of closure**", as the most seaward point of interest. It is considered the deepest point showing significant morphodynamic activity on yearly to decadal time-scales, see Figure 3.24. For the Holland coast the DoC ranges from MSL -6 m to MSL -12 m (Bosboom & Stive, 2011).
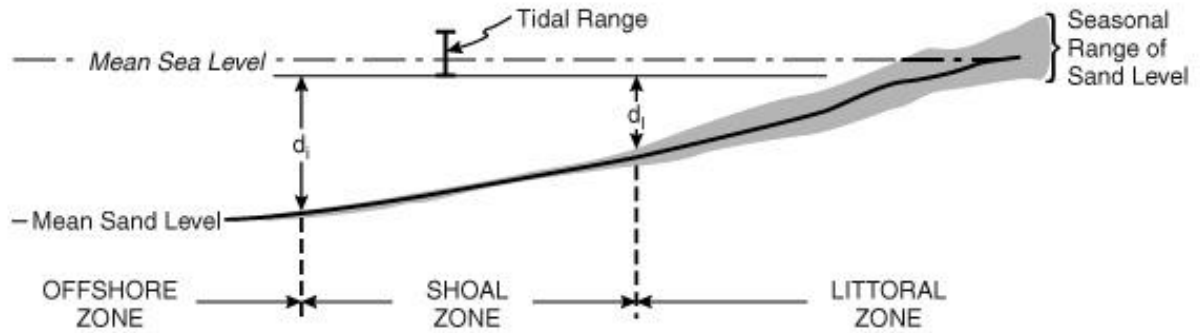
Figure 3.24: Envelope of beach profiles measured over a period of months to years, including both calm and storm conditions; d_l is the depth of closure as defined by Hallermeier(Equation 3.9) (Bosboom & Stive, 2011)

The formula given by Hallermeier (1983) for the estimation of the 'outer' closure depth is the following:

Equation 3.9

$$h_{out} = 0.01 \cdot H_m \cdot T_m \cdot H_m \sqrt{\frac{g}{D_{50} \cdot (s-1)}}$$

Where H_m is the median wave height, T_m is the median wave period, g is the acceleration of gravity, D_{50} is the median sediment diameter (considered stable and equal to 0.2 mm for the Holland coast) and s is the ratio of specific gravity of sand to that of fluid (about 2.65).

The active coastal zone represents the coastal area along which sediment transport processes take place (Figure 3.25). The seaward boundary corresponds to the depth of closure and the landward limit to a part of the front dune that can be eroded by storm waves (Dronkers, 2018). The height of the active profile is defined by the depth of closure and an upper limit which depends from the behaviour of the beach profile. If it is an erosive profile, then the upper limit should be the dune height whereas if it is an accretive profile, then the upper limit is defined by the representative wave run-up added to the high-water level (Bosboom & Stive, 2011). However, in this work the upper limit is calculated from the average profile measurements of the JarKus dataset. As upper limit is chosen the point until which it is observed changes of the dune profile.
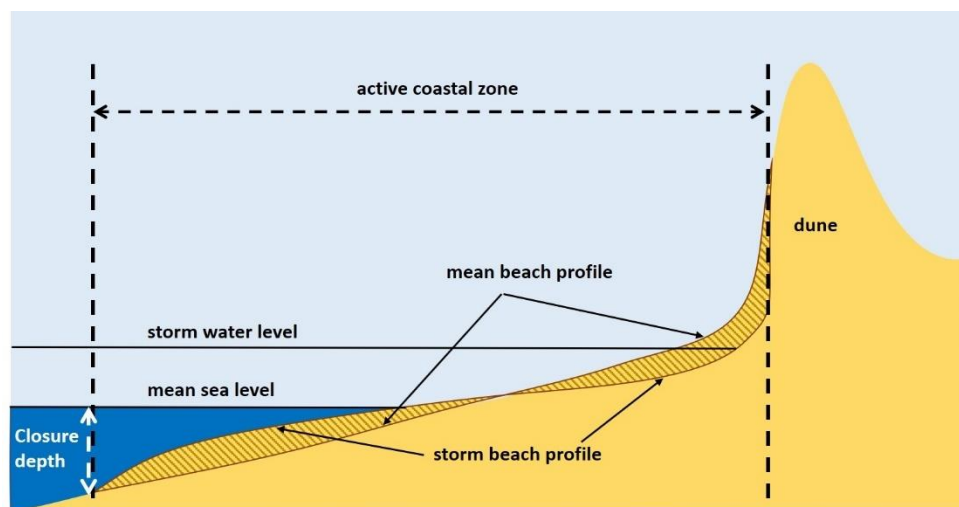
Figure 3.25: Active coastal zone (Dronkers, 2018)

Methods

The results of the new methodology for the PCR framework are presented at this chapter. First, the new methodology compares the three approaches for calibrating the recovery rates-before and after the expansion of the longshore sediment transport. The updated model is implemented for three SLR scenarios and finally the estimates of the PCR model are compared to those raised from the Bruun rule formula. An overview of the differences in time and space is presented and an interpretation is provided in the necessary nourishment volumes, in terms of 'hold-the-line' policy, for the three SLR scenarios.

4.1   PCR set up for Holland coast

The storm detection, the storm data analysis, the generation of the synthetic storm time series (SSTS) and the sensitivities of the erosion model to its main variables are presented in Appendix B. In this section the coastal profiles of Holland coast, where the PCR model is implemented, are presented and then the longshore sediment transport rates are defined for these profiles. After, the PCR model is tested for the three ways of calibrating the RR described in section 3.5 and by comparing the results a better insight of the contribution of the longshore sediment transport to the PCR upgrade is gained.

Longshore sediment transport

In this study, the PCR model is implemented at eleven locations along the Holland, see Figure 4.1 and Table 4.1.

Figure 4.1: Location of the coastal profiles where the PCR model is applied

Table 4.1: Location info of the coastal profiles

Profile (starting South to North)	JarKus transect	Region	Area
1	9011700	Delfland	Westland (South)
2	9011109	Delfland	Westland
3	9009795	Delfland	Wassenaar- Den Haag
4	8008700	Rijnland	Katwijk
5	8007600	Rijnland	Noordwijk
6	8006200	Rijnland	Bloemendaal
7	7005100	Noord-Holland	Heemskerk
8	7004100	Noord-Holland	Bergen (South)
9	7003100	Noord-Holland	Bergen (North)
10	7001990	Noord-Holland	Schagen
11	7000508	Noord-Holland	Den Helder

The alongshore sediment transport is estimated by a coastline model of the Holland coast in UNIBEST and it is assumed that remains constant in time. The longshore sediment transport is defined for each profile using the available RAY-files, generated by the UNIBEST. First, the location of the coastal profile in interest is identified with reference to the closest available rays of the UNIBEST model (Figure 3.16). For example, the cross-shore profile 9 is detected between RAY 80 and RAY 81 of the available UNIBEST model. Each RAY-file includes the computed transports (S) as a function of the relative coastal angle (Figure 4.2, Figure 4.3).

The spatial alongshore sediment transport can be seen in Table 4.2. For the conversion from erosion volume rate to coastal retreat rate and vice versa, the active profile height of each profile is used which is estimated by using the observations of the JarKus dataset. For each location, the active height is defined by the depth of closure and an upper limit which here is chosen as the point until which it is observed changes of the dune profile during the years. The level of the dune crest identified and used for each coastal profile can be found in Appendix C.
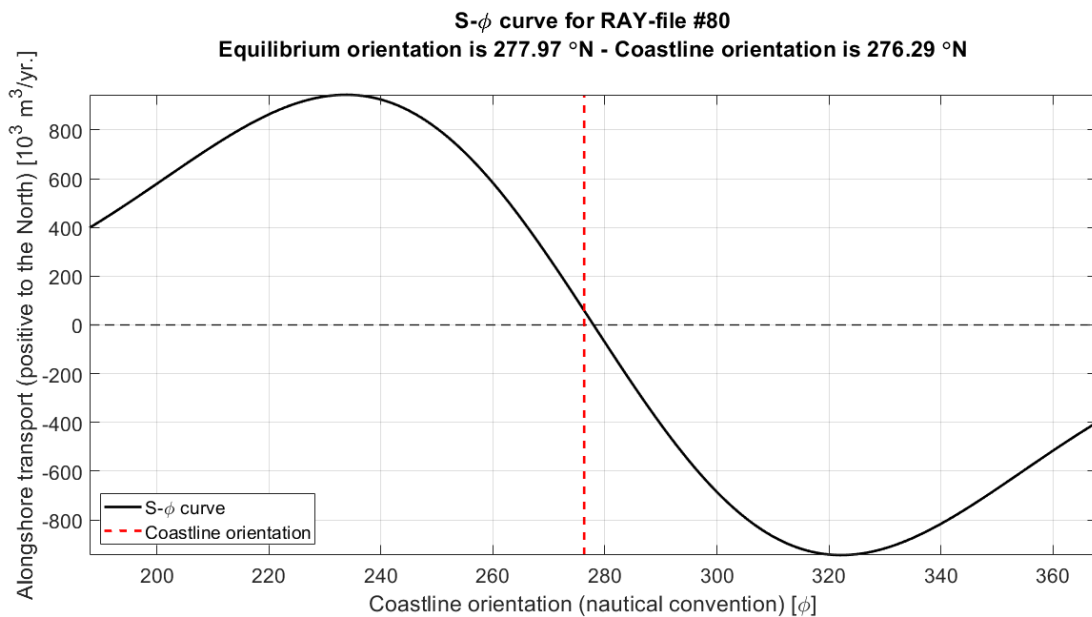
Figure 4.2: S-φ curve for RAY 80
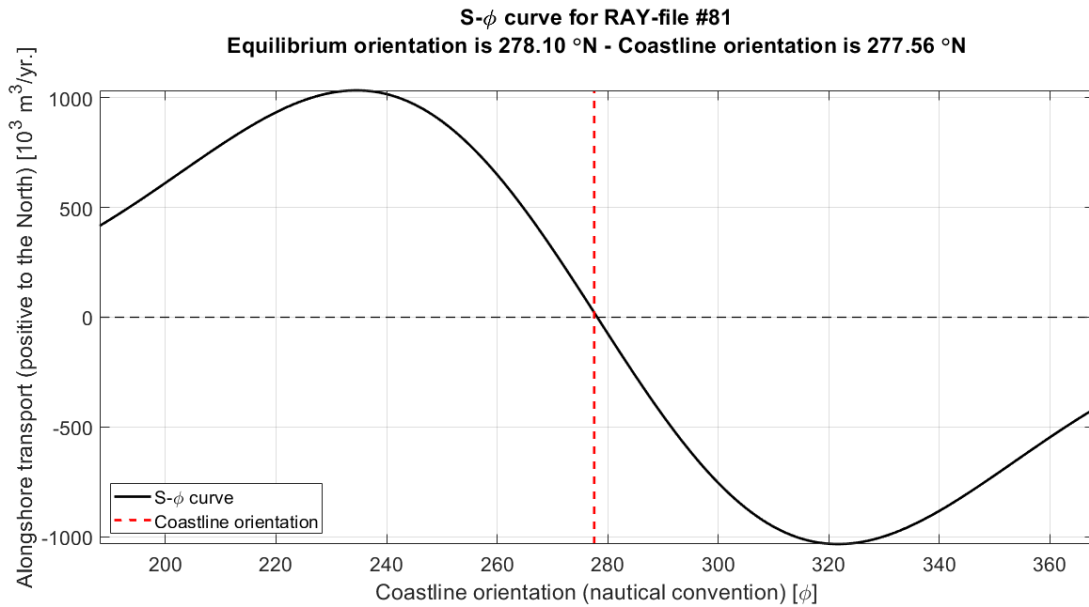
Figure 4.3: S-φ curve for RAY 81

Table 4.2: Alongshore sediment transport rates along the Holland coast; the negative values indicate an erosive process whereas the positive an accretive

Profile	LSTR [m/yr]	LSTR [m³/m /yr]
1	0.15	3.99
2	2.63	66.29
3	-0.16	-4.88
4	-0.31	-7.27
5	0.03	0.62
6	1.24	43.713
7	1.88	66.0
8	0.01	0.46
9	1.22	36.79
10	-11.34	-306.22
11	-0.58	-18.39

The longshore sediment transport rate is used for the calibration of the RR in cross-shore direction when following Approach 3.

Recovery rate

In section 3.5 three approaches for calibrating the recovery rate were presented. First, the RR is calibrated in the three ways and then the PCR is implemented for a period of 80 years (without including SLR) (Figure 4.4). The values of the RR for the eleven profiles following the three approaches can be seen in Table 4.3 and the relative change among the approaches in Table 4.4.

Results   41
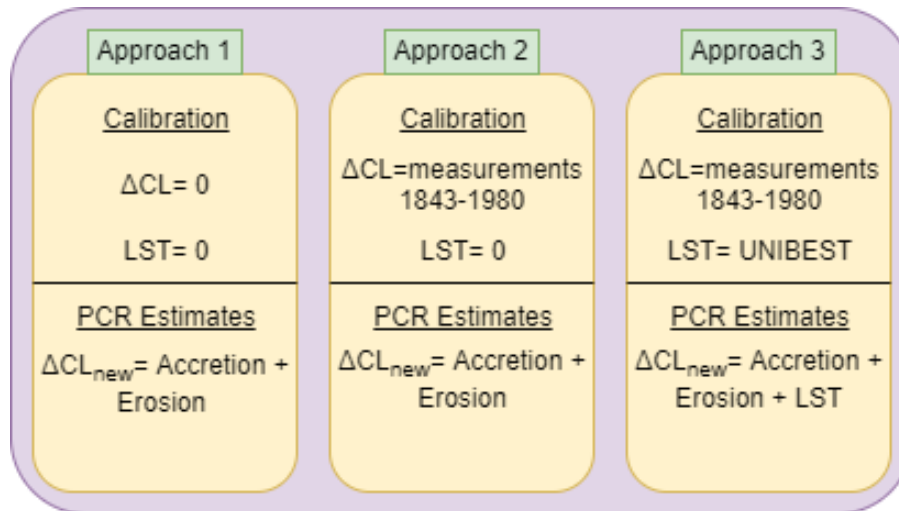
Figure 4.4: Three approaches of calibrating the recovery rate

Table 4.3: Recovery rate along the Holland coast

Profile	Approach 1 (m/yr)	Approach 1 (m³/m/yr)	Approach 2 (m/yr)	Approach 2 (m³/m/yr)	Approach 3 (m/yr)	Approach 3 (m³/m/yr)
1	37.0	*960*	37.7	*978*	37.5	*974*
2	42.9	*1082*	42.3	*1069*	39.6	*999*
3	26.8	*845*	27.3	*859*	27.4	*864*
4	60.2	*1400*	60.2	*1400*	60.5	*1408*
5	24.1	*803*	24.4	*816*	24.4	*815*
6	21.8	*768*	22.4	*791*	21.1	*746*
7	22.8	*799*	22.7	*795*	20.7	*725*
8	19.7	*721*	19.9	*727*	19.9	*726*
9	33.6	*1009*	32.8	*985*	31.5	*946*
10	38.9	*1050*	38.0	*1027*	49.9	*1348*
11	21.0	*662*	20.0	*632*	20.6	*651*

Table 4.4: Relative change in RR

Profile	Approach 1-Approach 2 Relative change [%]	Approach 1-Approach 3 Relative change [%]	Approach 2-Approach 3 Relative change [%]
1	1.8	1.4	-0.4
2	-1.3	-7.7	-6.5
3	1.8	2.3	0.5
4	0	0.5	0.5
5	1.5	1.5	-0.1
6	3.0	-3.0	-5.9
7	-0.5	-9.3	-8.8
8	0.7	0.7	-0.1
9	-2.4	-6.2	-3.9
10	-2.3	-28.3	31.3
11	-4.5	-1.7	2.9

It is noticed that for the profiles where the longshore sediment transport rate is high (profiles: 2, 6, 7, 9 and 10), this process is also reflected on the RR, leading to **relative differences in the calibration of RR that range from 3 % to 31 %.** The relative difference between Approach 1 and Approach 3 in terms of coastal retreat is estimated for the profiles showing an erosive trend in the past observations (2, 7, 9, 10 and 11). Table 4.5 shows the relative difference between the two approaches. It should be noted that since the longshore sediment transport was assumed a constant value therefore the recession of Approach 2 and 3 are the same because the effect of the LST is covered by the calibration process of the RR. The difference in the two ways can only be seen in the values of the RR and their relative change.

Table 4.5: PCR implementation for 80 years for the Approach 1 and Approach 3; Relative difference in coastal retreat (using p50 % values)

Coastal profile	Recession [m] Approach 1	Recession [m] Approach 3	Relative change [%] (Approach 3-Approach 1)
2	13.3	53.8	306
7	7	17.2	146
9	10.4	71.2	587
10	12.4	78.5	535
11	6.9	80	1055

According to the findings, without the expansion of the LST and the use of the coastline change rate as an indicator for tuning accordingly the RR (Approach 1), the RR is being overestimated and therefore the estimated retreats of the updated model (Approach 3) show a **relative increase in coastal recession ranging from 146 % to 1055 %** (the retreat values correspond to p50 % values). Figure 4.5 and Figure 4.6 show the results of the implementation of the PCR model for a period of 80 years (without SLR) for the three different concepts of calibrating the recovery rate for profile 9. The results of the rest profiles can be found in Appendix C.

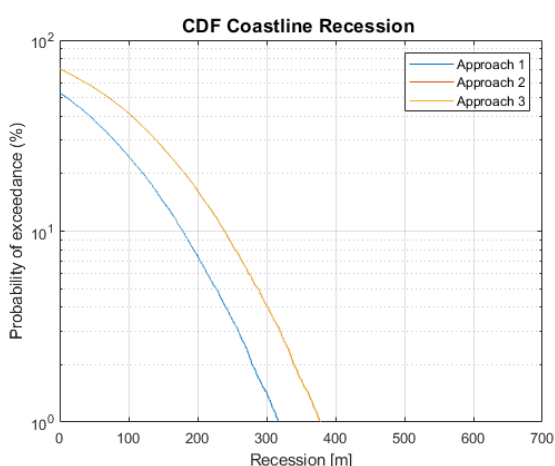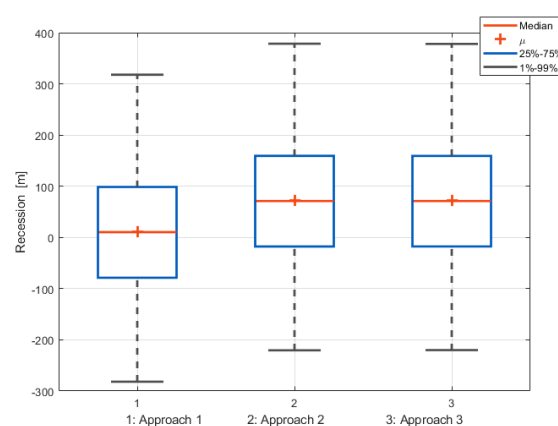*Figure 4.5: Comparison among the three RR approaches*

Figure 4.6: Recession range for the profile 9, for the three RR

It is evident that the extension of the longshore sediment transport affects the PCR model. However, for the profiles where both the longshore sediment transport and the erosion/accretion coastline rate are in line and comparable, the omittance of this extension in the calibration of the

RR wouldn't affect much the model because in this case the LST is the major factor for the coastal erosion and it is reflected directly in the ΔCL_rate.

It can be concluded that following Approach 2, the RR works as a good estimator for coastal retreat because it includes the LST into the historic measurements. However, the expansion of the PCR framework (Approach 3) in this study is significant because the approach followed allows investigating the ability of the model for future coastal retreat estimates when a construction of a hard defence structure or a port may change abruptly the longshore sediment transport.

In order to get a better feeling of the contribution of the LST expansion to the PCR model, the updated model (Approach 3) is tested for a period of 80 years (without SLR) for the case that the LST is equal to zero (Figure 4.7). In Table 4.6 can be seen the results raised for these two different concepts (using the p50 values). It is seen that the LST accounts for a range of 1 m-907 m along the Holland coast. The range of the **relative difference** between the two cases **fluctuates from 7 % to 1149 %**. As expected, the biggest differences are detected to the profiles where the LST is high.
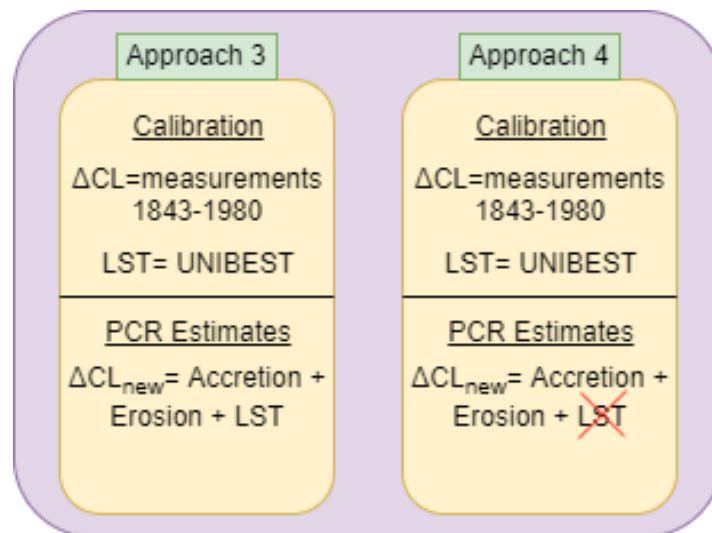

Figure 4.7: Test contribution of LST

Table 4.6: PCR implementation for 80 years for the Approach 3 and Approach 4; Relative change in coastal retreat and erosion volume (using p50 % values)

Profile	Approach 3 Retreat [m]	Approach 4 Retreat [m]	Retreat Difference [m]	Erosion Difference [m³/m]	Factor change [-]	Approach 3- Approach 4 Relative change [%]
1	-40	-28	-12	-312	0.7	-30
2	54	263	-210	-5303	4.9	-388
3	-27	-39	13	410	1.4	47
4	17	-9	26	582	0.5	135
5	-22	-20	-2	-67	0.9	-7
6	-43	56	-99	-3497	1.3	-230
7	17	167	-150	-5253	9.8	-874
8	-6	-5	-1	-37	0.8	-18
9	71	169	98	2944	2.4	137
10	79	-823	907	24484	10	1149
11	80	34	46	1453	0.4	58

In this work, a constant value of the LST was used, however, a temporal expansion of the longshore sediment transport component would give extra value to PCR model. The cumulative erosion or the accretion to the coast induces changes in the coastal orientation and thus changes to the longshore sediment transport, and this is something that still needs to be explored and incorporated into the model.

Furthermore, since the DUNERULE formula is adjusted in a specific coastal profile of the Holland coast, following the same approach for all the profiles (i.e. adjusting the DUNERULE formula for each profile) would lead to a more representative insight of the recovery rates along the coast and would make the model more robust.

4.2   PCR implementation for the SLR scenarios

For every selected coastal profile (Figure 4.1) the methodology explained in chapter 3 was implemented and PCR simulations were carried out for each profile. The duration of the synthetic time series was 81 years (2020-2100) and for every simulation, the location of coastline on the first day of each calendar year was recorded (Figure 4.8). Hence, a construction of an empirical distribution of coastline recession for every future year was recorded. Another record was also constructed, this time using the most landward position of the coastline for every future year.
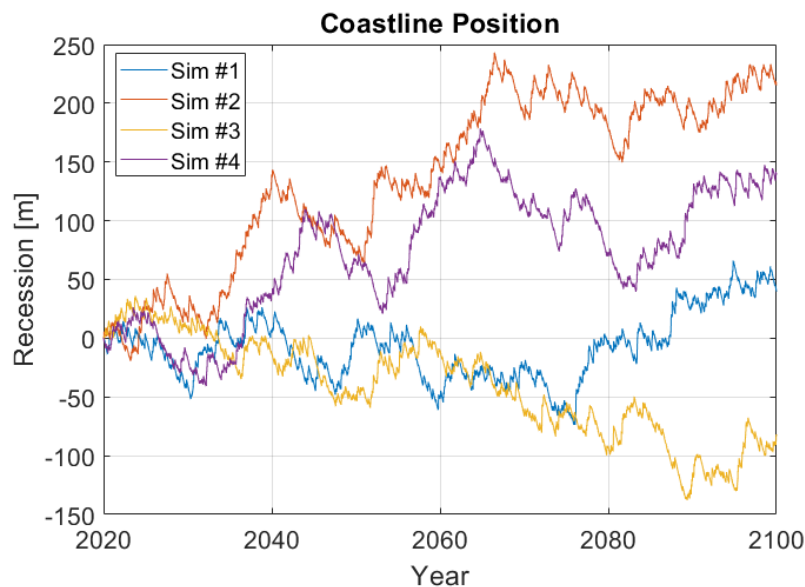

Figure 4.8: Time-series of coastline position

20,000 simulations of 81 years (2020-2100) were conducted for eleven profiles along the Holland coast, for each considered scenario of SLR (RCP4.5, RCP8.5 and Deltascenario). In this work, RCP4.5 was used as a low SLR scenario, RCP8.5 as a medium to high SLR scenario and Deltascenario as a high SLR scenario. Exceedance probability curves of coastal recession were constructed for all the years and the years 2040, 2070 and 2100 were chosen for presenting the results.

For illustration purposes, the results of the erosive profile 9 at North Bergen *(JarKus 7003100)* were selected for presentation. In Appendix D can be found the results of the rest profiles.

Figure 4.9 shows the exceedance probability curves of coastal recession for the profile 9 in Bergen, for the years 2040, 2070 and 2100 under three SLR scenarios and one scenario without SLR; the red dot acts as verification point for the assumption that in case there is no SLR, there is a 50 % probability that the coastline would retreat by (ΔCL_rate x 81 years) by 2100. Table 4.7

presents the values of coastal retreat for the different exceedance probabilities (p50 %, p10 % and p1 %) the years 2040, 2070 and 2100. It should be noted that the recessions are relative to the coastline position in the beginning of the simulated period, at 1-1-2020.
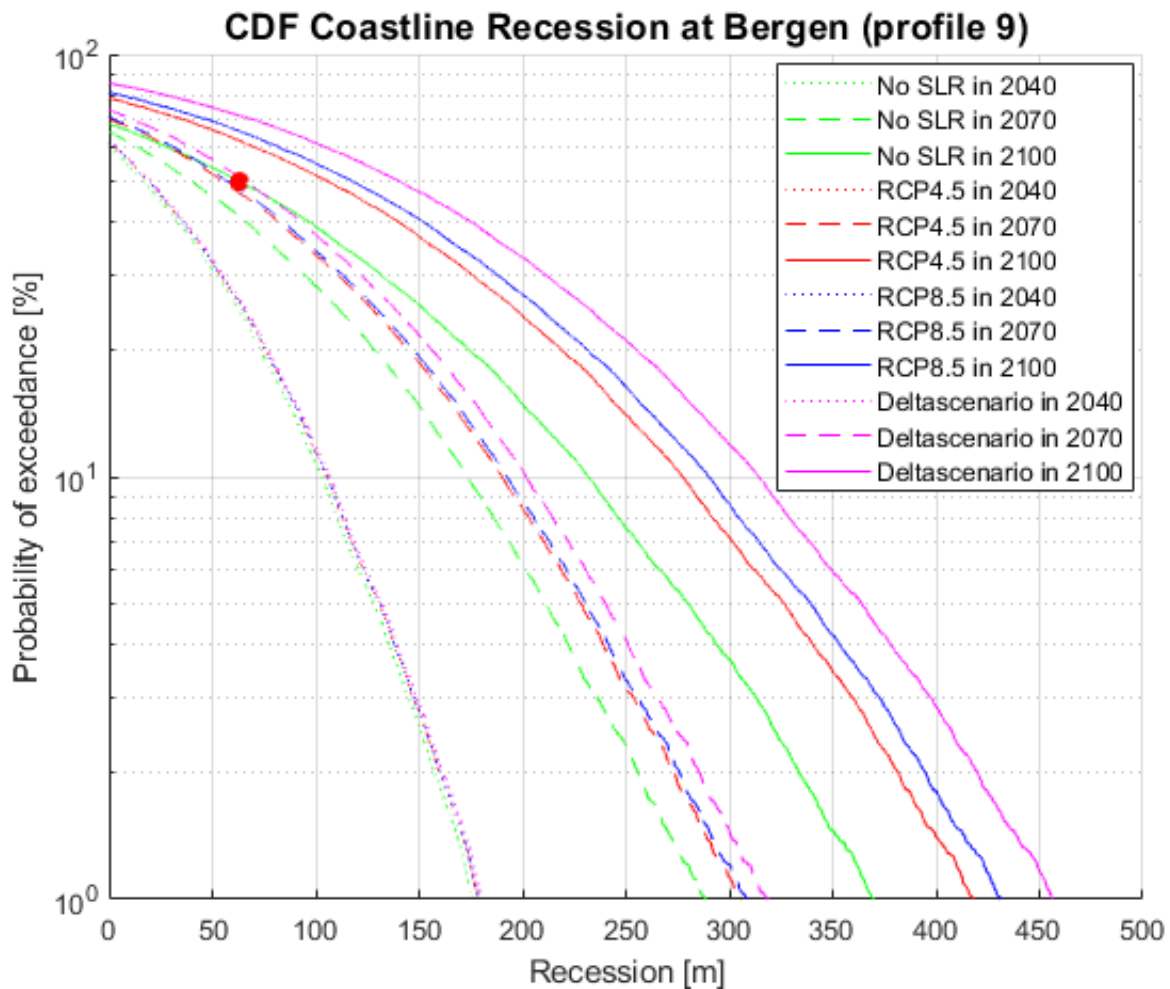

Figure 4.9: Exceedance probability curves of coastal recession for profile 9 in Bergen for different years, for several SLR scenarios; for every simulation, the location of the coastline on the first day of each calendar year was used

The probability of exceedance that someone reads from the graph above is the probability of the coastline being landwards from the initial position (i.e. coastline location in 2020). For example, in Table 4.7 can be seen that for the Deltascenario the probability of the coastline retreating more than 141 m in 2100 (relative to 2020) is 50 %. It appears that in the first years of the simulations the differences between sea level rise scenarios are very low. However, the more we are getting into the future, the differences are getting more clear.

Table 4.7: Coastal recession values in [m] associated with different exceedance probabilities of the three SLR scenarios, for several years (relative to 2020); the colours depict the SLR scenarios and are related to the legend of Figure 4.9

Prob. of exceed.	Year								
	2040			2070			2100		
P50%	19	19	20	55	58	66	106	118	141
P10%	106	106	109	190	193	202	278	290	314
P1%	179	179	180	307	309	319	418	431	456

At Table 4.8 is presented the results of another record of empirical distributions of coastline recession; this time using **the most landward position** of the coastline for every future year.

Following the same line of the most landward position, Figure 4.10 presents the results in a form that is useful and comprehensible for the public and decision makers, by showing the annual probability of coastal recession reaching a fixed value (140, 200 m and 300 m).

Table 4.8: Most landward coastal recession values in [m] associated with different exceedance probabilities of the three SLR scenarios, for several years (relative to 2020); the colours depict the SLR scenarios and are related to the legend of Figure 4.9

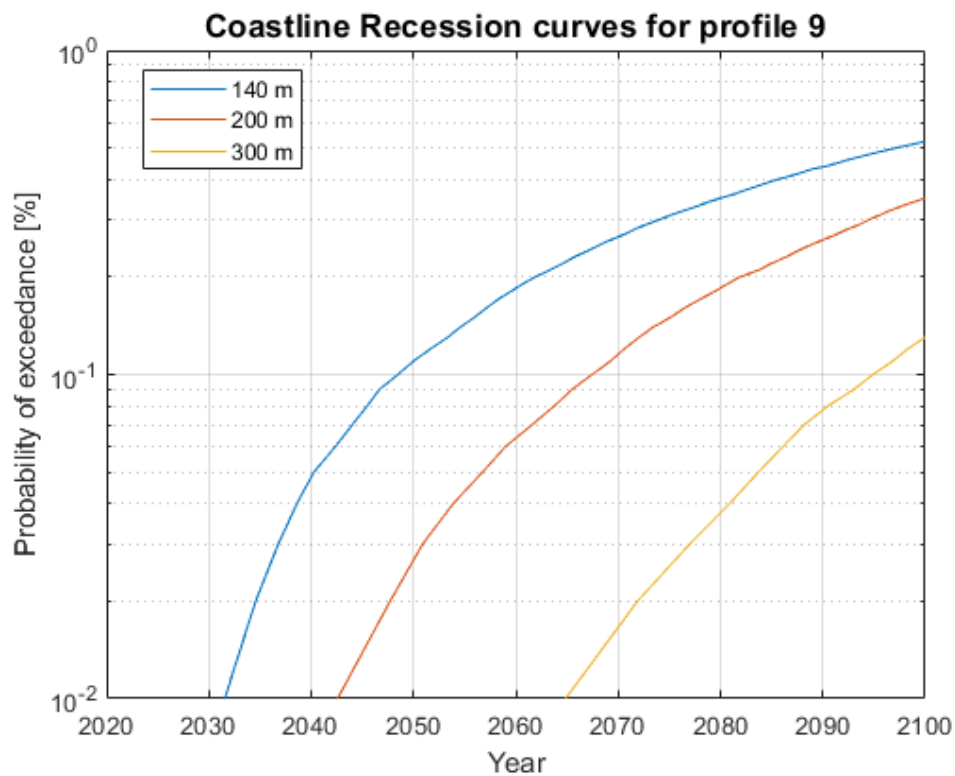| Prob. of exceed.	Year								
	2040			2070			2100		
P50%	27	27	28	62	65	73	114	125	148
P10%	112	112	114	197	200	209	284	297	320
P1%	185	185	187	314	317	327	425	439	465

Figure 4.10: Annual probability of coastal recession at Bergen reaching fixed location at 140 m, 200 m and 300 m (Deltascenario)

However, the beach width at Bergen is approximately 140 m, therefore any erosion after this point has not a physical meaning. This can be seen in Figure 4.11 where it is pointed out that no recession higher than the beach width should be considered (shaded area). Also, Figure 4.12 presents the annual probability of exceedance of the available beach width (140 m) for the several SLR scenarios.
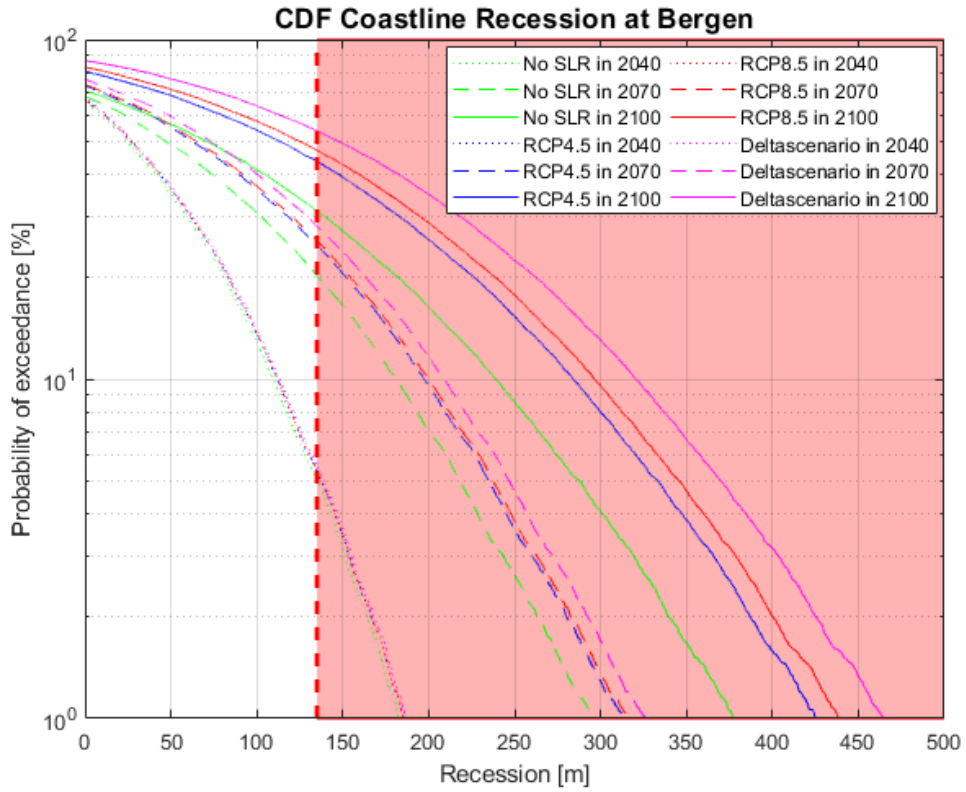
Figure 4.11: CDF record of the most landward position during the future years, for three SLR scenarios; recessions higher than the beach width are denoted in the graph with shading

Table 4.9: Probability of exceedance (from the CDF of the most landward retreat), for several fixed recessions, for the years 2040, 2070 and 2100 under the Deltascenario

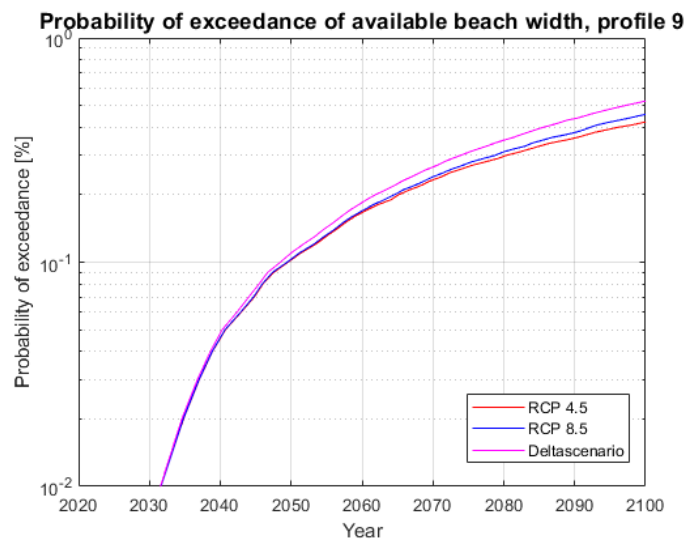| Recession/ Year	2040	2070	2100
0	67 %	76 %	87 %
50	37 %	59 %	77 %
140	5 %	27 %	52 %
200	0.6 %	12 %	35 %
400		0.1 %	3 %

Figure 4.12: Annual exceedance probability of available beach width for the several SLR scenarios

Table 4.10 presents the results from PCR model of the coastal retreat and coastal erosion for the profile 9, for different years and SLR scenarios. The results for the other profiles can be found in Appendix D.

Table 4.10: Coastal retreat of profile 9, for the year 2040, 2070 and 2100

Profile 9 Recession [m]	Year		
Prob. of exceedance	2040	2070	2100
No SLR			
P50%	25	47	71
P10%	110	181	239
P1%	183	297	378
RCP4.5			
P50%	27	62	114
P10%	112	197	284
P1%	185	314	425
RCP8.5			
P50%	27	65	125
P10%	112	200	297
P1%	186	317	439
Deltascenario			
P50%	28	73	148
P10%	113	209	320
P1%	187	327	465

Table 4.11: Coastal erosion of profile 9, for the year 2040, 2070 and 2100

Profile 9 Erosion volume [m³]	Year		
Prob. of exceedance	2040	2070	2100
No SLR			
P50%	742	1421	2140
P10%	3292	5438	7181
P1%	5490	8915	11355
RCP4.5			
P50%	803	1881	3419
P10%	3363	5928	8541
P1%	5571	9444	12766
RCP8.5			
P50%	808	1949	3770
P10%	3369	6002	8911
P1%	5577	9522	13192
Deltascenario			
P50%	841	2202	4452
P10%	3406	6274	9626
P1%	5618	9814	13967

For this profile, the **relative increase** of Deltascenario compared to the concept that there is no SLR is approximately 108 % more (for the probability of exceedance of 50 %) or 34 % and 23 % for p10 % and p1 % respectively. The range of the retreat for the rest of the profiles can be seen in the next figures, for the different years and the several SLR scenarios (see Figure 4.13, Fig D.1).
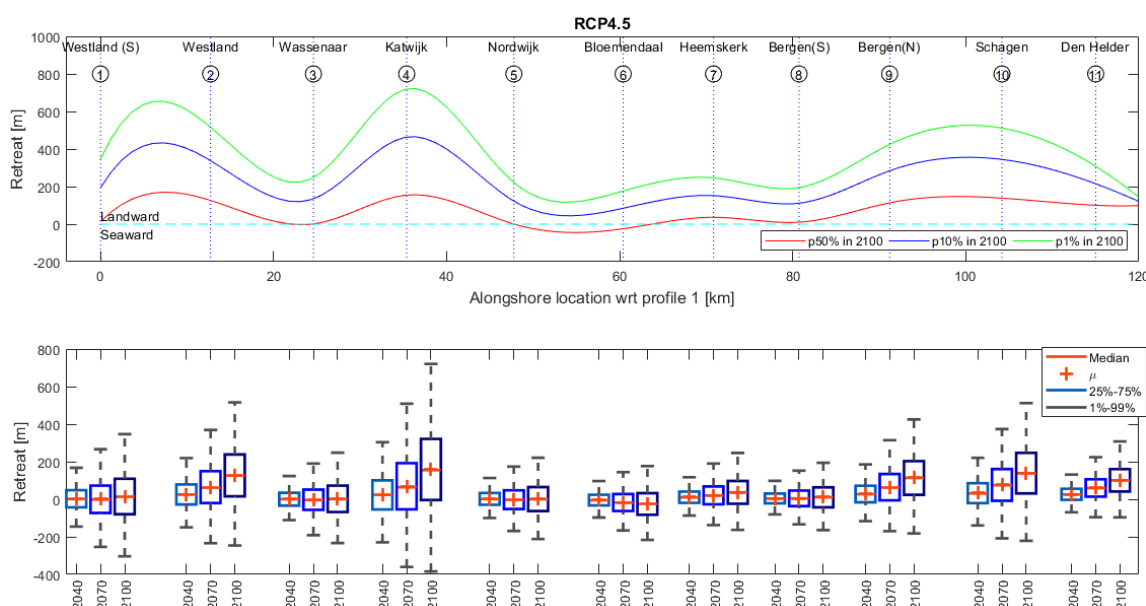

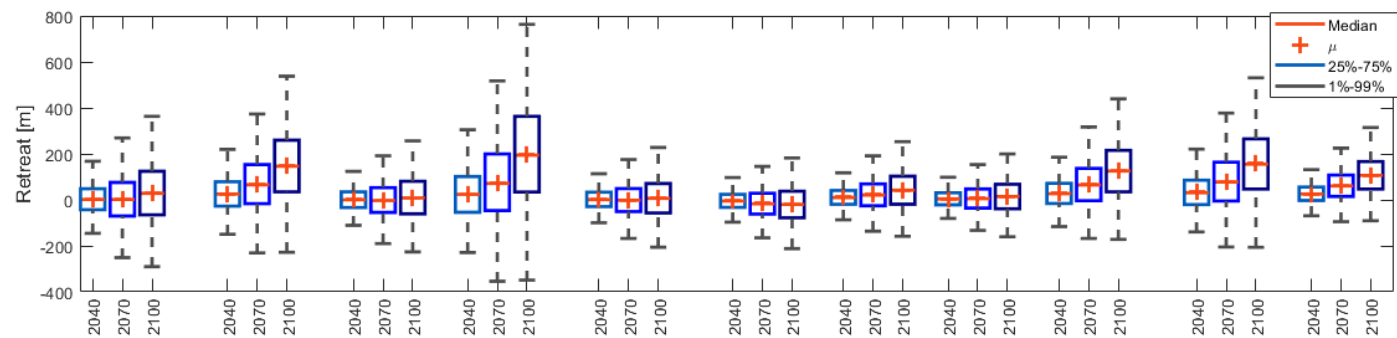*Figure 4.13: Coastal retreat along the Holland coast for the RCP4.5 scenario*
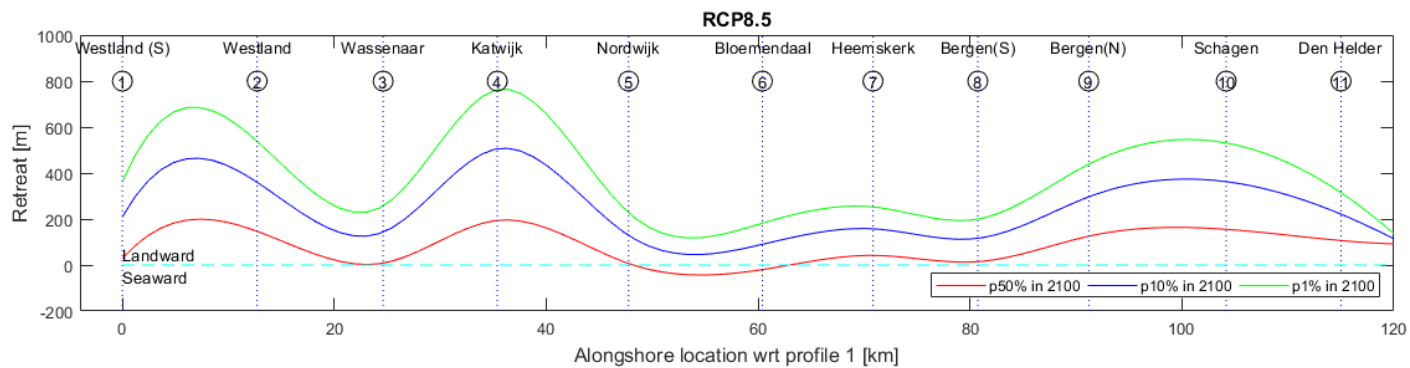
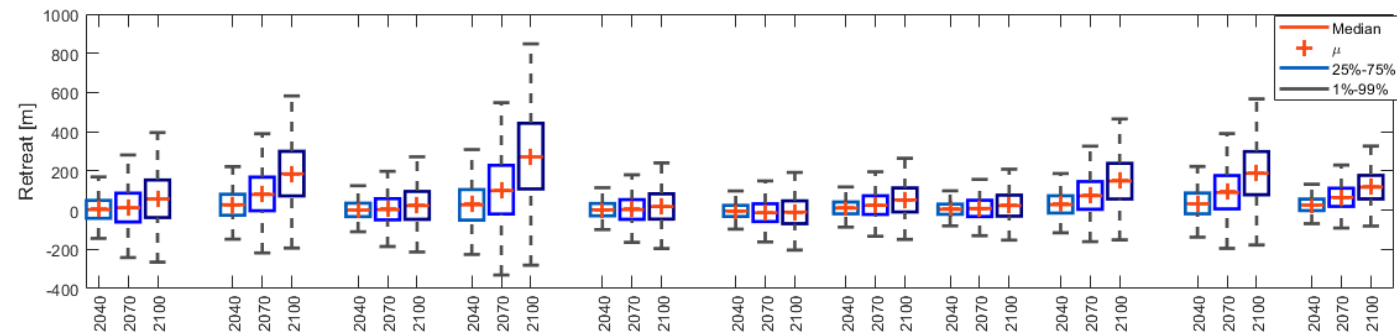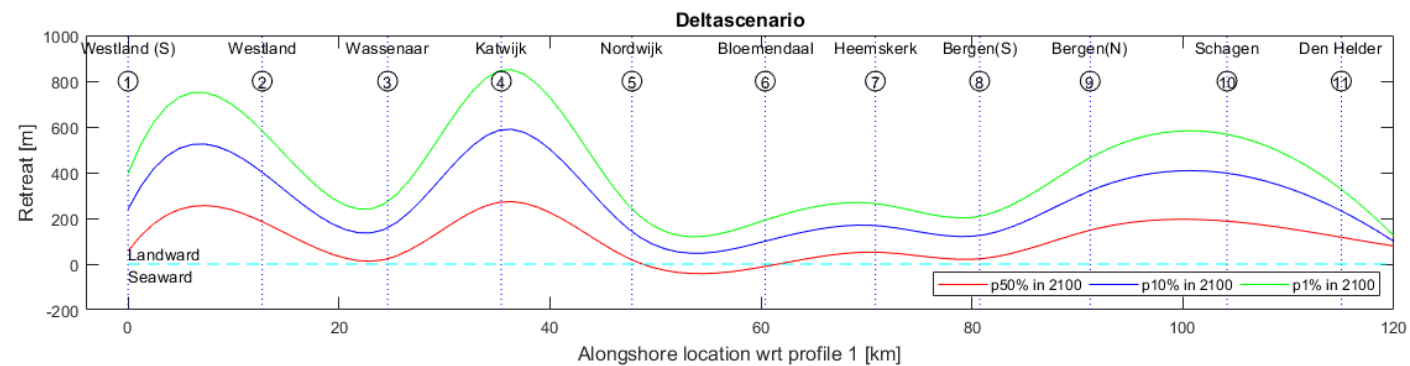*Figure 4.14: Coastal retreat along the Holland coast for the RCP8.5 scenario*

Figure 4.15: Coastal retreat along the Holland coast for the Deltascenario

The ranges of the expected retreats in 2100 (relative to 2020) for the different SLR scenarios are: 0.5 m-155 m (for RCP4.5), 6 m-194 m (for RCP8.5) and 18 m-172 m (for Deltascenario), for the p50 % values of the cdf of the coastline retreat. The average values of the coastal retreat for 2100 are 61 m, 73 m and 97 m for RCP4.5, RCP 8.5, and Deltascenario respectively. The relevant average volume losses by 2100 are 1664 m³/m, 2005 m³/m and 2665 m³/m.

If the Holland coast is divided into 11 areas/cells, each one being represented by the results raised from the coastal profiles located there (Figure 4.16), then the relative increase in volume losses due to SLR is shown in Table 4.12.

Figure 4.16: Holland coast divided into 11 areas

Table 4.12: Relative increase in nourishment schemes for 2100 (relative to 2020), using p50% values of the most landward position record

Cell	SLR scenario	Retreat [m]	Relative increase [%] Compared to No_SLR
Cell 1	No SLR	-40	
	RCP4.5	14	134
	RCP8.5	28	170
	Deltascenario	57	242
Cell 2	No SLR	54	
	RCP4.5	126	135
	RCP8.5	146	172
	Deltascenario	185	244
Cell 3	No SLR	-27	
	RCP4.5	1	103

	RCP8.5	8	131
	Deltascenario	23	186
Cell 4	No SLR	16	
	RCP4.5	155	854
	RCP8.5	194	1097
	Deltascenario	272	1573
Cell 5	No SLR	-22	
	RCP4.5	0.3	102
	RCP8.5	6	130
	Deltascenario	18	184
Cell 6	No SLR	-43	
	RCP4.5	-25	42
	RCP8.5	-20	54
	Deltascenario	-10	76
Cell 7	No SLR	17	
	RCP4.5	37	113
	RCP8.5	42	144
	Deltascenario	52	204
Cell 8	No SLR	-6	
	RCP4.5	10	282
	RCP8.5	15	358
	Deltascenario	23	503
Cell 9	No SLR	71	
	RCP4.5	114	60
	RCP8.5	125	76
	Deltascenario	148	108
Cell 10	No SLR	79	
	RCP4.5	138	76
	RCP8.5	155	98
	Deltascenario	188	139
Cell 11	No SLR	80	
	RCP4.5	101	26
	RCP8.5	106	33
	Deltascenario	117	46

It is estimated that the relative increase in current nourishments that is required in order to maintain the 'hold-the-line' policy is ranging from 26 % to 1573% depending on the SLR scenario. According to the findings of the erosive profiles 2, 4, 7, 9, 10 and 11, in 2100, the relative increase in volume loss along the Holland coast is expected to be 95 %, 121 % and 173 % respectively for RCP4.5, RCP8.5 and Deltascenario (Table 4.13).

Table 4.13: Calculation of volume loss per year for the erosive cells 2,4,7,9,10 and 11

Volume loss [M m³/yr]			
No SLR	**RCP4.5**	**RCP8.5**	**Deltascenario**
1.4	2.6	3.0	3.7

4.3   Comparison PCR model to Bruun Rule

In this section the results obtained using the Bruun rule formula were compared to those raised using the PCR model. The Bruun rule has been implemented for the eleven locations along the Holland coast for the three SLR scenarios: RCP4.5, RCP 8.5, and Deltascenario. The retreats found using the Bruun rule formula (Table 4.14) were associated to the probabilities of exceedance obtained from the CDF curves of the PCR model so a conclusion about the comparison between the two models can be drawn.

Table 4.14: Coastal recessions estimated using the Bruun rule for three SLR scenarios, for the years 2040, 2070 and 2100 (relative to 2020), for profile 9

SLR scenario	RCP4.5		
Year	2040	2070	2100
Recession [m]	9	26	45
SLR scenario	RCP8.5		
Year	2040	2070	2100
Recession [m]	10	32	66
SLR scenario	Deltascenario		
Year	2040	2070	2100
Recession [m]	15	47	83

Table 4.15: Association of Bruun rule estimates to probabilities of exceedance of PCR model (most landward cdf curves), for RCP4.5, RCP8.5 and Deltascenario, for profile 9

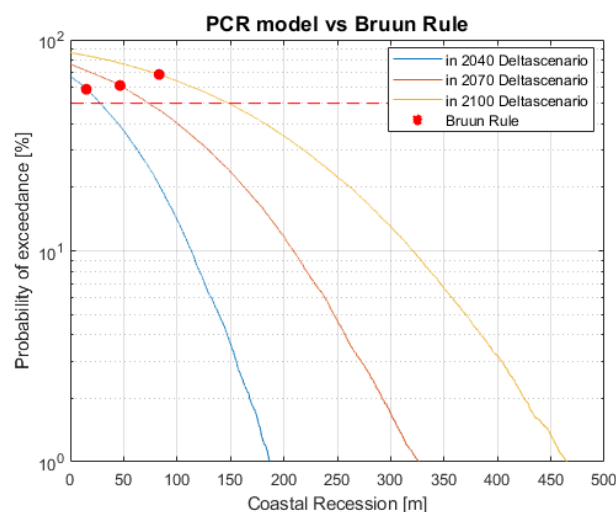| Year	2040	2070	2100
RCP4.5	61 %	64 %	70 %
RCP8.5	60 %	63 %	67 %
Deltascenario	58 %	61 %	68 %

Figure 4.17: PCR vs Bruun rule for Deltascenario, for profile 9

Table 4.16: Bruun rule estimates of coastal retreat for 2100 (relevant to 2020) for the three SLR scenarios

Profile	Retreat [m]		
	RCP4.5	RCP8.5	Delta-scenario
1	48	70	89
2	47	69	87
3	49	71	91
4	56	81	103
5	37	54	68
6	45	66	84
7	51	75	95
8	28	40	51
9	45	66	83
10	45	65	82
11	16	23	30

Table 4.17: Associated exceedance probabilities for 2100 (relevant to 2020) for the three SLR scenarios

Profile	Associated exceedance Probabilities [%]		
	RCP4.5	RCP8.5	Delta-scenario
1	40.2	38.4	41.24
2	68.4	68.0	72.19
3	32.7	28.1	26.76
4	66.2	68.4	75.8
5	35.2	31.1	30.3
6	20.5	15.7	13.7
7	43.7	35.8	32.0
8	41.4	37.2	36.0
9	69.7	67.2	68.5
10	72.3	71.4	74.2
11	83.4	82.9	83.9

From the Table 4.17, it can be concluded that most of the profiles showing an erosive trend in the past (ΔCL<0), raised slightly more conservative results when implementing the PCR model rather than when applying the Bruun rule method. The opposite applies for the accretive profiles.

- For the erosive profiles [2,4,7,9,10,11]:
  - The estimated coastal recession for 2100 (relevant to 2020) ranges from 16 m to 95 m with an average of 41 m, 59 m and 75 m for the RCP4.5, RCP8.5 and Deltascenario.
  - The associated exceedance probabilities of PCR model ranges from 32 % to 84 %, with an average of 67 %, 65 % and 66 % for the RCP4.5, RCP8.5 and Deltascenario respectively for 2100 (relevant to 2020).
  - Comparing with the Bruun rule results, it is seen that the PCR model is getting more conservative over time (the associated exceedance probabilities are increasing over time).
  - The differences between the several SLR scenarios are more clear for the Bruun rule. For the PCR model the ranges of relative increase of Deltascenario compared to RCP4.5 fluctuate from 16 %-47 % and for RCP8.5 - Deltascenario from 10 %-26.5 %. In Bruun rule formula the relative increase is more (84 % and 27 % respectively).

- For the accretive profiles [1,3,5,6,8]:
  - The range of the coastal recession is from 28 m to 103 m, with an average of 44 m, 64 m and 81 m for the RCP4.5, RCP8.5 and Deltascenario respectively for 2100 (relative to 2020).
  - The associated exceedance probabilities of PCR model ranges from 14 % to 76 %, with an average of 39 %, 36 % and 37 % for the RCP4.5, RCP8.5 and Deltascenario respectively for 2100 (relevant to 2020).
  - Comparing with the results of the PCR model, it is seen that the Bruun rule is getting more conservative over time (the associated exceedance probabilities of PCR are getting smaller over time).

o   The differences between the several SLR scenarios are more clear for the PCR model. For the PCR model the ranges of relative increase for RCP4.5 – Deltascenario fluctuate from 75 %-5135 % and for RCP8.5-Deltascenario from 40 %-181 %. In Bruun rule formula the relative increase is less (84 % and 27 % respectively).
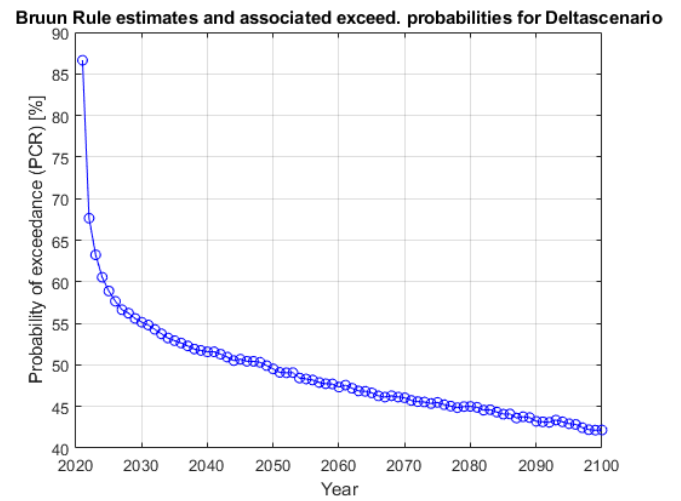
It is also observed a temporal evolution between the Bruun rule estimates and the associated probabilities of exceedance of PCR, with the estimates of Bruun rule getting more conservative as more into the future is applied for the accretive profiles. As expected, for the erosive profiles the Bruun rule method is getting less conservative over time.
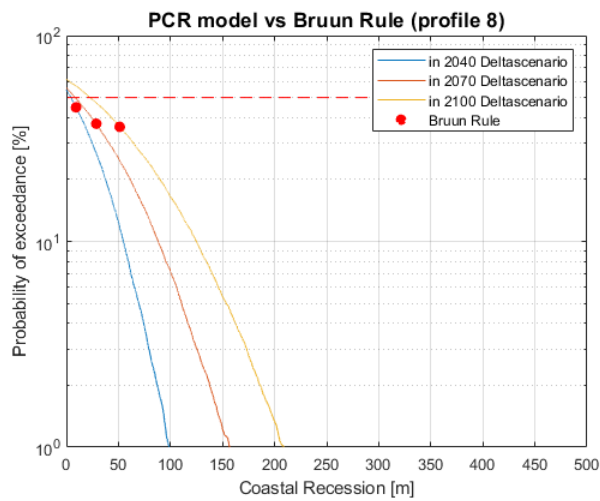
Figure 4.18: PCR vs Bruun rule for Deltascenario, for profile 8

Figure 4.19: Temporal evolution between the Bruun rule estimates and the associated probabilities of exceedance of PCR

5 Discussion

This chapter includes a discussion over the results of the previous chapter. It presents the assumptions and limitations of this study and it suggests any further research.

Improvements, application opportunities and further research

The methods followed in this study allow the PCR model to explore locations where the longshore sediment transport is not negligible. It is estimated that the contribution of the LST expansion is important for the Holland coast, reaching a relative change in the results of the order of 388 % to 1150 % -if omitted.

In this work, a constant value of the LST was used. However, the approach followed allows investigating the ability of the model for future coastal retreat estimates when a construction of a hard defence structure or a port may change abruptly the longshore sediment transport.

This study can be a valuable assistance in the course of further improving the model. A temporal expansion of the longshore sediment transport component would give extra value to the PCR model. The cumulative erosion or the accretion to the coast induces changes in the coastal orientation and thus changes to the longshore sediment transport, and this is something that still needs to be explored and incorporated into the model. In addition, nourishment adaptation schemes should be included into the PCR framework in the scope of a safer coastal management. Moreover, maps of economical setback lines can be defined using the output of the upgraded PCR model (see Dastgheib et al., 2018).

Moreover, in this study the adjusted PCR model has been implemented for eleven locations along the Holland coast using the wave climate existing at each site. It is suggested to implement the PCR model with wave data from other locations for each profile and investigate the sensitivity of the model to wave climate.

Assumption and limitations

The choice of the period (years in past) based on which the coastline change rate is calculated is an important parameter in this thesis. For some profiles the nourishments schemes have been implemented before the 'hold-the-line' policy (in 1990) thus this choice is different for every profile (see Appendix C- years of observations). This parameter is important for the calibration of the recovery rate and thus for the future estimates of the coastline retreat. It defines the trend of the coastline profile and this choice was a bit tricky almost for all coastal profiles. A slightly different choice would have led to different coastline change rate, different recovery rate and finally different future coastline estimates. Since the results of this work do not reflect the approximate 12 M m^3 of nourishment schemes needed in the Dutch coast every year, it is recommended from the reader interested in the results of this thesis to reconsider another option for the choice made about the years.

Another parameter that raises uncertainties is the choice of the dune crest level as an upper limit. As mentioned before a different choice of this parameter may yield different results. It is observed that the profiles having a smaller height of active profile, showed higher coastal retreat values. Thus, it is recommended to make some sensitivity analysis to check the range of uncertainty induced with this choice.

One main assumption of this work is that the cross-shore profile maintains its shape and only moves forwards and backwards. However, a more complex cross-shore profile that includes the changes in the profile due to SLR and due to the storm impact or accounts for the presence of

multiple dunes, may describe better the physical processes and therefore be a better choice for the PCR framework.

Moreover, another assumption regards the way inducing the SLR into the PCR. It was hard to implement the DUNERULE formula because it requires water levels and when SLR is introduced into the formula the erosion starts to increase sharply. This is not realistic because the coastline is also reshaping itself according to SLR. The erosion model (adjusted DUNERULE formula) used in this thesis, is might not the best choice for the estimation of the coastal recession when SLR occurs. Usually the SLR is included to the model through the variable of water level when the generation of new storms is performed. Since for DUNERULE this option raised unrealistic results, the SLR has finally been incorporated into the PCR model at the conversion of the dry erosion volume to coastal retreat (Equation 3.8).

The adjusted DUNERULE formula was chosen among other options in order to compare the results of this study with Li's work. However, to be able to compare the results obtained by the previous case study in the Netherlands the same methodology should be applied. In the end, the estimates calculated in this work were not comparable to the ones estimated by Li due to the following main reasons:

- Li introduced a term named 'storm potential erosive capability'; a conditional statement was applied and depending on the state of the dune and the capability of the storm, the event either rejected or proceeded. Thus, the number of storm events and the RR were different.
- Another difference between the two studies is the LST assumption and the method for calibrating the natural RR without the nourishment interventions.
- The integration of the SLR into the PCR framework was accomplished with the use of XBeach, whereas in this study a different approach was followed.
- The approached followed for the storm definition and the storm data analysis were different.

6   Conclusions and Recommendations

Coastline recession caused by sea level rise poses a threat to coastal communities and exposes billions worth of infrastructure to inundation from rising seas and erosion. Making reliable and robust predictions of the future coastline recession is becoming necessary now more than ever. The Bruun rule has been widely used in the past but its implementation started fading due to the questioning legitimacy of the assumptions behind the method (Passeri et al., 2015). The need of coastal planning to integrate the range of uncertainties of wave climate and stochastic forcing into the coastal management framework, has led to the development of approaches that yield estimates of coastal recession in probabilistic terms. The Probabilistic Coastline Recession (PCR) model departs from the Bruun rule's deterministic nature and is suggested as an appropriate model for estimating coastal retreat due to SLR.

The objective of this research was to test the applicability of the Probabilistic Coastline Recession model developed by Ranasinghe et al. (2012) for the stretch of the Holland coast, for several SLR scenarios in order to further develop this model in being capable to generate stochastic projections of coastline changes and later explore the effectiveness of adaptation strategies. To meet this objective the following research questions were posed:

1. *What are the relevant physical processes for the long-term coastline evolution of the Holland coast and to what extent does the current PCR model includes them? Which methodologies can be applied to improve the PCR model for the Holland coast?*
2. *What is the predicted coastline recession and required nourishment volumes for different SLR scenarios using the (updated) PCR model?*
3. *How do the results obtained from the (updated) PCR model compare to the estimates of the Bruun rule?*

6.1   Conclusions

What are the relevant physical processes for the long-term coastline evolution of the Holland coast and to what extent does the current PCR model includes them? Which methodologies can be applied to improve the PCR model for the Holland coast?

In past, the PCR model was implemented in the Netherlands for a coastal profile at Noordwijk, with the following main assumptions: 1. the alongshore sediment transport is negligible for the specific profile, 2. the recovery rate is calibrated by assuming that in the absence of climate change the coastline would remain in the same position for the year 2100 with a probability of 50 %, (equal probability of recession or accretion).

A physical process for the long-term coastline evolution is the **alongshore sediment transport.** Literature review showed that the littoral drift is not a trivial process along the Holland coast, thus, in this study the LST should be incorporated into the PCR framework.

Another important physical process is the redistribution of the sediment in the cross-shore direction during the calm periods. This is reflected on the PCR framework through the recovery rate. However, **nourishments schemes** have been applied to the Holland coast on a regular basis since 1990. Therefore, the calibration of the natural **recovery rate in cross shore direction** - before the nourishment interventions – would complicate the implementation of PCR to this coast.

Moreover, low energy processes like the SLR is considered to result in long-term, gradual shoreline retreat. In this study, three SLR scenarios are considered for the PCR implementation to the Holland coast.

Finally, since the PCR was applied to one profile of the Holland coast, a spatial expansion to more profiles along the coast would provide a better insight of this complex and unique coast.

In this study, the following extensions have been added to the PCR:
- The longshore sediment transport extension
- The calibration of the recovery rate, in three stepwise approaches, using both observations of the coastline change in the past and the longshore sediment transport rate
- Spatial expansion

Based on these improvements, the following can be concluded:
Longshore sediment transport
Since the longshore drift is an important process along the Holland coast, this study contributed to the integration of the LST into the PCR framework. The longshore sediment transport rate has been calculated using data from look-up tables (S-φ curves) generated by a coastline model of the Holland coast in UNIBEST. The present study showed that the effects of LST is not negligible. For the cases where the LST has an accretive effect on the profile, the omittance of the LST in the calibration of the RR would cause an underestimation of the RR. The opposite applies when the LST has an erosive effect on the profile.

The addition of the LST into the calibration of the RR yields differences in the RR values. The relative change observed varies from 0.1 % to 31 %. The relative change in the estimates of coastal retreat for the profiles with high LST ranges from 146 % to 1055 %.

Moreover, the LST was assumed constant in this study. However, if the LST is included into the calibration of the RR but omitted from the future estimation procedure, then the estimates of coastal retreat along the Holland coast would be different by a factor ranging from 0.4 to 10.

Recovery rate
In this study three approaches were considered for the calibration of the RR. The first approach didn't include the LST and the coastline change rate (based on observations of Dutch Beach Lines between 1843 and 1980). The second approach included only the coastline change rate and the last approach included both coastline change rate and the LST. It can be concluded that following Approach 2, the RR works as a good estimator for coastal retreat because it includes the LST into the historic measurements. However, the expansion of the PCR framework (Approach 3) in this study is significant because the approach followed allows investigating the ability of the model for future coastal retreat estimates when a construction of a hard defence structure or a port may change abruptly the longshore sediment transport.

Spatial expansion
The adjusted PCR model has been implemented for eleven locations along the Holland coast using the wave climate existing at each site.

What is the predicted coastline recession and required nourishment volumes for different SLR scenarios using the (updated) PCR model?

The new PCR model has been implemented for eleven locations along the Holland coast. CDFs of estimated coastline retreat based on the most landward position of the coastline of every year have been generated for the years 2040, 2070 and 2100 for each location, for several SLR scenarios. The following results are retrieved:

- The PCR model has been implemented for three SLR scenarios: **RCP4.5**, **RCP8.5** and **Deltascenario** counting as low, moderate and high SLR scenario. It is shown that for all the SLR scenarios the effect of the sea level rise is not very noticeable in the first years, but it is getting more profound over time.
- The ranges of the expected retreats in 2100 (relative to 2020) for the different SLR scenarios are: 0.5 m-155 m (for RCP4.5), 6 m-194 m (for RCP8.5) and 18 m-272 m (for Deltascenario), corresponding to the 50 % exceedance probability values of the cdf of the coastline retreat. The average values of the coastal retreat for 2100 are 61 m, 73 m and 97 m for RCP4.5, RCP 8.5, and Deltascenario respectively. The relevant average volume losses by 2100 are 1664 m³/m, 2005 m³/m and 2665 m³/m.
- According to the findings, in 2100 the relative increase in volume loss along the Holland coast is expected to be 95 %, 121 % and 173 % more, for RCP4.5, RCP8.5 and Deltascenario respectively.

How do the results obtained from the (updated) PCR model compare to the estimates of the Bruun rule?

The Bruun rule has been implemented for the eleven locations along the Holland coast for three SLR scenarios: RCP4.5, RCP 8.5, and Deltascenario. The Bruun rule estimates were compared to the findings of the PCR model. The following can be concluded:

- According to the findings, the majority of the profiles showing an erosive trend in the past (before the 'hold-the-line' policy) raised slightly more conservative results when implementing the PCR model rather than when applying the Bruun rule method- especially under the Deltascenario. On the other hand, the Bruun rule method is more conservative than PCR model for most of the accretive profiles.
- For the erosive profiles:
  - The estimated coastal recession for 2100 (relevant to 2020) ranges from 16 m to 95 m with an average of 41 m, 59 m and 75 m for the RCP4.5, RCP8.5 and Deltascenario.
  - The associated exceedance probabilities of PCR model ranges from 32 % to 84 %, with an average of 67 %, 65 % and 66 % for the RCP4.5, RCP8.5 and Deltascenario respectively for 2100 (relevant to 2020).
  - Comparing with the Bruun rule results, it is seen that the PCR model is getting more conservative over time (the associated exceedance probabilities are increasing over time).
  - The differences among the SLR scenarios are more clear for the Bruun rule compared to PCR model.
- For the accretive profiles:
  - The range of the coastal recession is from 28 m to 103 m, with an average of 44 m, 64 m and 81 m for the RCP4.5, RCP8.5 and Deltascenario respectively for 2100 (relative to 2020).
  - The associated exceedance probabilities of PCR model ranges from 14 % to 76 %, with an average of 39 %, 36 % and 37 % for the RCP4.5, RCP8.5 and Deltascenario respectively for 2100 (relevant to 2020).
  - Comparing with the results of the PCR model, it is seen that the Bruun rule is getting more conservative over time (the associated exceedance probabilities of PCR are getting smaller over time).
  - The differences among the SLR scenarios are clearer for the PCR model compared to Bruun rule.

6.2 Recommendations

A set of recommendations for future research have been identified and presented below:

- In this work, a constant value of the longshore sediment transport was used. However, setting as a variable the longshore sediment transport would give extra value to PCR model. The cumulative erosion (or accretion) of the coast induces changes to the coastal orientation and thus changes to the longshore sediment transport. This is something that still needs to be explored and incorporated into the model. This temporal expansion of the PCR framework would be significant, especially for future estimations of the coastal recession after the construction of a hard defence structure or a port that will change abruptly the longshore sediment transport.

- The updated PCR model can be further adjusted to incorporate nourishment schemes. This nourishment-scheme expansion in combination with the temporal expansion of the recovery rate will greatly improve the model.

- The initial form of the erosion function (DUNERULE) used for the specific case study raised very high erosion results when the SLR was induced into the water level variable. So, the DUNERULE formula needed further adjustment in order to be able to incorporate the sea level increase into the PCR framework. Due to this adjustment, maybe the DUNERULE is not the best choice for the specific case and it is recommended to either use more complex models such XBeach (Roelvink et al. 2009) to compare and verify the findings of this research or to check the sensitivity into the water level increase of another simple empirical erosion model like DUROS+(Ruessink et al. 2012) and compare the results with those of this research.

- The DUNERULE formula used in this research is adjusted and calibrated according to a specific coastal profile of the Holland coast. In case the reader would like to use the findings of this work, it is recommended to calibrate the DUNERULE formula for every profile in the way Li did in his work (Li, 2014). This would let us gain further insight of the rates of the dune recovery process along the coast.

- In the Netherlands, JarKus dataset provides information of the coastal profiles in an annual base. It is suggested to apply the updated PCR model to regions where there are available post-storm data of the coastal profiles. Da Cruz (2018) indicates that performance of PCR is much better when the storms events are defined from high erosion events instead of high wave events.

- Since there were no erosion time series available, wave thresholding was used as storm detection method. The choice of the threshold is smoothed by the recovery rate calibration. However, it would be interesting to further research the sensitivity of the model to the choice of storm detection method.

- It is suggested to implement the PCR model with wave climates from other locations and investigate the sensitivity of the model.

- The effect of climate change in the variables used for the synthesis of the storm time series was not considered. It would be interesting to explore this aspect and how it affects the PCR model, including also the storm frequency as a variable.

7 References

Bird, E. C. (1996). Coastal erosion and rising sea-level. In *Sea-Level Rise and Coastal Subsidence* (pp. 87-103). Springer, Dordrecht.

Bosboom, J., & Stive, M. J. (2012). *Coastal dynamics I: lectures notes CIE4305*.

Brière, C., & van den Boogaard, H. F. P. (2009). Kustlijnzorg Project.

Bruun, P. (1962). Sea-level rise as a cause of shore erosion. *Journal of the Waterways and Harbors division*, *88*(1), 117-132.

Burnham, K. P., & Anderson, D. R. (2004). Multimodel inference: understanding AIC and BIC in model selection. *Sociological methods & research*, *33*(2), 261-304.

Callaghan, D. P., Nielsen, P., Short, A., & Ranasinghe, R. (2008). Statistical simulation of wave climate and extreme beach erosion. *Coastal Engineering*, *55*(5), 375-390.

Church, J. A., & White, N. J. (2011). Sea-level rise from the late 19th to the early 21st century. *Surveys in geophysics*, *32*(4-5), 585-602.

Church, J. A., Clark, P. U., Cazenave, A., Gregory, J. M., Jevrejeva, S., Levermann, A., ... & Payne, A. J. (2013). *Sea level change*. PM Cambridge University Press.

Collins, M. B., & Balson, P. S. (2007). Coastal and shelf sediment transport: an introduction. *Geological Society, London, Special Publications*, *274*(1), 1-5.

Cooper, J. A. G., & Pilkey, O. H. (2004). Sea-level rise and shoreline retreat: time to abandon the Bruun Rule. *Global and planetary change*, *43*(3-4), 157-171.

Da Cruz, C. M. (2018). *Stochastic projections of coastline variations: application to Hasaki beach, Japan* (Master's thesis, UNESCO-IHE).

Dastgheib, A., Jongejan, R., Wickramanayake, M., & Ranasinghe, R. (2018). Regional scale risk-informed land-use planning using probabilistic coastline recession modelling and economical optimisation: East coast of Sri Lanka. *Journal of Marine Science and Engineering*, *6*(4), 120.

De Fockert A., Luijendijk A. (2011) Wave look-up table: Building with Nature. Memo 1002337-002-ZKS-0001. Deltares, Delft, the Netherlands

De Ronde, J. G., Mulder, J. P. M., & Spanhoff, R. (2003, November). Morphological developments and coastal zone management in the Netherlands. In *International Conference on Estuaries and Coasts November* (pp. 9-11).

de Vries, S., de Schipper, M. A., & Stive, M. (2014). Measured gradients in alongshore sediment transport along the Dutch coast. *Coastal Engineering Proceedings*, *1*(34), 58.

den Heijer, C. K., Baart, F., & van Koningsveld, M. (2012). Assessment of dune failure along the Dutch coast using a fully probabilistic approach. *Geomorphology*, *143*, 95-103.

Doody, J. P. (2012). *Sand dune conservation, management and restoration* (Vol. 4). Springer Science & Business Media.

Dronkers J. (2018, April 24). Active coastal zone. Retrieved from http://www.coastalwiki.org/wiki/Active_coastal_zone

Elias, E.P.L. (2017). *Kustgenese 2.0; Available Measurements and Bathymetric Data at Ameland Inlet, The Netherlands*. Memo 1220339-007-ZKS-0001. Deltares, Delft, the Netherlands

Frank, F. (2013). Assessment of the integration based method to calculate profile likelihoods for mathematical models in biology.

Fuss, S., Canadell, J. G., Peters, G. P., Tavoni, M., Andrew, R. M., Ciais, P., ... & Le Quéré, C. (2014). Betting on negative emissions. *Nature climate change*, *4*(10), 850.

Gao, G. (2018). Multivariate Modelling Using Copulas. In *Bayesian Claims Reserving Methods in Non-life Insurance with Stan* (pp. 153-183). Springer, Singapore.

Giardino, A., Santinelli, G., & Bruens, A. (2012). The state of the coast (Toestand van de kust). Case study: North Holland. *Deltares report 1206171-003 for Rijkwaterstaat, waterdienst.*

Giardino, A., Schrijvershof, R., Nederhoff, C. M., de Vroeg, H., Brière, C., Tonnon, P. K., ... & Schellekens, J. (2018). A quantitative assessment of human interventions and climate change on the West African sediment budget. *Ocean & Coastal Management*, *156*, 249-265.

Giardino, A., Diamantidou, E., Pearson, S., Santinelli, G., & den Heijer, K. (2019). A Regional Application of Bayesian Modeling for Coastal Erosion and Sand Nourishment Management. *Water*, *11*(1), 61.

Hallermeier, R. J. (1983, March). Sand transport limits in coastal structure designs. In *Coastal Structures' 83* (pp. 703-716). ASCE.

Hamm, L., Capobianco, M., Dette, H. H., Lechuga, A., Spanhoff, R., & Stive, M. J. F. (2002). A summary of European experience with shore nourishment. *Coastal engineering*, *47*(2), 237-264.

Hanley, M. E., Hoggart, S. P. G., Simmonds, D. J., Bichot, A., Colangelo, M. A., Bozzeda, F., ... & Trude, R. (2014). Shifting sands? Coastal protection by sand banks, beaches and dunes. *Coastal Engineering*, *87*, 136-146.

Hanson, H., Brampton, A., Capobianco, M., Dette, H. H., Hamm, L., Laustrup, C., ... & Spanhoff, R. (2002). Beach nourishment projects, practices, and objectives—a European overview. *Coastal engineering*, *47*(2), 81-111.

Harman, B. P., Heyenga, S., Taylor, B. M., & Fletcher, C. S. (2013). Global lessons for adapting coastal communities to protect against storm surge inundation. *Journal of Coastal Research*, *31*(4), 790-801.

Heslenfeld, P., Jungerius, P. D., & Klijn, J. A. (2008). European coastal dunes: ecological values, threats, opportunities and policy development. In *Coastal dunes* (pp. 335-351). Springer, Berlin, Heidelberg.

Inman, D. L. (1994). Types of coastal zones: similarities and differences. *Environmental Science in the Coastal Zone: Issues for Further Research*, 67-84.

Kane, E. J. (1948). Economic statistics and econometrics.

Larson, M., Erikson, L., & Hanson, H. (2004). An analytical model to predict dune erosion due to wave impact. *Coastal Engineering*, *51*(8-9), 675-696.

Larson, M., & Kraus, N. C. (1998). *SBEACH: Numerical Model for Simulating Storm-Induced Beach Change. Report 5: Representation of Nonerodible (Hard) Bottoms* (No. CERC-89-9). COASTAL ENGINEERING RESEARCH CENTER VICKSBURG MS.

Li, F. (2014). Probabilistic estimation of dune erosion and coastal zone risk.

Luijendijk, A., Hagenaars, G., Ranasinghe, R., Baart, F., Donchyts, G., & Aarninkhof, S. (2018). The state of the world's beaches. *Scientific reports*, *8*(1), 6641.

Mangor, K., Drønen, N. K., Kærgaard, K. H., & Kristensen, N. E. (2017). Shoreline management guidelines. *DHI https://www. dhigroup. com/marine-water/ebook-shoreline-management-guidelines.*

Marchand M. (201). Concepts and Science for Coastal Erosion Management. Concise report for policy makers. Deltares, Delft.

Mendoza, E. T., & Jiménez, J. A. (2006). A storm classification based on the beach erosion potential in the Catalonian Coast. In *Coastal Dynamics 2005: State of the Practice* (pp. 1-11).

Miller, J. K., & Dean, R. G. (2004). A simple new shoreline change model. *Coastal Engineering*, *51*(7), 531-556.

Minneboo, F. A. J. (1995). Jaarlijkse kustmetingen: Richtlijnen voor de inwinning, bewerking, en opslag van gegevens van jaarlijkse kustmetingen. *RIKZ-95.022.*

Mulder, J. P., Hommes, S., & Horstman, E. M. (2011). Implementation of coastal erosion management in the Netherlands. *Ocean & coastal management*, *54*(12), 888-897.

Passeri, D. L., Hagen, S. C., Medeiros, S. C., Bilskie, M. V., Alizad, K., & Wang, D. (2015). The dynamic effects of sea level rise on low-gradient coastal landscapes: A review. *Earth's Future*, *3*(6), 159-181.

Pender, D., & Karunarathna, H. (2013). A statistical-process based approach for modelling beach profile variability. *Coastal Engineering*, *81*, 19-29.

Pit, I. R., Griffioen, J., & Wassen, M. J. (2017). Environmental geochemistry of a mega beach nourishment in the Netherlands: Monitoring freshening and oxidation processes. *Applied geochemistry*, *80*, 72-89.

Pontee, N. (2013). Defining coastal squeeze: A discussion. *Ocean & coastal management*, *84*, 204-207.

Pot, R. (2011). System description Noord-Holland Coast (master's thesis). Retrieved from repository of TU Delft (http://resolver.tudelft.nl/uuid:ae808e51-7d9f-464a-a7d6-07703f4240e8).

Ranasinghe, R., & Stive, M. J. (2009). Rising seas and retreating coastlines. *Climatic Change*, *97*(3), 465-468.

Ranasinghe, R., Callaghan, D., & Stive, M. J. (2012). Estimating coastal recession due to sea level rise: beyond the Bruun rule. *Climatic Change*, *110*(3-4), 561-574.

Ranasinghe, R. W. M. R. J. B., Callaghan, D., & Roelvink, D. (2013). Does a more sophisticated storm erosion model improve probabilistic erosion estimates? In Coastal Dynamics 2013: *7th International Conference on Coastal Dynamics, Arcachon, France, 24-28 June 2013*. Bordeaux University.

Ranasinghe, R. (2016). Assessing climate change impacts on open sandy coasts: A review. *Earth-science reviews*, *160*, 320-332.

Riahi, K., Rao, S., Krey, V., Cho, C., Chirkov, V., Fischer, G., ... & Rafaj, P. (2011). RCP 8.5—A scenario of comparatively high greenhouse gas emissions. *Climatic Change*, *109*(1-2), 33.

Rijkswaterstaat, 2011, Kustlijnkaartenboek 2012

Roelvink, D., Reniers, A., Van Dongeren, A. P., de Vries, J. V. T., McCall, R., & Lescinski, J. (2009). Modelling storm impacts on beaches, dunes and barrier islands. *Coastal engineering*, *56*(11-12), 1133-1152.

Ruessink, B. G., Boers, M., Van Geer, P. F. C., De Bakker, A. T. M., Pieterse, A., Grasso, F., & De Winter, R. C. (2012). Towards a process-based model to predict dune erosion along the Dutch Wadden coast. *Netherlands Journal of Geosciences*, *91*(3), 357-372.

Salman, A., Lombardo, S., & Doody, P. (2004). Living with coastal erosion in Europe: Sediment and Space for Sustainability. *Eurosion project reports*.

Shand, T., Shand, R., Reinen-Hamill, R., Carley, J., & Cox, R. (2013). A review of shoreline response models to changes in sea level. In *Coasts and Ports 2013: 21st Australasian Coastal and Ocean Engineering Conference and the 14th Australasian Port and Harbour Conference* (p. 676). Engineers Australia.

Sistermans, P., & Nieuwenhuis, O. (2004). Holland coast (the Netherlands). *Eur. Case Study*, *31*, 1-17.

Stive, M. J., Ranasinghe, R., & Cowell, P. J. (2010). Sea level rise and coastal erosion. In *Handbook of coastal and ocean engineering* (pp. 1023-1037).

Stocker, L., Kennedy, D., Kenchington, R., & Merrick, K. (2012). Sustainable coastal management. *Sustainable coastal management and climate adaptation, global lessons from regional approaches in Australia*, 29-56.

Tawn, J. A. (1988). Bivariate extreme value theory: Models and estimation. Biometrika 75 397–415. *Mathematical Reviews (MathSciNet): MR967580 Zentralblatt MATH*, *653*.

Toimil, A., Losada, I. J., Camus, P., & Díaz-Simal, P. (2017). Managing coastal erosion under climate change at the regional scale. *Coastal Engineering*, *128*, 106-122.

Tribbia, J., & Moser, S. C. (2008). More than information: what coastal managers need to plan for climate change. *Environmental science & policy*, *11*(4), 315-328.

Van Koningsveld, M., & Mulder, J. P. M. (2004). Sustainable coastal policy developments in the Netherlands. A systematic approach revealed. *Journal of Coastal Research*, 375-385.

Van Koningsveld, M., Otten, C., & Mulder, J. P. M. P. M. (2007, May). Dunes: the Netherlands soft but secure sea defences. In Proceedings 18th World dredging congress, Florida USA, WODA.

van Rijn, L. C. (2009). Prediction of dune erosion due to storms. Coastal Engineering, 56(4), 441-457.

van Rijn, L. (2013). Erosion of coastal dunes due to storms. Sourced from www. leovanrijn-sediment. com.

van Vessem, P., & Stolk, A. (1991). Sand Budget of the Dutch Coast: The Dutch Coast: Paper No. 4. In *Coastal Engineering 1990* (pp. 1895-1908).

Van Vuuren, D. P., Edmonds, J., Kainuma, M., Riahi, K., Thomson, A., Hibbard, K., ... & Masui, T. (2011). The representative concentration pathways: an overview. *Climatic change*, *109*(1-2), 5.

Vellinga, P., 1986. *Beach and dune erosion during storm surges*. Doctoral Thesis, Delft University of Technology, Delft, The Netherlands (Publication 372, Delft Hydraulics)

Wang, P., Rosati, J. D., & Roberts, T. M. (Eds.). (2011). *The Proceedings of the Coastal Sediments 2011* (Vol. 3). World Scientific.

Williams, J. J., de Alegría-Arzaburu, A. R., McCall, R. T., & Van Dongeren, A. P. (2012). Modelling gravel barrier profile response to combined waves and tides using XBeach: Laboratory and field results. *Coastal Engineering*, *63*, 62-80.

Wit, E., Heuvel, E. V. D., & Romeijn, J. W. (2012). 'All models are wrong...': an introduction to model uncertainty. *Statistica Neerlandica*, *66*(3), 217-236.

Woodroffe, C. D., Cowell, P. J., Callaghan, D. P., Ranasinghe, R., Jongejan, R., Wainwright, D. J., ... & Dougherty, A. J. (2012). Approaches to risk assessment on Australian coasts: A model framework for assessing risk and adaptation to climate change on Australian coasts.

Zhu, X., Linham, M. M., & Nicholls, R. J. (2010). *Technologies for climate change adaptation-Coastal erosion and flooding*. Danmarks Tekniske Universitet, Risø Nationallaboratoriet for Bæredygtig Energi.

Appendix A

Erosion function

In this thesis, an adjusted formula of the DUNERULE erosion model is used which is an empirical model developed by van Rijn (van Rijn, 2009). DUNERULE is based on the CROSMOR2007-model which is a process-based profile model used for cross-shore modelling of dune erosion. It uses the wave by wave approach, solving the wave energy equation for every individual wave. Basic dune erosion processes have been added to CROSMOR model and sensitivity analyses were implemented to find the effect of key parameters on the computation of dune erosion volume for a very severe storm, defined as the Reference Case Storm, as proposed by Vellinga (Vellinga, 1986), see Table_ A.1.

Table_ A.1 The Reference Case Storm characteristics and the parameters of Dutch coastal profile (van Rijn, 2013)

Parameter	Prototype conditions used by Vellinga (1986)
Offshore wave height [m]	7.6 (Pierson and Moskowitz spectrum)
Offshore wave period [sec]	12
Offshore water depth [m]	21
Storm surge level above MSL* [m]	+5 m NAP during 5 hours
Median sediment diameter [μm]	225
Median fall velocity [m/sec]	0.0267
Water temperature (°C)	10
Cross-shore profile	a) dune height at +15 m NAP, b) dune face with slope of 1 to 3 down to a level of +3 m NAP, c) slope of 1 to 20 between +3m and 0 m NAP, d) slope of 1 to 70 between 0 and -3 m NAP, e) slope of 1 to 180 seaward of -3 m NAP line
*Remark: Mean Sea Level (MSL) is about equal to NAP	

The results of the sensitivity study, with the storm surge level (S) and bed material diameter (d_{50}) being the most influential, conducted for a range of conditions, were parameterized and used for the development of DUNERULE-model, a simplified dune erosion rule (van Rijn, 2013). In Fig A.1 is depicted the dune erosion of a cross-shore profile.
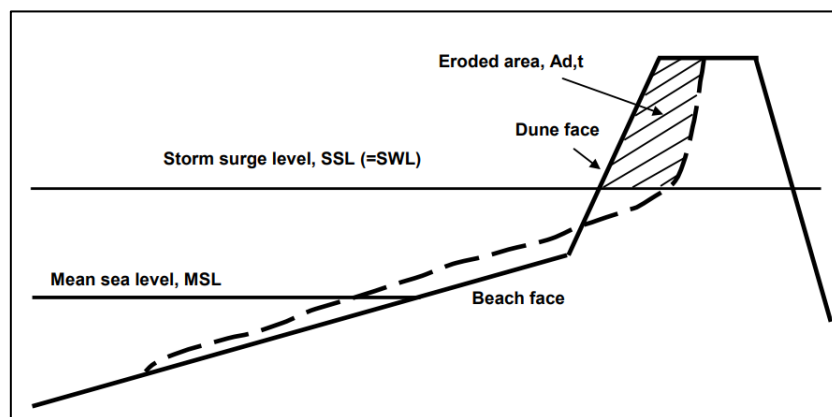
Fig A.1: Dune erosion (van Rijn, 2009)

The eroded area in Fig A.1 is estimated as follows:

Equation_ A.1

$$V_{d,t=5} = V_{d,ref} \cdot (d_{d,ref} / d_{50})^{a1} \cdot (h_{max} / h_{max,ref})^{a2} \cdot (H_{s,0} / H_{s,0,ref})^{a3} \cdot (T_p / T_{p,ref})^{a4} \cdot (\tan \beta / \tan \beta_{ref})^{a5} \cdot (1 + \theta_0 / 100)^{a6}$$

And the time development over 100 hours is estimated:

Equation_ A.2

$$V_{d,t} = V_{d,t=5} \cdot (t/t_{ref})^{a7}$$

Where, in Table_ A.2 it is provided more information about Equation_ A.1 and Equation_ A.2.

Table_ A.2: DUNERULE variables

Variable	Description of variable	Value in R.C.*	Units
$V_{d,t=5}$	Dune erosion area above storm surge level after 5 hours	170	[m³/m]
h_{max}	Storm surge level above mean sea level	5	[m]
$H_{s,0}$	Offshore significant wave height	7.6	[m]
T_p	Peak wave period	12	[sec]
d_{50}	Median bed material diameter	0.000225	[m]
$\tan\beta$	Coastal slope gradient defined as the slope between the -3 m depth contour (below MSL) and the dune toe (+3 m)	0.0222 (1 to 45)	
θ_0	Offshore wave incidence angle to coast normal		[deg]
α_1, α_5	exponents	1.3	
α_2	exponent	1.3 for S<S$_{ref}$ 0.5 for S>S$_{ref}$	
α_3, α_4, α_6	exponents	0.5	
$V_{d,t}$	Dune erosion area above storm surge level after t hours		[m³/m]
t	time	5	[hrs]
α_7	exponent	0.5 for dur<dur$_{ref}$ 0.2 for dur>dur$_{ref}$	[hrs]
*Remark: R.C. is the Reference Case storm; it regards all the variables with -,**ref**			

According to van Rijn (2009), the validity of Equation_ A.1 is higher for major storm events, but it yields accurate results for minor storms as well.

Li (2014) refers that DUNERULE must be calibrated by historical data from the study site for which is going to be implemented. Since, these measurements are not available, the coastal profile was calibrated and validated by Li, using XBeach, for a coastal profile at the Noordwijk coast. For this case, roughly 300 storm events, with several combinations of storm characteristics have been used for the calibration of DUNERULE's parameters. By keeping the wave direction stable and by applying the trial and error method, Li determined the model's parameters based on the results having the minimum deviation from XBeach estimates (Fig A.2).
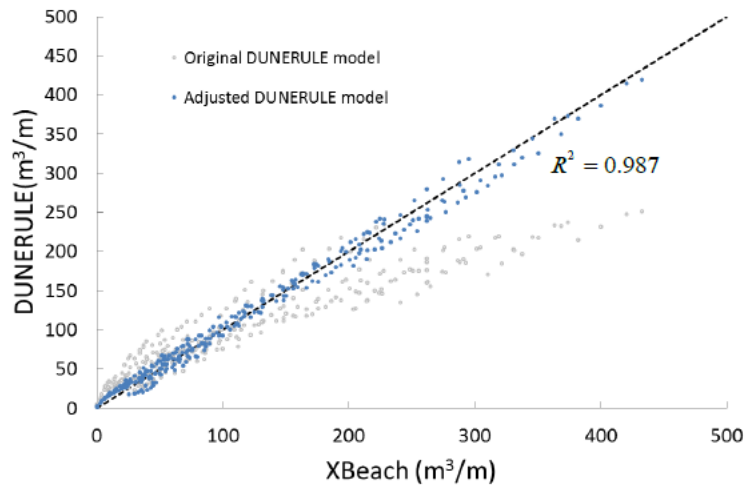
Fig A.2: Original DUNERULE model vs adjusted DUNERULE model, as calibrated by Li (2014); R2 is the coefficient of determination

The next figure shows the differences in coastal erosion estimation of the two erosion functions, the original DUNERULE formula and the calibrated DUNERULE formula by Li (2014).
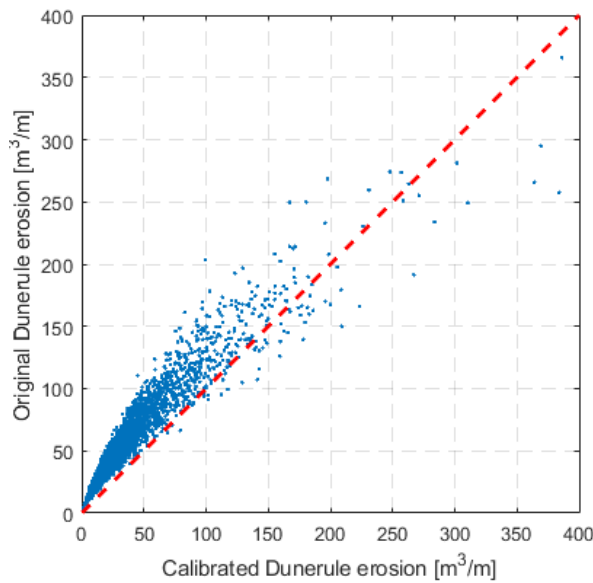
Fig A.3: Original DUNERULE formula VS adjusted DUNERULE formula

In Fig A.3 it can be seen that for major storms the original DUNERULE formula is more conservative than the formula calibrated by Li using XBeach as an indicator of reality. However, for less extreme storm events the coastal erosion estimations predicted by the original formula are greater than the estimations calculated by Li's calibrated formula for the coastal profile 8008250 at Noordwijk. Using the original DUNERULE formula raises more conservative results compared to Li's formula for DUNERULE, since the events generated within a Monte Carlo simulation are in the majority less extreme. In this study, it is assumed that the storm events and their relevant erosion volume are better described by the calibrated DUNERULE formula by Li, hereinafter referred to as *adjusted DUNERULE formula*.

Appendix B

Analyses

This chapter presents the analyses performed, based on the methods in chapter 3. It includes the data collection, the storm detection and storm data analyses. It presents the dependencies between the storm characteristics. It includes the fitted SLR curves and lastly it describes the Bruun rule implementation for the Holland coast.

Storm detection and data analysis

As mentioned in methodology, as storm events are defined the periods of time within which the significant wave height exceeds the threshold of 95% percentile of all available observations H_s. There are two limitations; one regarding the independence among the storms and therefore a minimum opening of 3 hrs is set between two storms otherwise these two events are merged and considered as one event. The other limitation is about the duration of a storm event and in this thesis a minimum duration of 6 hrs is defined. At profile 9 the threshold is equal to 2.44 m. Fig B.1 and Fig B.2 show the process of storm detection for the period from 1979 until 2018.
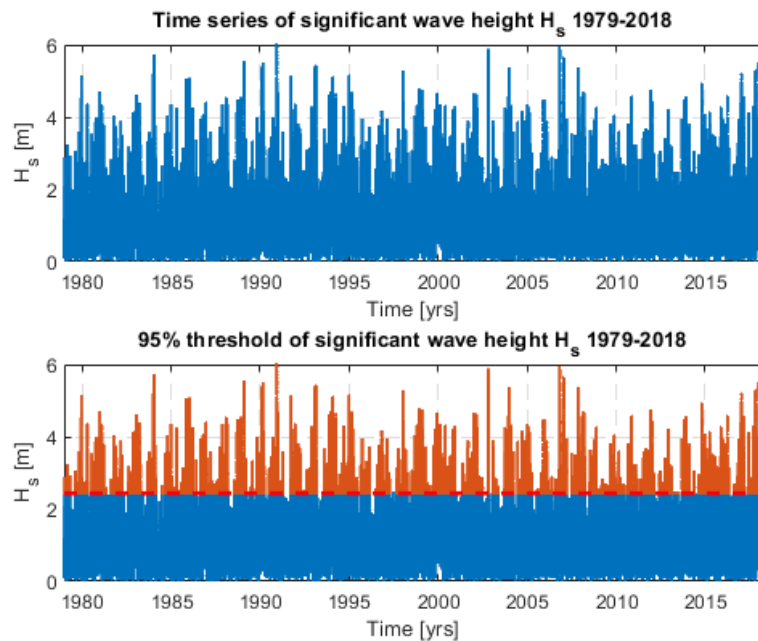
Fig B.1: Storm events identified over a 39-year period
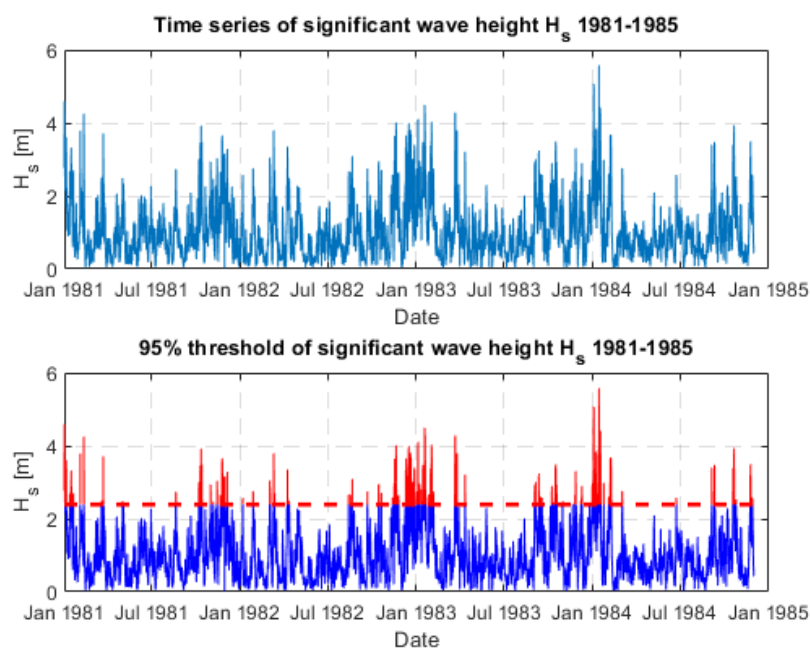
Fig B.2: Zoom-in plot of a 5-year period from 1981 to 1985

In the case of (North) Bergen, (profile 9), setting as threshold the 95th percentile significant wave height raised 797 events over a 39-year period, which is approximately 20 events per year (Fig B.3). The overall number of storms detected over the 39-year period in the different coastal profiles is around 794 storms, or on average around 20 storms per year.
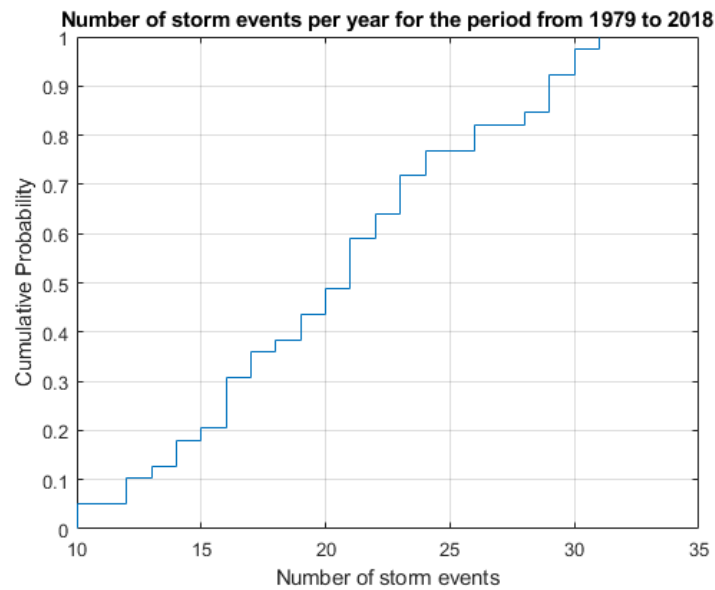
Fig B.3: Annual number of storm events for the 39-year period (1979-2018), for the coastal profile 9

After detecting the storm events for all the coastal profiles, it follows the statistical analyses of the data. The 797 storm events detected for the coastal profile 9 (North Bergen) are used for illustration purposes of the methodology used for statistical analyses. Fig B.4 presents the main storm characteristics of this coastal profile, which are the maximum significant wave height (H_s) during the storms, the mean peak period of waves (T_p) during the storms, the average wave direction (θ) during the storms (Fig B.5), the maximum (positive) water level during the storms and the duration of the storms.
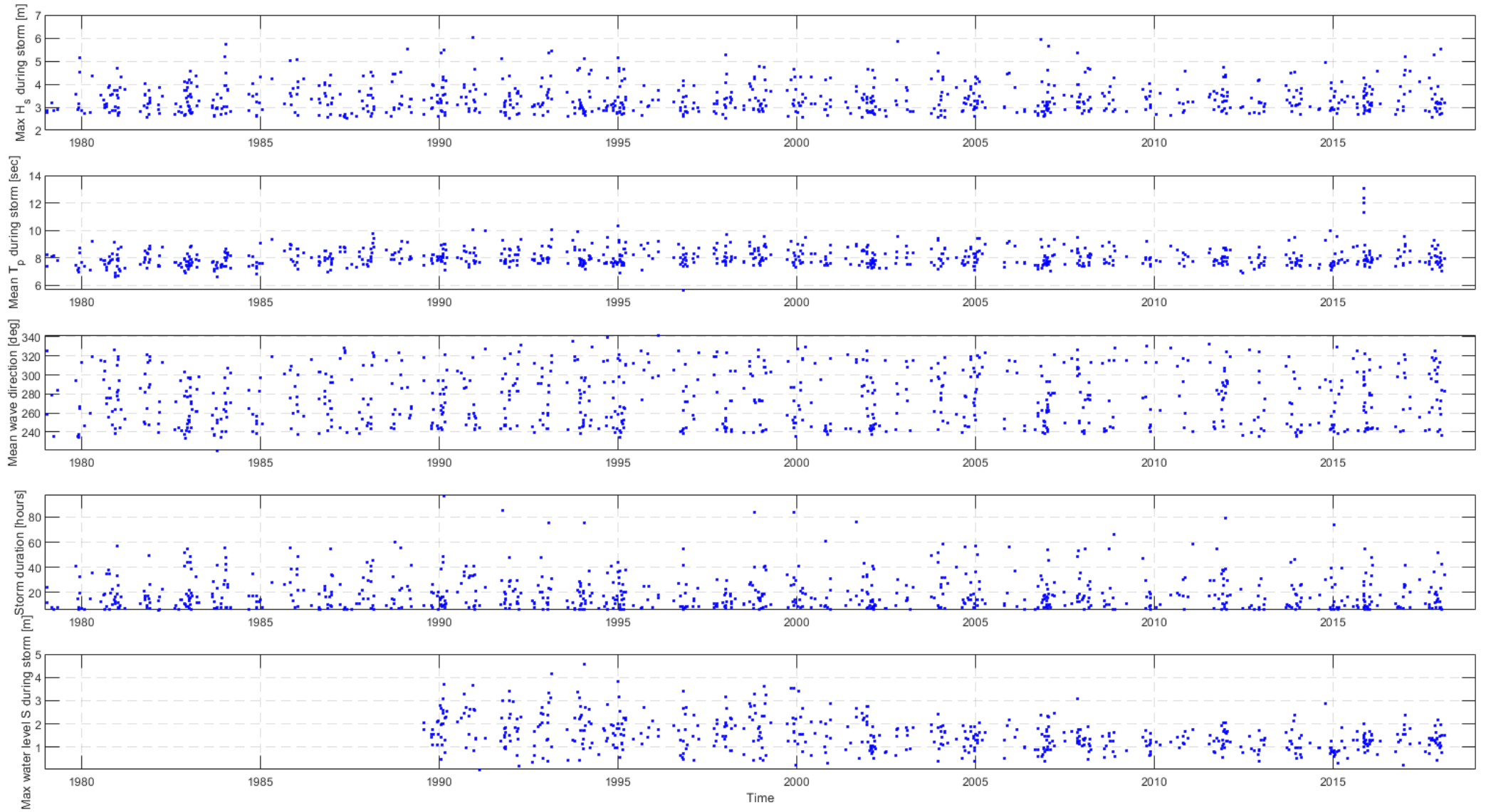
Fig B.4: Storm characteristics at profile 9 for the period from 1979 to 2018
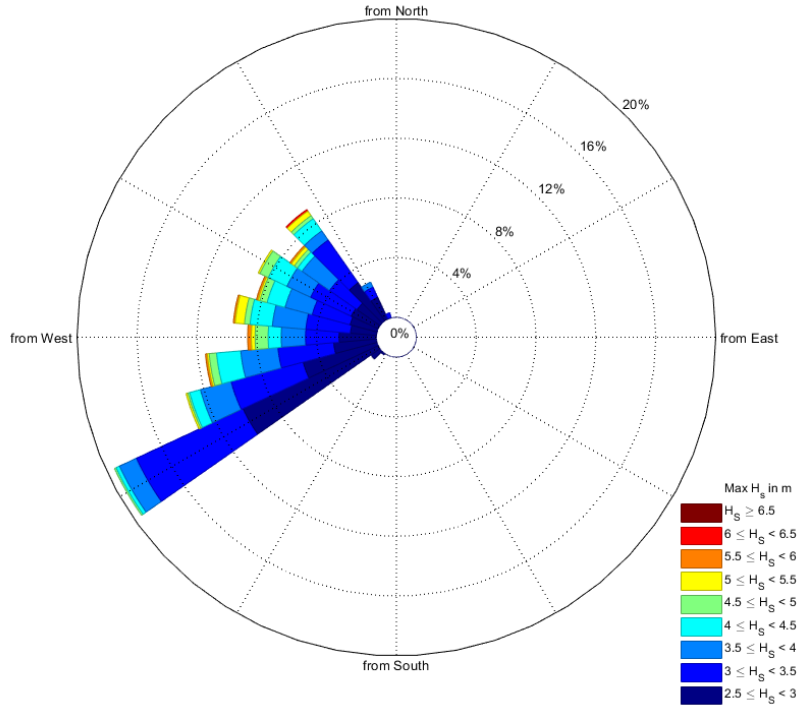
Fig B.5: Wave rose for the coastal profile 9, at the location with depth 17 m

To use these data in coastline recession simulation, generalised pareto (GP) distribution functions are fitted to the storm characteristics H_s, T_p, *dur* and *S*. An empirical cumulative distribution function is used for the average wave direction during storms (Fig B.9). Since in this study seasonality is not included, the intermediate time between two consecutive storms (i.e. storm gaps) are simulated using an empirical distribution function (Fig B.10).
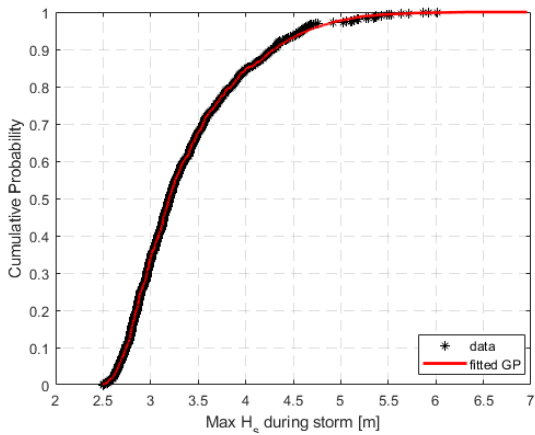
Fig B.6: Cumulative distribution function and fitted GP of maximum significant wave height Hs
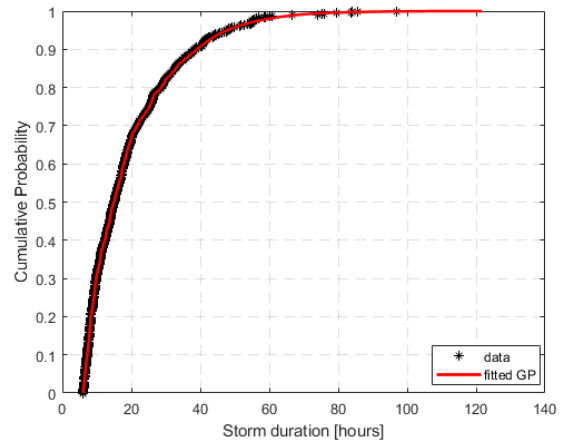
Fig B.7: Cumulative distribution function and fitted GP of storm duration
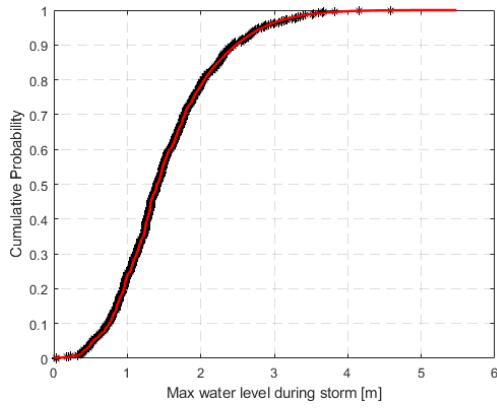
Fig B.8: Cumulative distribution function and fitted GP of maximum water level hmax [m]
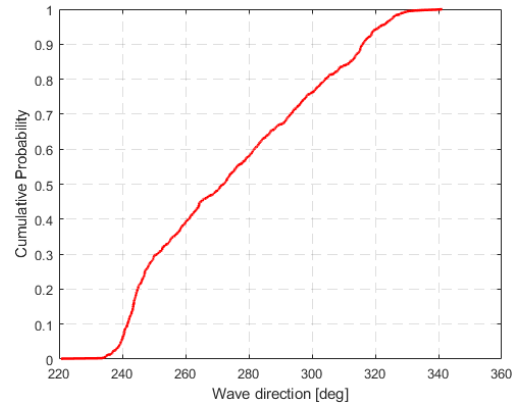
Fig B.9: Empirical distribution function of average wave direction [deg]
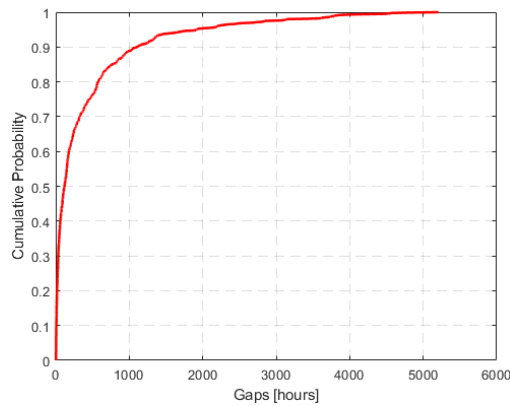
Fig B.10:Empirical distribution function of storm gaps [hours]

The statistical analysis is completed when the dependencies between different storm characteristics is set. For this scope, the maximum significant wave height during the storm is chosen as the main parameter and its dependencies against other parameters is examined. Fig B.11-Fig B.13 show the dependency between maximum significant wave height and storm duration, the dependency between maximum significant wave height and maximum water level during storms and the dependency between maximum significant wave height and the average wave direction during storms. The figures regard profile 9 (North Bergen).

The pair of maximum significant wave height and storm duration and the pair of maximum significant wave height and maximum water level during storms are positively correlated (i.e. the increase of the one variable is in line with the increase of the other variable). The correlation of the two pairs is 0.64 and 0.56 respectively. On the contrary, the maximum significant wave height and the average wave direction are hardly related, showing a low correlation of 0.18.
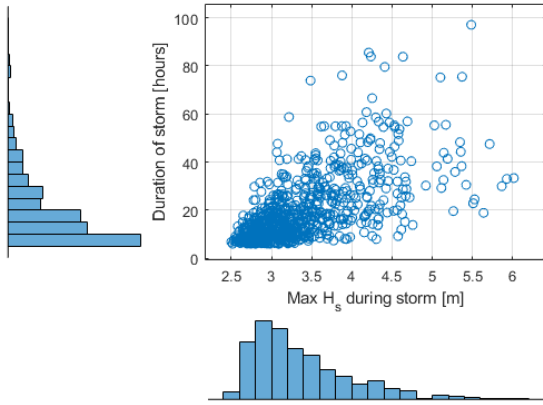
Fig B.11: Dependency between maximum significant wave height and storm duration
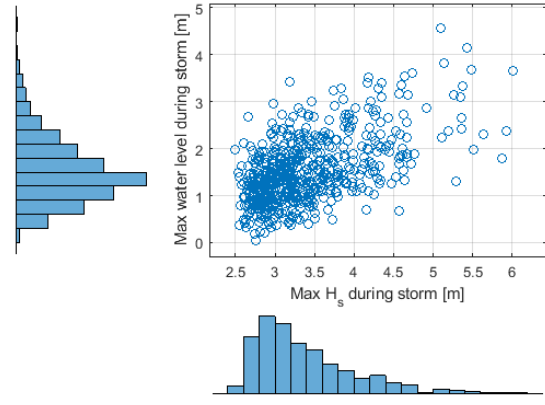
Fig B.12: Dependency between maximum significant wave height and maximum water level during storms
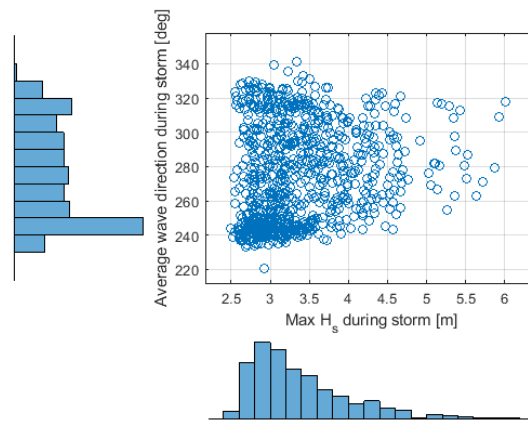
Fig B.13: Dependency between maximum significant wave height and average wave direction during storms

The next step is to employ a copula method in order to establish the dependency distribution that describes the observed dependency between maximum significant wave height and storm duration and the observed dependency between maximum significant wave height and maximum water level during storms. Copulas are basically a family of multivariate cumulative distribution functions for which the marginal distribution of each variable is uniform (Gao, 2018). in this study, the 'Gumbel' and the 'Frank' copula have been used for the two pairs respectively(Fig B.14,Fig B.15).
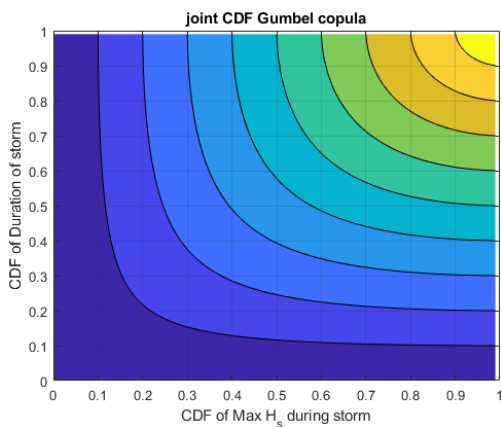
Fig B.14: Fitted joint CDF of H_S and storm duration using Gumbel copula
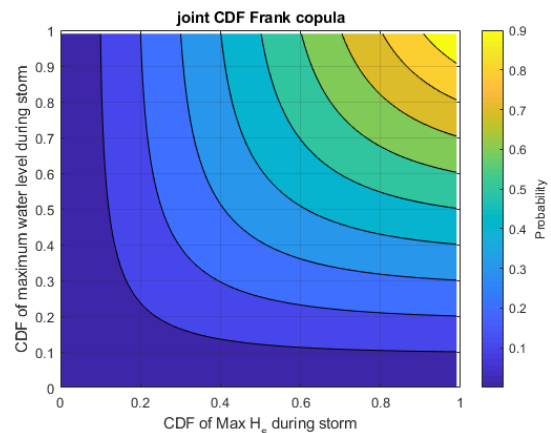
Fig B.15: Fitted joint CDF of H_S and maximum water level using Frank copula

Similar to previous studies, the maximum significant wave height and average wave period are related through linear fitting of the data, as shown in Fig B.16
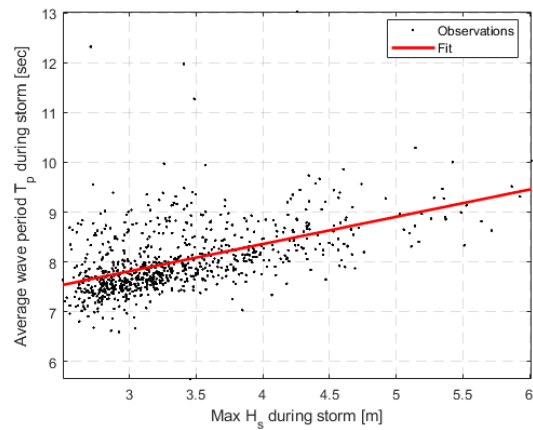
Fig B.16: Linear fit between Hs and Tp, profile 9

Fig B.17 show the synthetic storm characteristics and the relevant erosion they cause from one simulation, for the period 2020-2100.
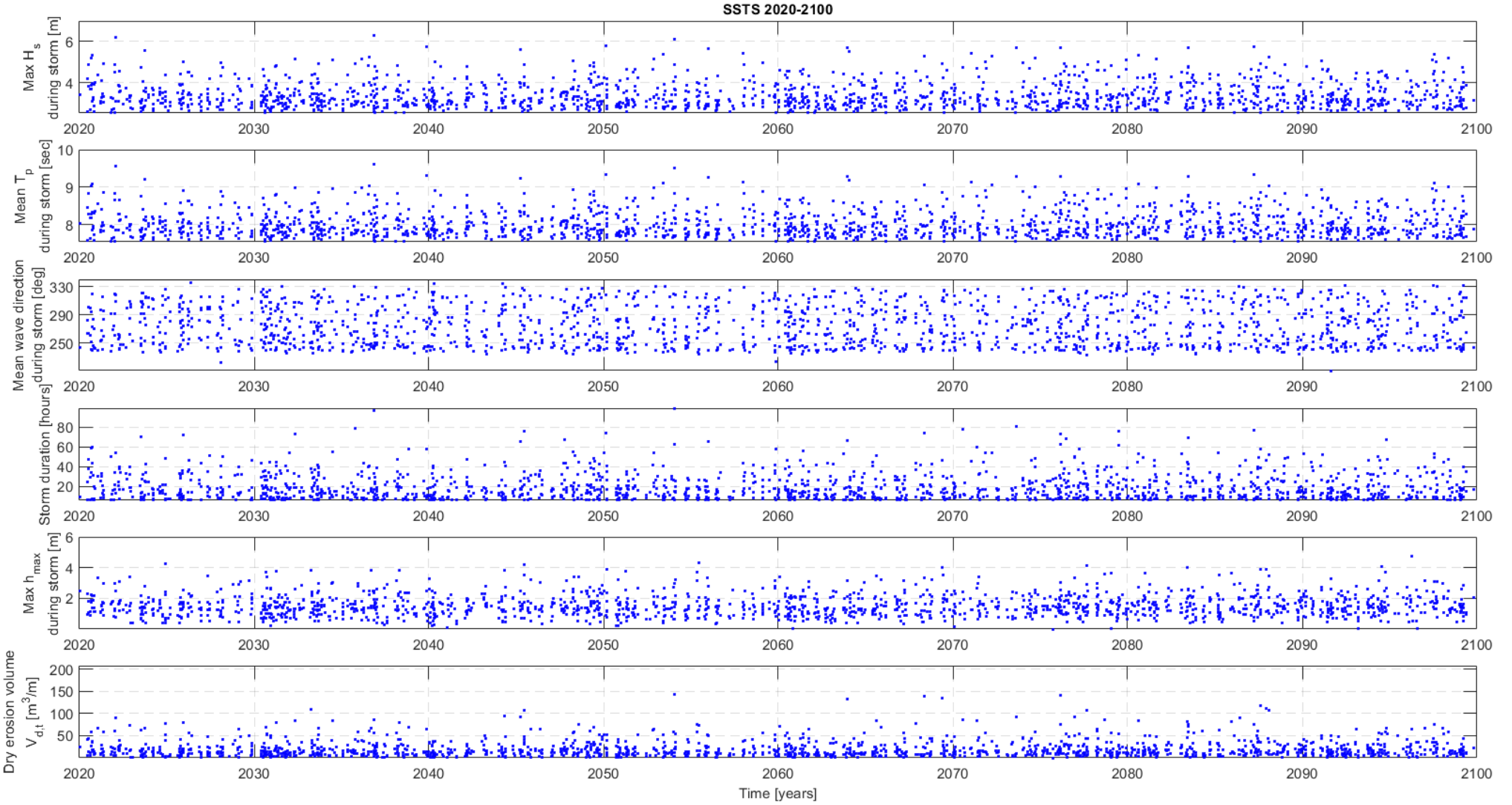
Fig B.17:Synthetic storm characteristics and relevant erosion (DUNERULE) at profile 9 for the period from 2020 to 2100, sim #1

Erosion model

The section of the erosion model is described in more detail in section 3.4. A comparison between the range of the dry erosion volumes (m³/m) of the detected storm measurements (797 events over a 39-year period) and the generated storm events (39,000,000 events), for profile 9 is shown in Fig B.18 and Fig B.19.
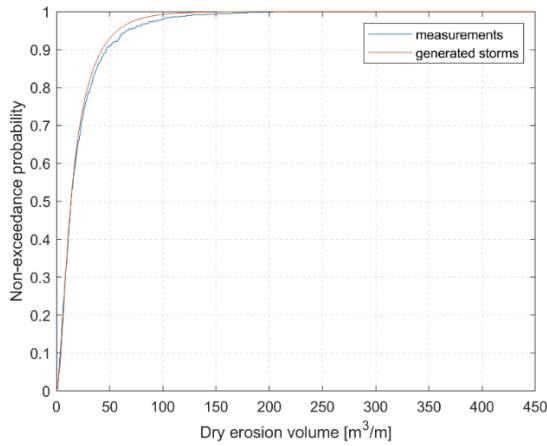
Fig B.18: CDF of erosion volumes for storm measurements and generated storms
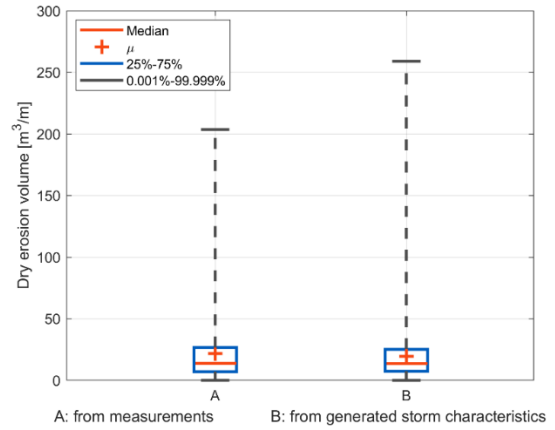
Fig B.19: Erosion volumes for storm measurements and generated storms

In the following figures the adjusted DUNERULE formula was tested on some of its main parameters for profile 9. This accomplished by using the mean values of the parameters as constants in the formula and changing the value of the variable in interest.
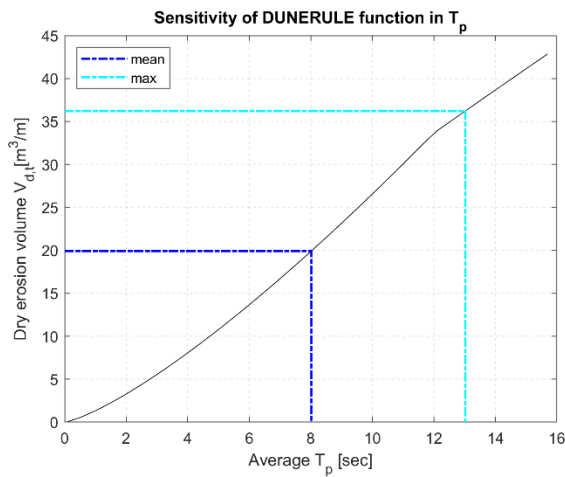
Fig B.20: Sensitivity of adjusted DUNERULE in Tp
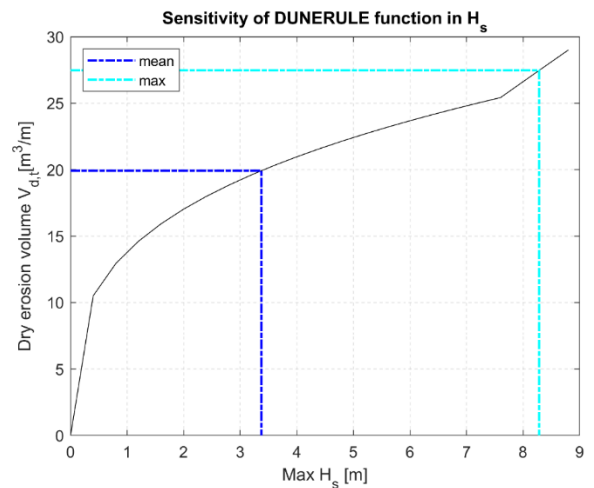
Fig B.21: Sensitivity of adjusted DUNERULE in Hs
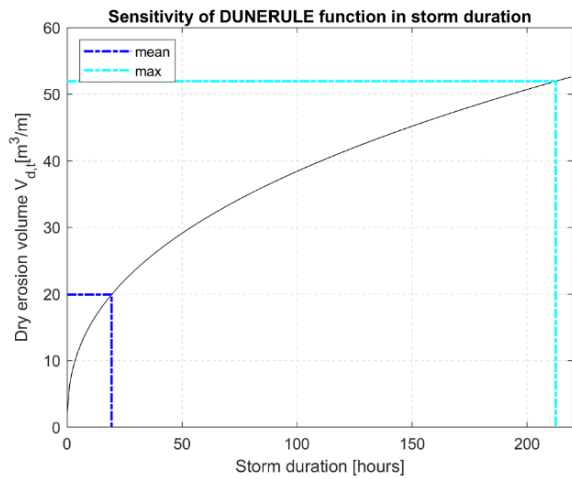
Fig B.22: Sensitivity of adjusted DUNERULE in storm duration
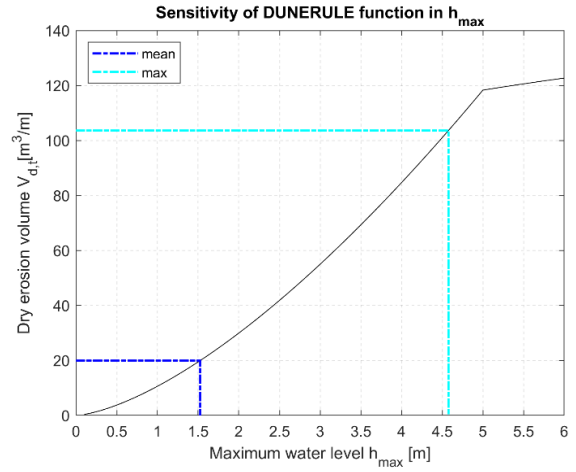
Fig B.23: Sensitivity of adjusted DUNERULE in hmax

It is seen that the adjusted DUNERULE is more sensitive to water level variable among the other parameters. Due to this, the SLR is included into the PCR framework in the way described in section 3.6.

Bruun rule

In this section the SLR driven coastline recession is estimated using the Bruun rule formula. The recession of the coast is calculated using Equation_ B.1 as it is described in section 2.4.2.

Equation_ B.1

$$R = \frac{L \cdot SLR}{B + h_*}$$

Where R is the coastal recession of the cross-shore profile in response to a SLR, h_* is the maximum depth until which there is exchange of material between nearshore and offshore, L is the horizontal distance from the shoreline to depth h_*, and B is the berm or dune elevation estimate for the eroded area.

In this work the dune elevation level (*or the dry height of the dune*) B is calculated from the average profile measurements of the JarKus dataset. As dune elevation level is chosen the point until which it is observed changes of the dune profile (Fig B.24). The (outer) depth of closure is calculated using **Equation 3.9** (Hallermeier, 1983). The values of **H_m** and **T_m** used in this equation, are defined from the available data of the 39-year period, from January 1979 to December 2018. Once the DoC is estimated then the horizontal distance L, from the shoreline to DoC, is defined using the average profile measurements of the JarKus dataset.

The sea level rise S respect to the year 2020 is obtained from the fitted KNMI's projection curve of Deltascenario and the fitted IPCC curves for scenarios RCP4 and RCP8.5. For illustration purposes, the results of the erosive profile 9 at North Bergen *(JarKus 7003100)* were selected for presentation. The projected recessions of profile 9, according to Bruun rule, are calculated using the calculated inputs presented in Table_ B.1. The relevant recessions R corresponding to the several SLR scenarios (Table 3.1) are shown in Table_ B.2. The estimates of the coastal retreat for the years 2020-2100 are shown in Fig B.25.
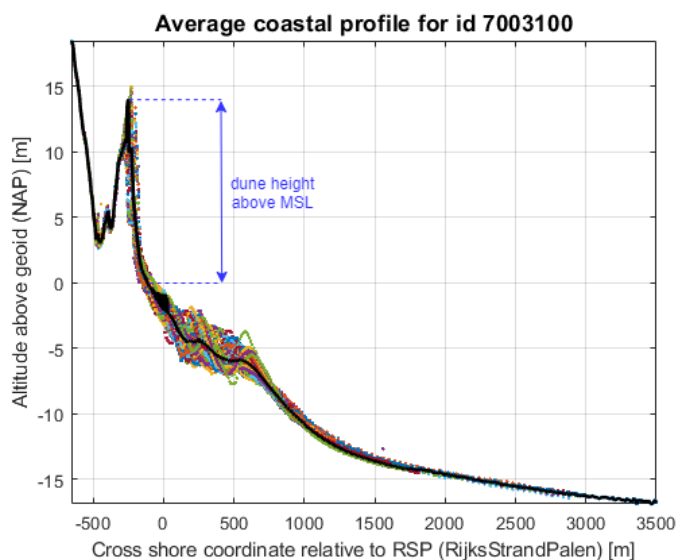
Fig B.24: Definition of dune height above MSL

Table_ B.1:Inputs for Bruun rule, profile 9

H_m [m]	T_m [m]	h_* [m]	L [m]	B [m]
0.93	5.6	15.9	3048	14

Table_ B.2: Coastal recession R for the scenarios RCP4.5, RCP8.5 and Deltascenario

Years	R [m]		
	RCP4.5	**RCP8.5**	**Deltascenario**
2040	9.3	10.2	15.0
2070	26.3	32.2	46.6
2100	45.1	65.7	83.2
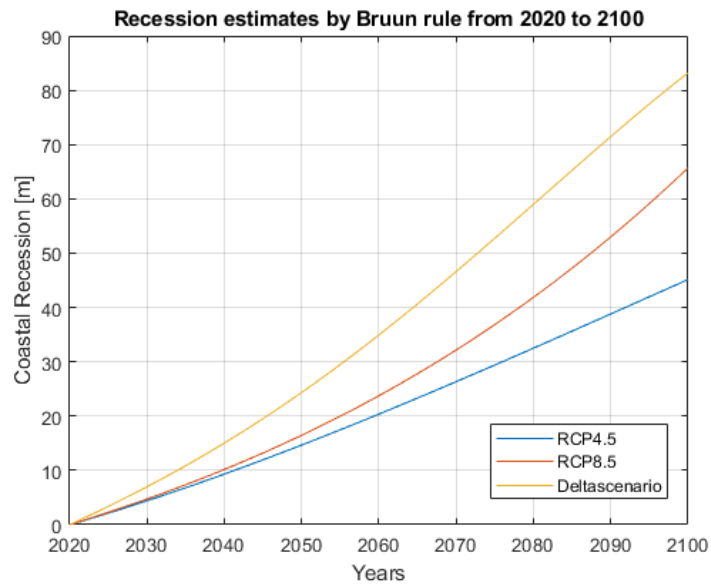
Fig B.25:Estimated recessions using Bruun rule for profile 9

Appendix C

Coastal profiles info and results

In this appendix the following info is provided for each profile:

- The JarKus id that corresponds to the specific cross-shore profile.
- The chosen level of the dune crest above NAP, as observed from the JarKus profile.
- The height of the active profile (summation of the dune crest level above NAP and the DoC)
- The chosen years in the past (indicated as years of observations) for which the coastline change rate is estimated.
- The coastline change rate (trend).
- The rays of the UNIBEST model within which lays the cross-shore profile and the longshore sediment transport rates for each of the two rays.

This appendix also includes the following results for every profile (in figures):

- Exceedance probability curves of coastal recession, under no SLR scenario
- PCR estimates vs Bruun rule, for Deltascenario
- The range of retreats for the three different approaches of calibrating the recovery rate

Profile 1

JarKus id	9011700
Dune crest level above NAP	12.5 m
Active height	25.96 m
Years of observations	1843-1970
Trend	Accretive ΔCL_rate = 0.64 m/year
UB Rays	4-5
S_1	0.332 M m³/yr
S_2	0.328 M m³/yr
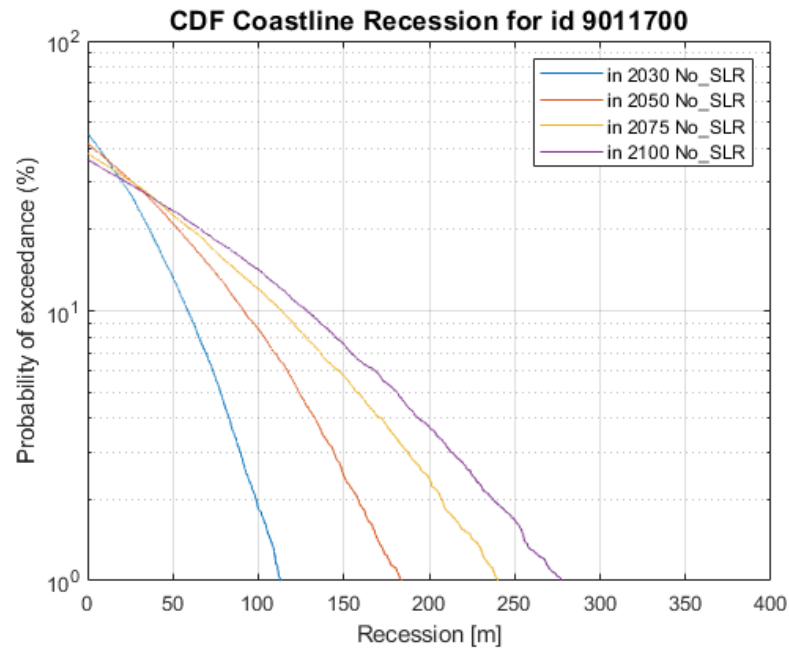
Fig C.2: Dutch Beach Lines between 1843 and 1980

Fig C.1: Exceedance probability curves of coastal recession, under no SLR scenario
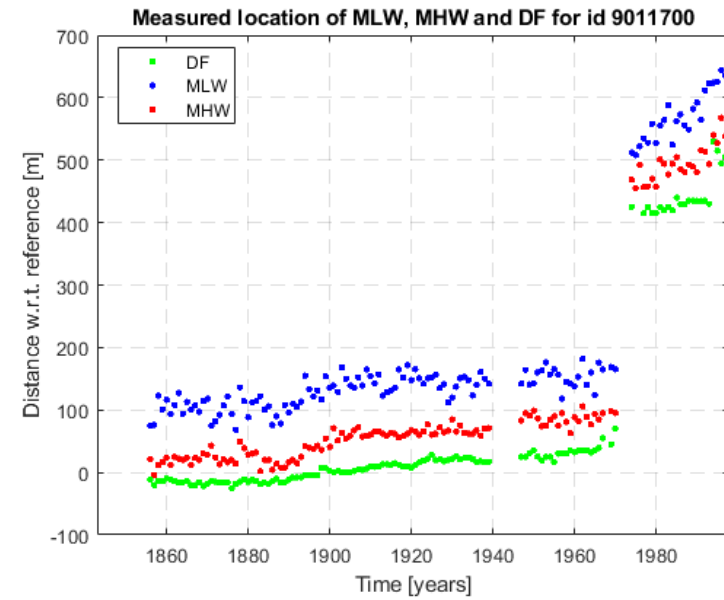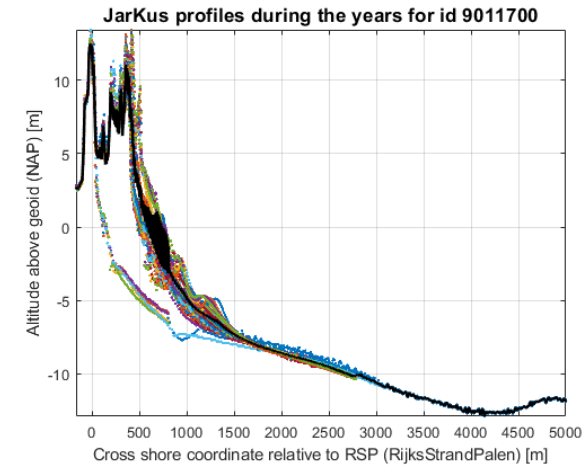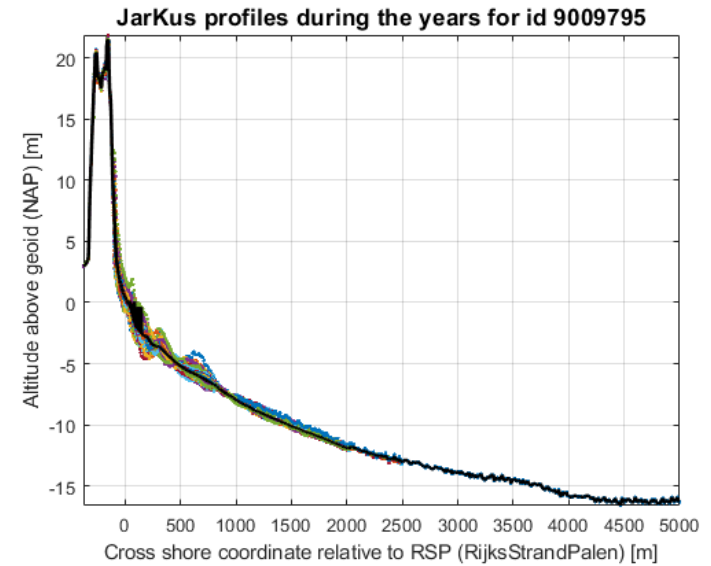

*Fig C.3: JarKus transect (measurements from 1965 up to present)*
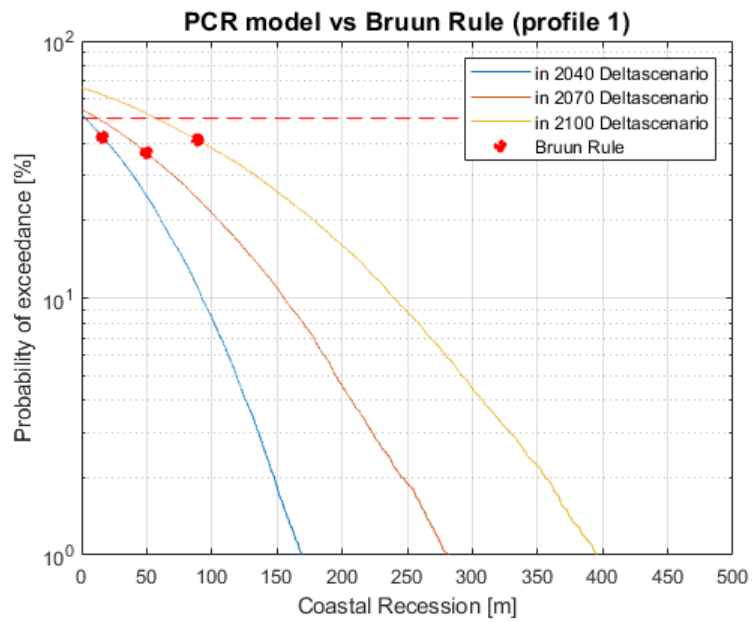
Fig C.4: PCR vs Bruun rule for Deltascenario
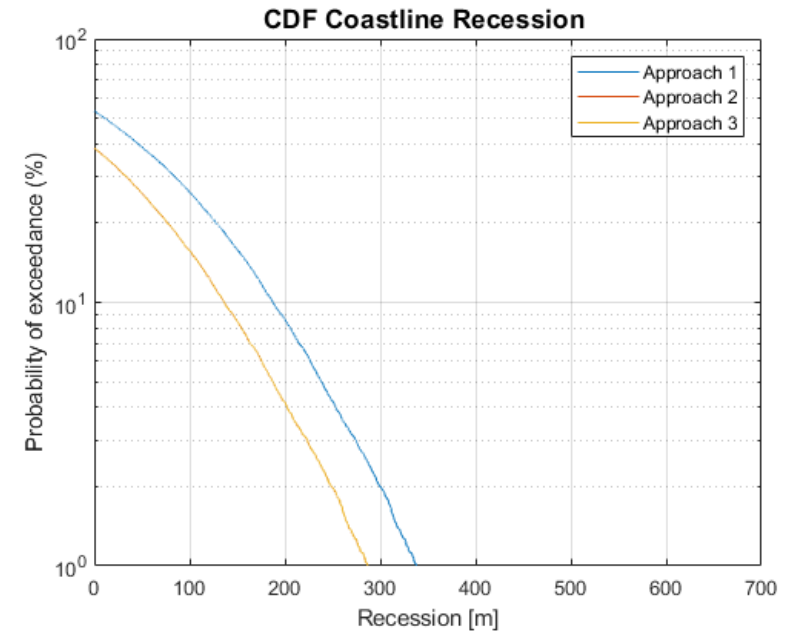
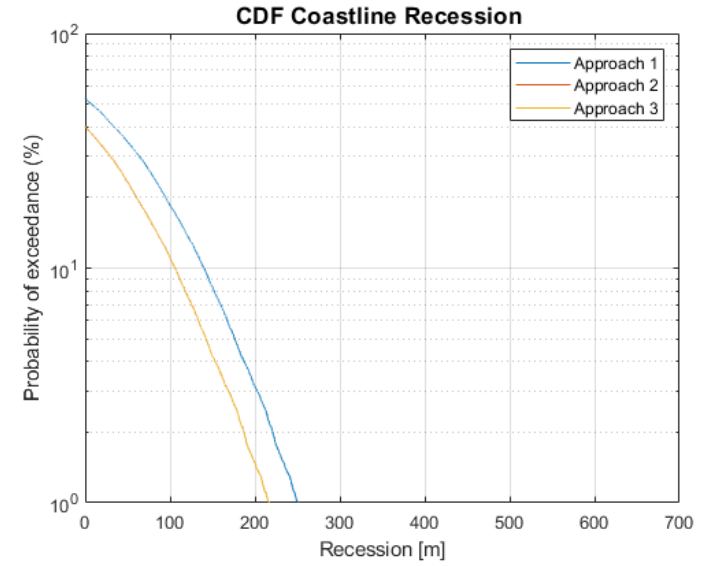*Fig C.6: Recession range for the profile 1, for the three RR*
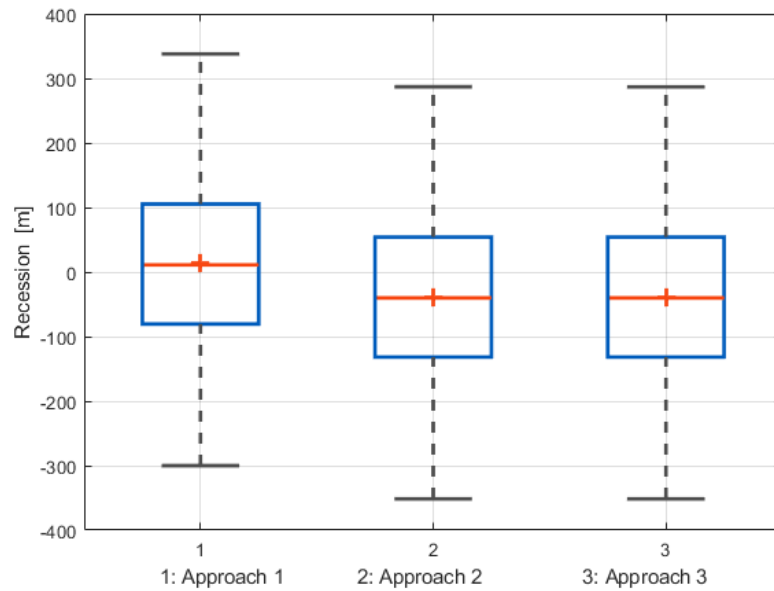
Fig C.5: Comparison among the three RR approaches

Profile 2

JarKus id	9011109
Dune crest level above NAP	11 m
Active height	25.25 m
Years of observations	1843-1960
Trend	Erosive ΔCL_rate = -0.51 m/year
UB Rays	10-11
S_1	-0.09 M m³/yr
S_2	-0.17 M m³/yr
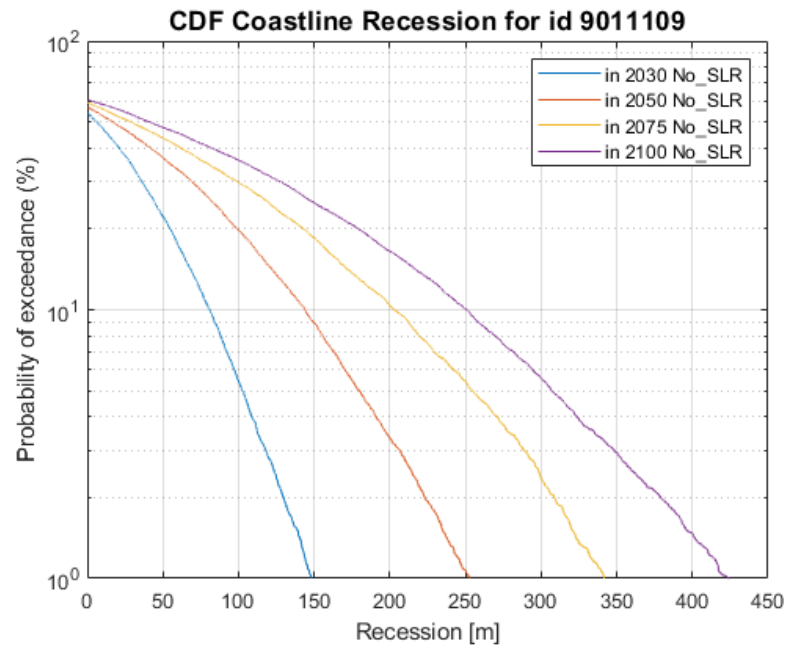
Fig C.8: Dutch Beach Lines between 1843 and 1980

Fig C.7: Exceedance probability curves of coastal recession, under no SLR scenario
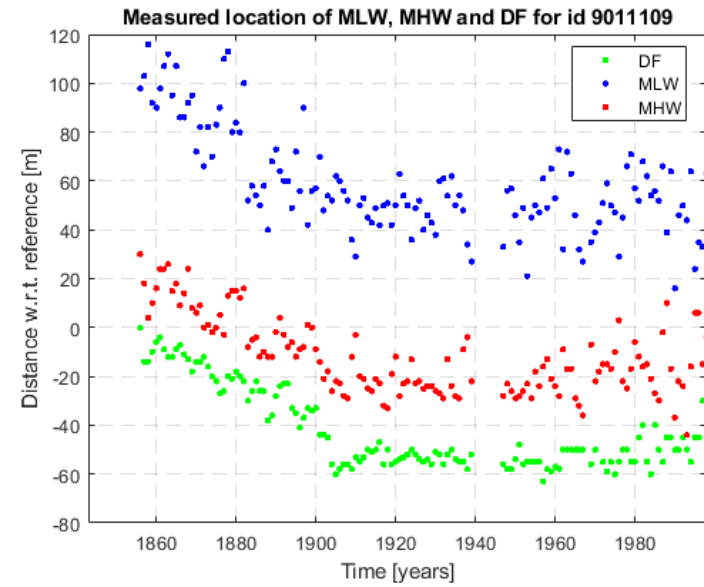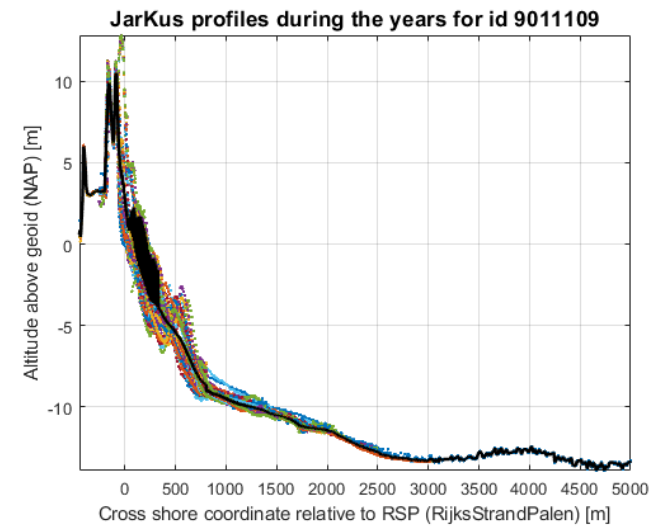
Fig C.9: JarKus transect (measurements from 1965 up to present)
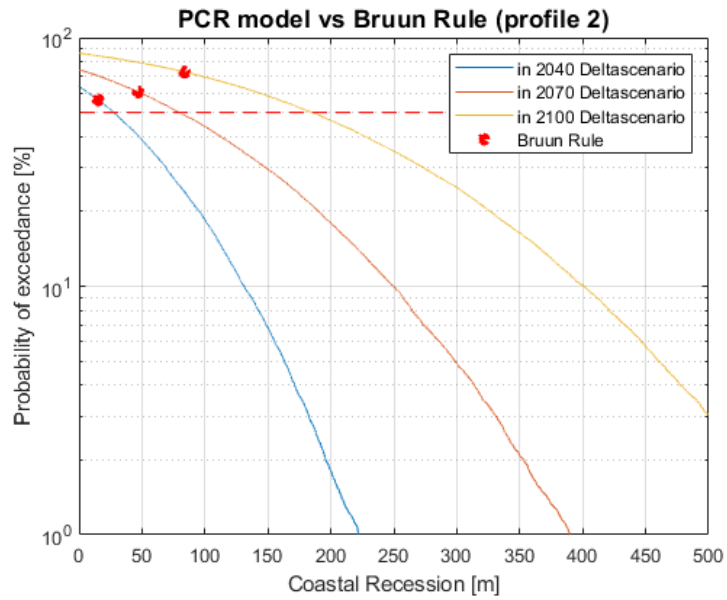
Fig C.10: PCR vs Bruun rule for Deltascenario
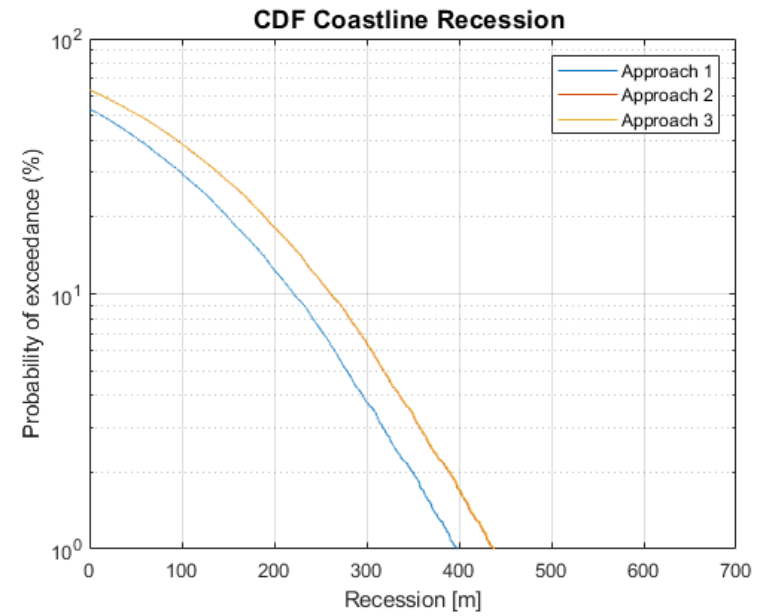
Fig C.12: Recession range for the profile 2, for the three RR
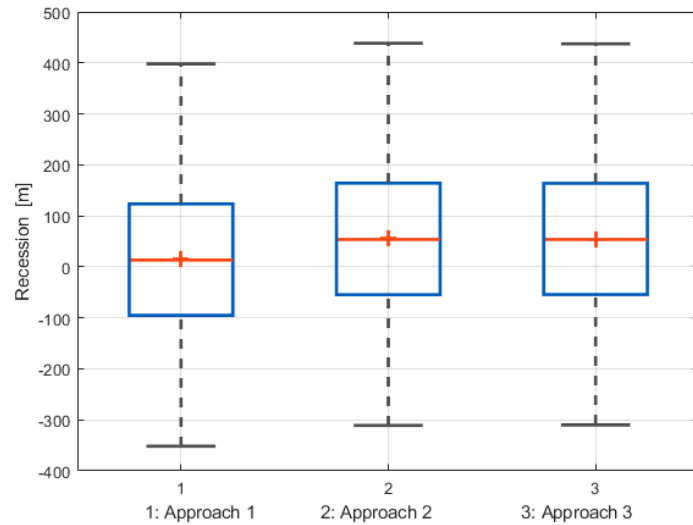
Fig C.11: Comparison among the three RR approaches

Profile 3

JarKus id	9009795
Dune crest level above NAP	17 m
Active height	31.50 m
Years of observations	1920-1970
Trend	Accretive ΔCL_rate = 0.43 m/year
UB Rays	22-23
S_1	-0.360 M m³/yr
S_2	-0.355 M m³/yr

Fig C.14: Dutch Beach Lines between 1843 and 1980
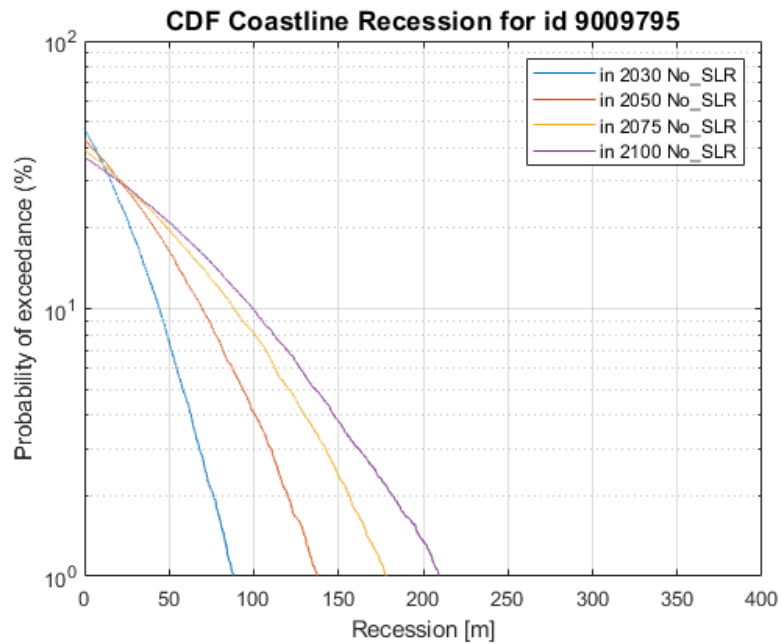
Fig C.13: Exceedance probability curves of coastal recession, under no SLR scenario
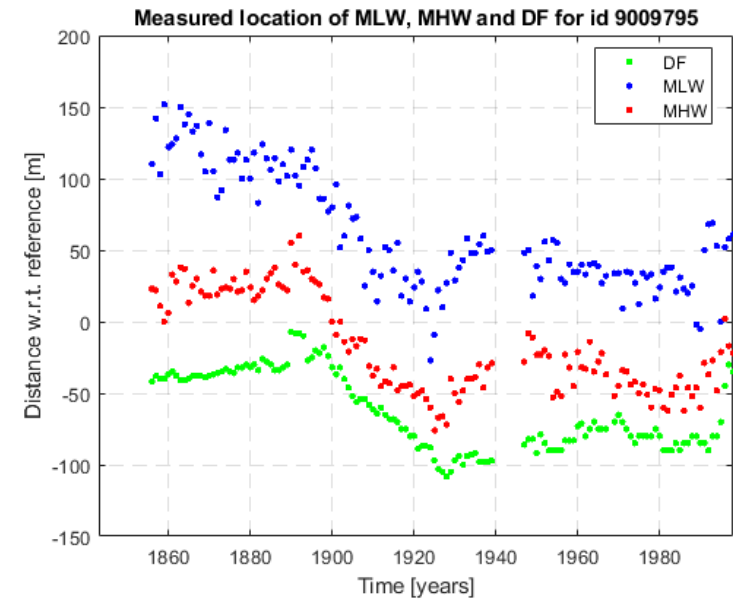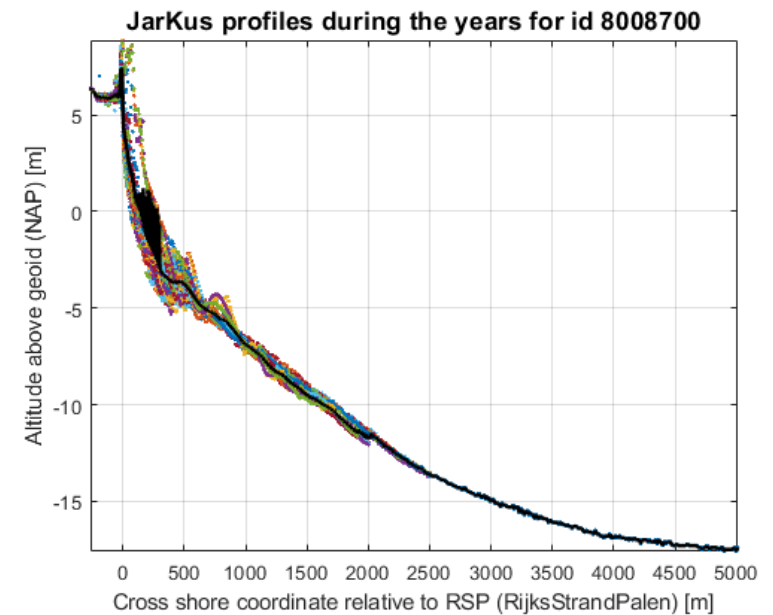

*Fig C.15: JarKus transect (measurements from 1965 up to present)*
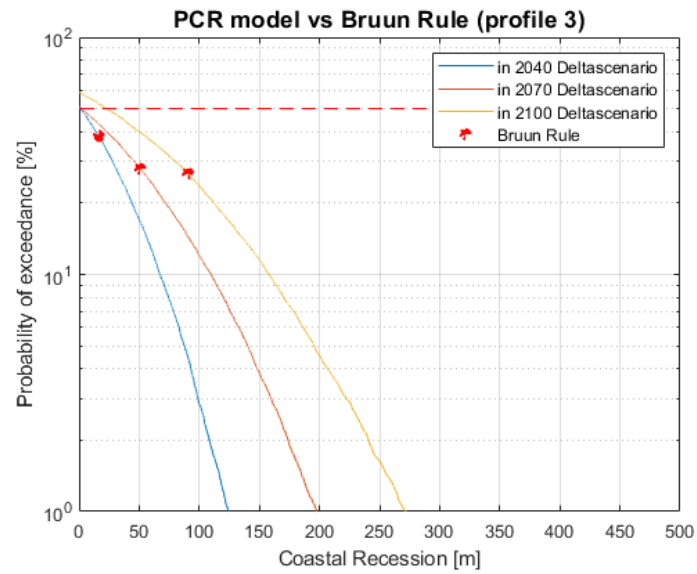
Fig C.16: PCR vs Bruun rule for Deltascenario

Fig C.18: Recession range for the profile 3, for the three RR
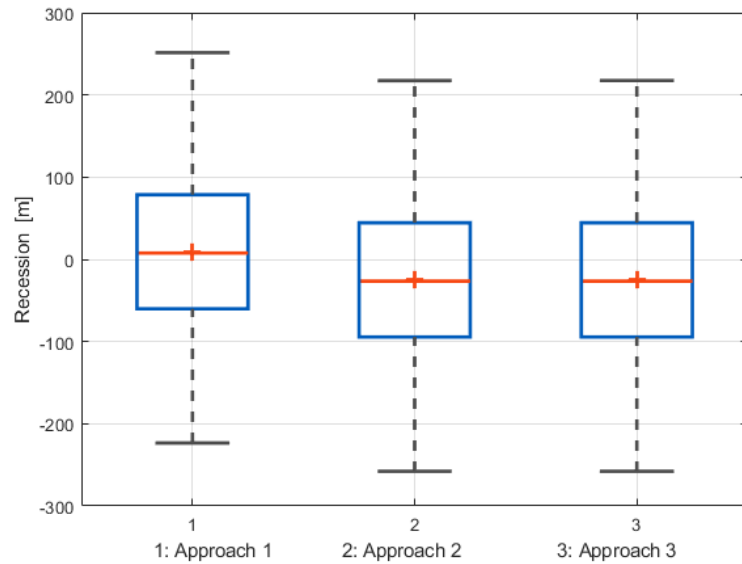
Fig C.17: Comparison among the three RR approaches

Profile 4

JarKus id	8008700
Dune crest level above NAP	8.5 m
Active height	23.27 m
Years of observations	1910-1980
Trend	Accretive ΔCL_rate = 0.002 m/year
UB Rays	31-32
S_1	-0.264 M m³/yr
S_2	-0.257 M m³/yr
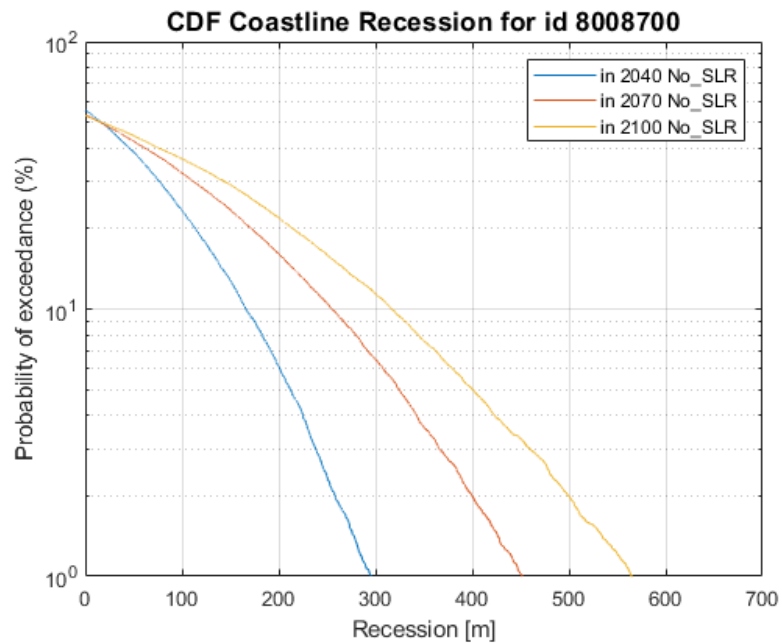
Fig C.20: Dutch Beach Lines between 1843 and 1980

Fig C.19: Exceedance probability curves of coastal recession, under no SLR scenario
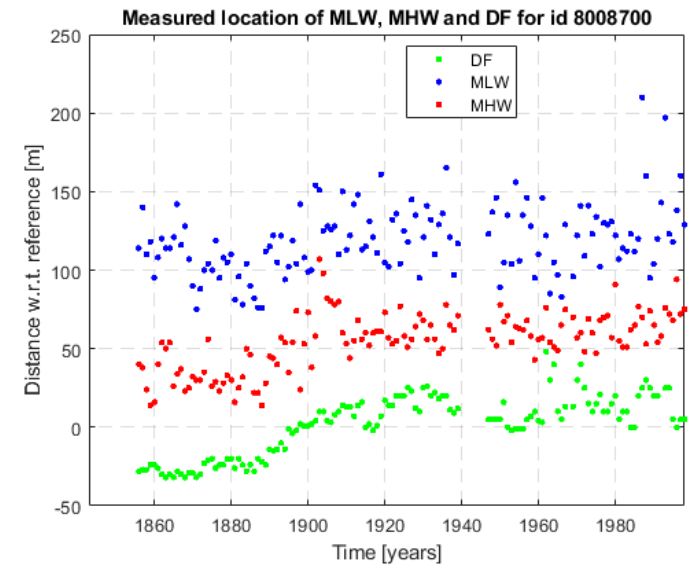
Fig C.21: JarKus transect (measurements from 1965 up to present)
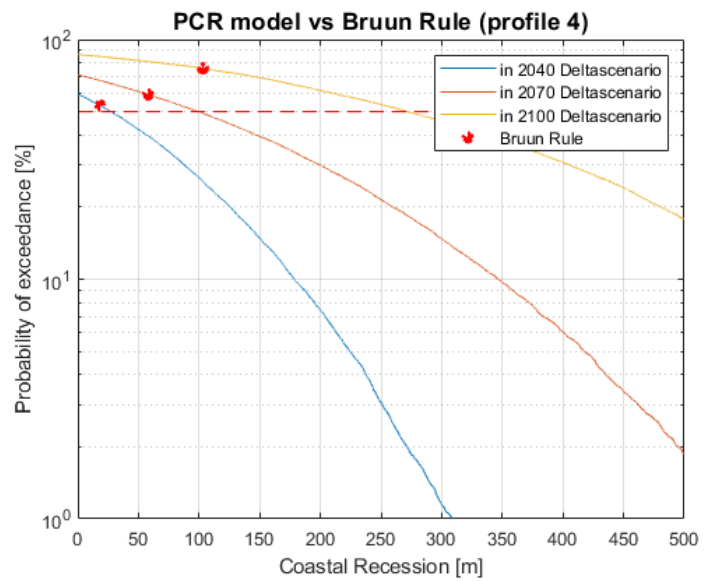
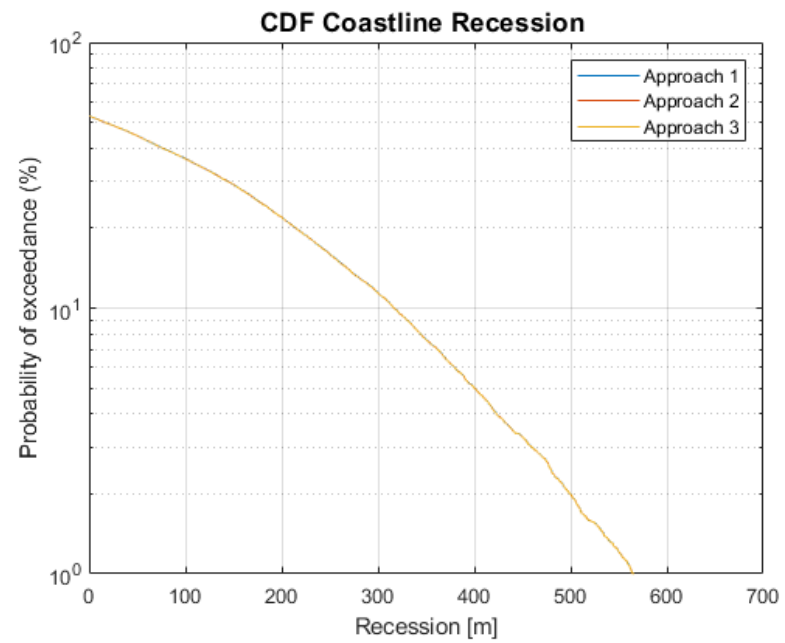*Fig C.22: PCR vs Bruun rule for Deltascenario*

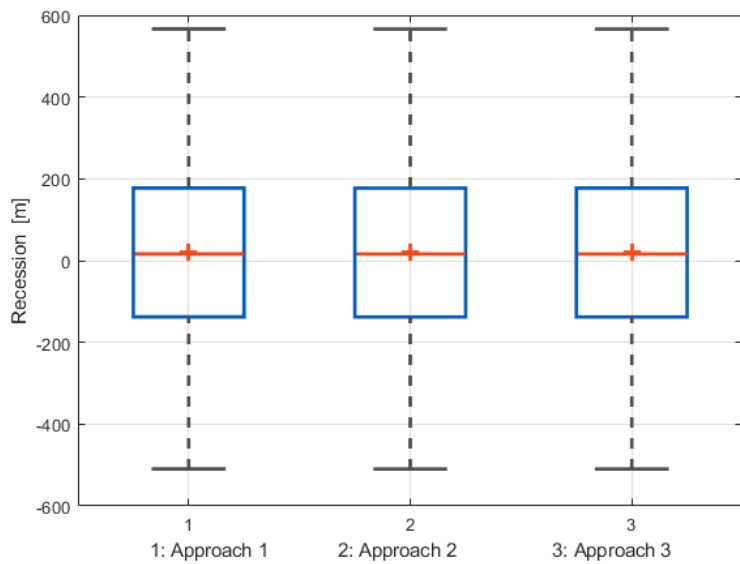*Fig C.24: Recession range for the profile 4, for the three RR*

Fig C.23: Comparison among the three RR approaches

Profile 5

JarKus id	8007600
Dune crest level above NAP	18.5 m
Active height	33.39 m
Years of observations	1843-1970
Trend	Accretive ΔCL_rate = 0.37 m/year
UB Rays	40-41
S_1	-0.168 M m³/yr
S_2	-0.169 M m³/yr

Fig C.26: Dutch Beach Lines between 1843 and 1980

Fig C.25: Exceedance probability curves of coastal recession, under no SLR scenario
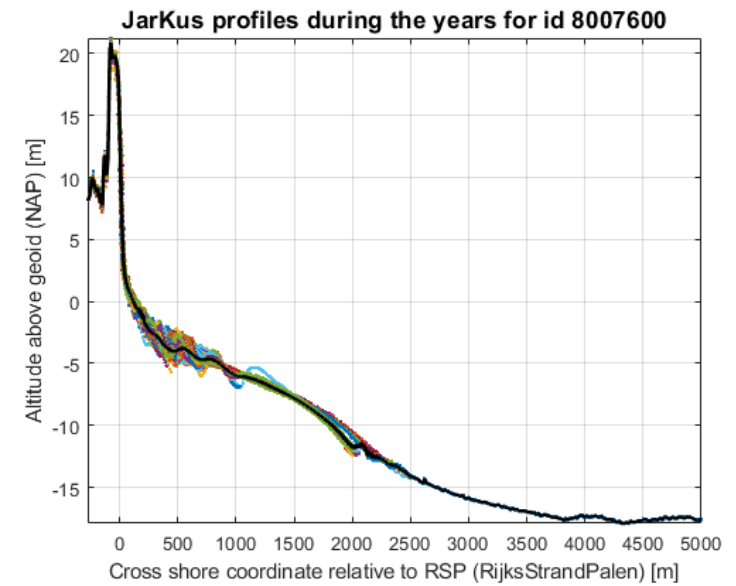

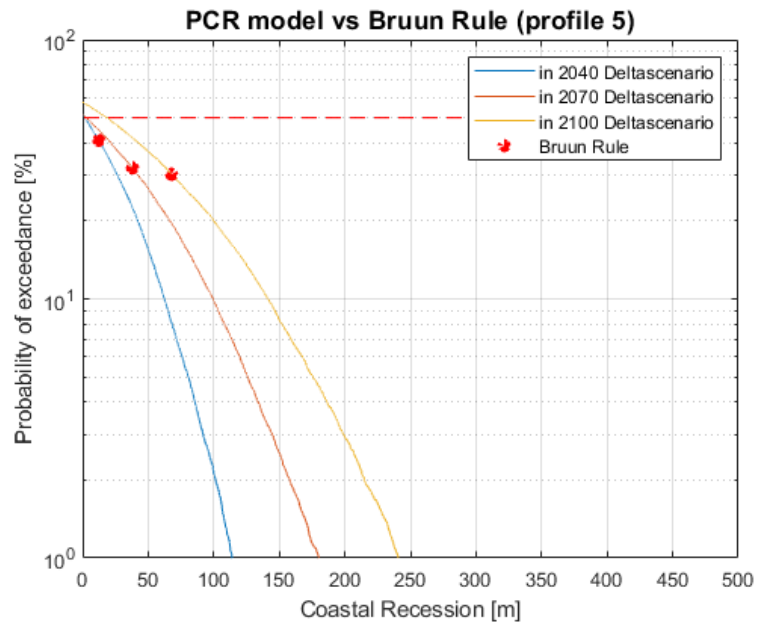*Fig C.27: JarKus transect (measurements from 1965 up to present)*

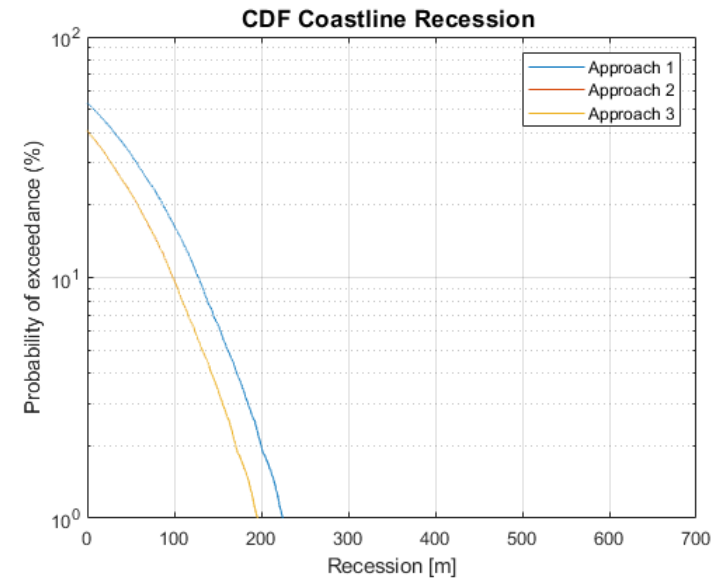Fig C.28: PCR vs Bruun rule for Deltascenario

Fig C.30: Recession range for the profile 5, for the three RR
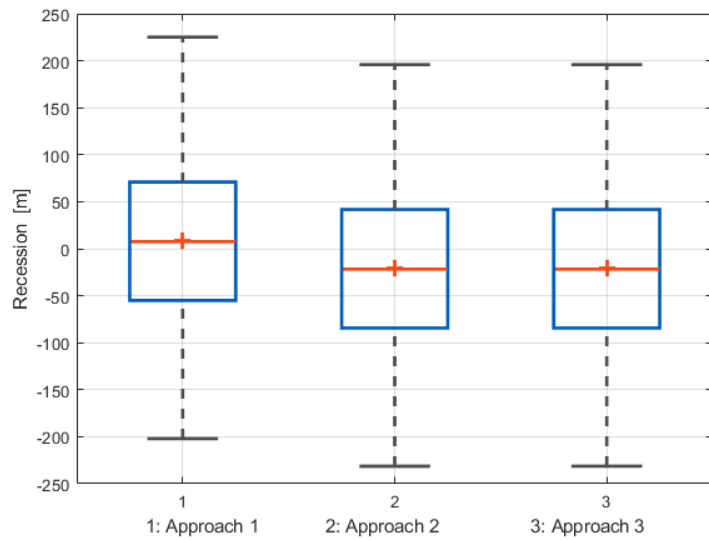
Fig C.29: Comparison among the three RR approaches

Profile 6

JarKus id	8006200
Dune crest level above NAP	20.5 m
Active height	35.33 m
Years of observations	1843-1966
Trend	Accretive ΔCL_rate = 0.63 m /year
UB Rays	50-51
S_1	-0.16 M m³/yr
S_2	-0.22 M m³/yr
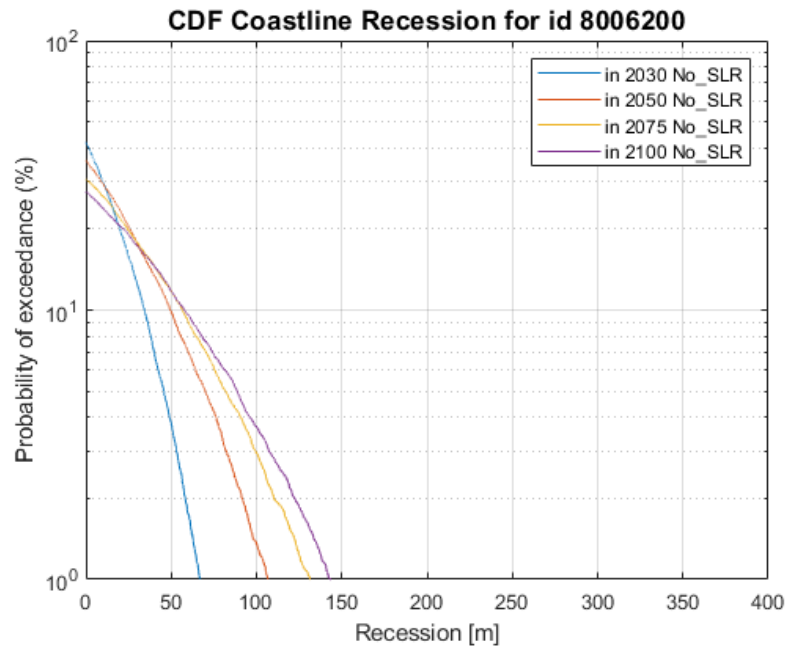
Fig C.32: Dutch Beach Lines between 1843 and 1980

Fig C.31: Exceedance probability curves of coastal recession, under no SLR scenario
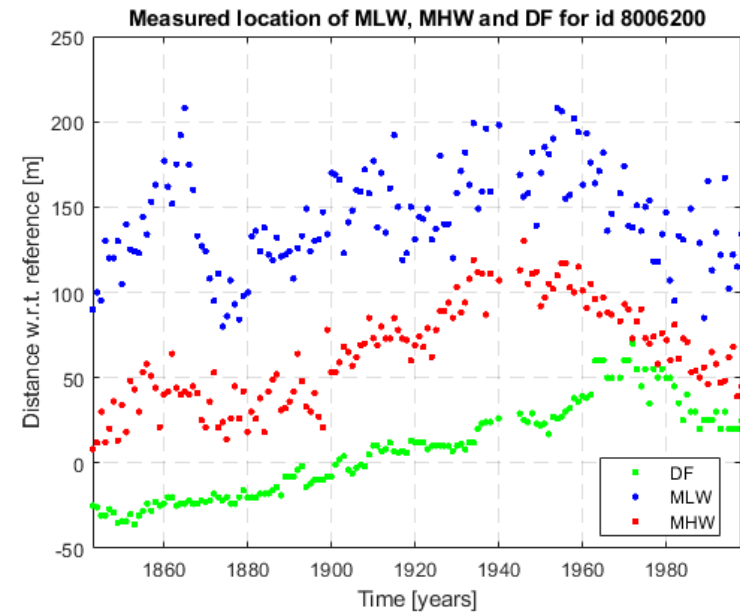
Fig C.33: JarKus transect (measurements from 1965 up to present)
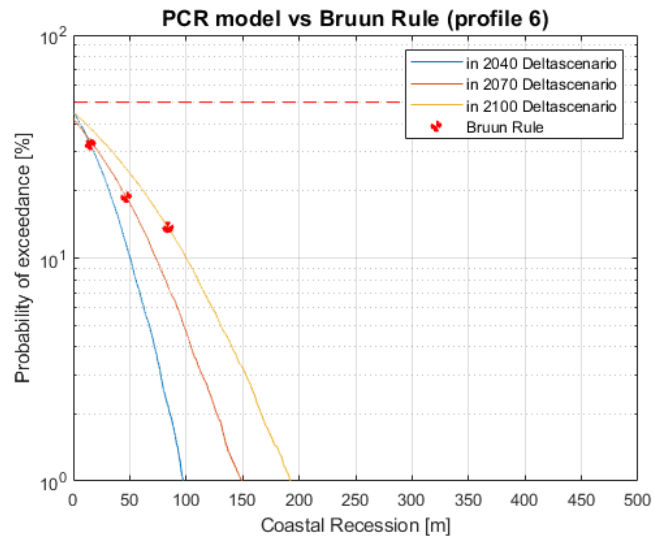
Fig C.34: PCR vs Bruun rule for Deltascenario
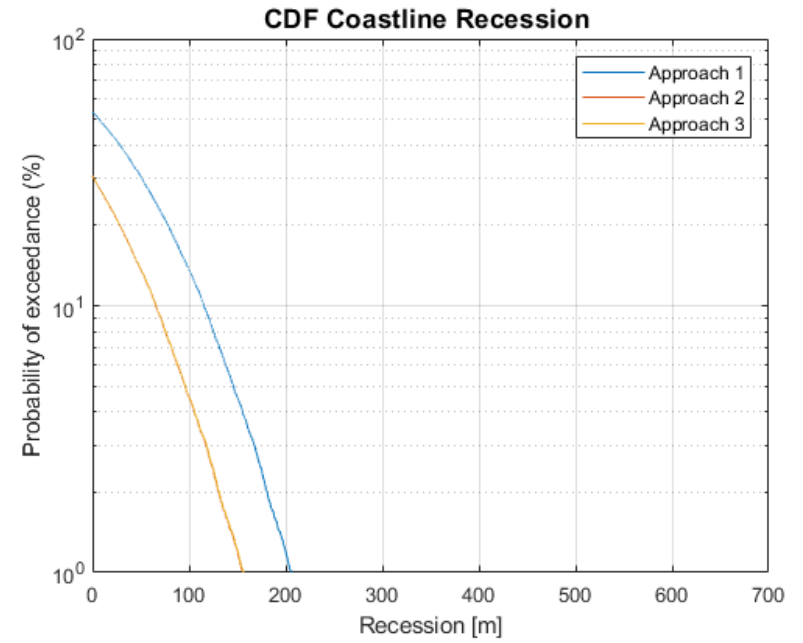
Fig C.36: Recession range for the profile 6, for the three RR
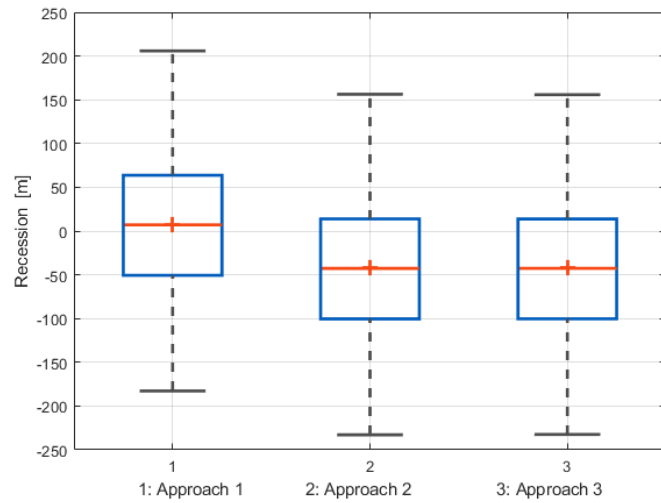
Fig C.35: Comparison among the three RR approaches

Profile 7

JarKus id	7005100
Dune crest level above NAP	20
Active height	35.02 m
Years of observations	1843-1960
Trend	Erosive ΔCL_rate = -0.13 m/year
UB Rays	60-61
S_1	0.14 M m³/yr
S_2	0.10 M m³/yr
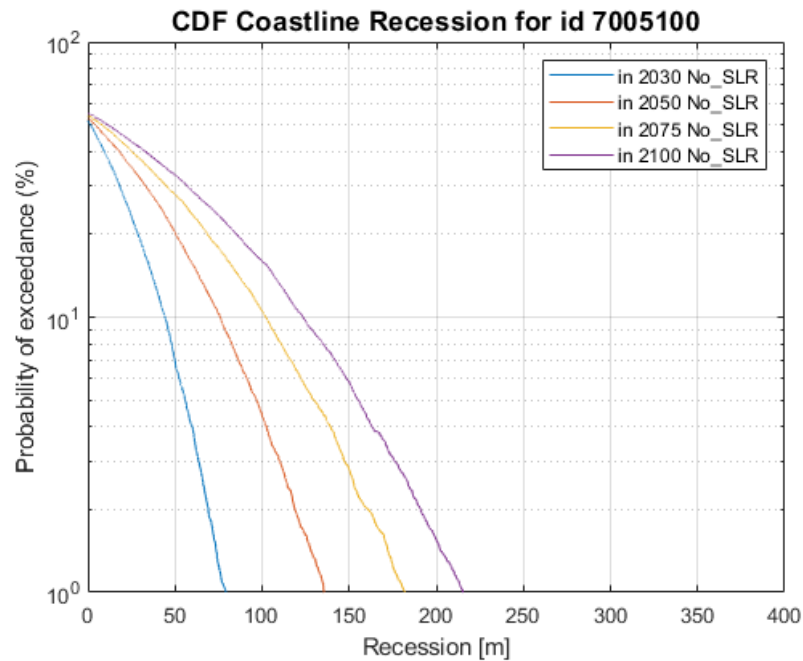
Fig C.38: Dutch Beach Lines between 1843 and 1980

Fig C.37: Exceedance probability curves of coastal recession, under no SLR scenario
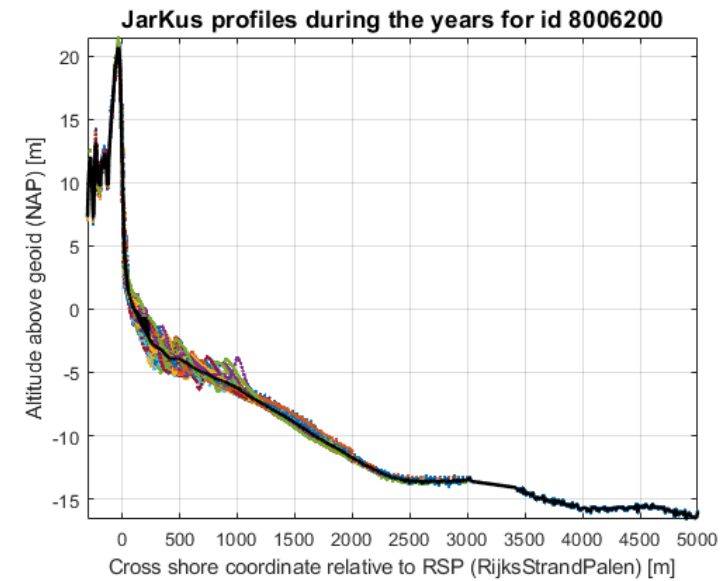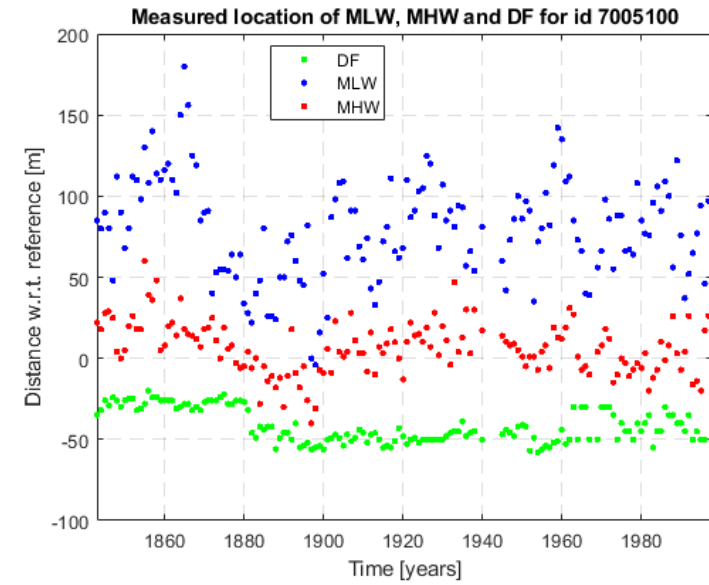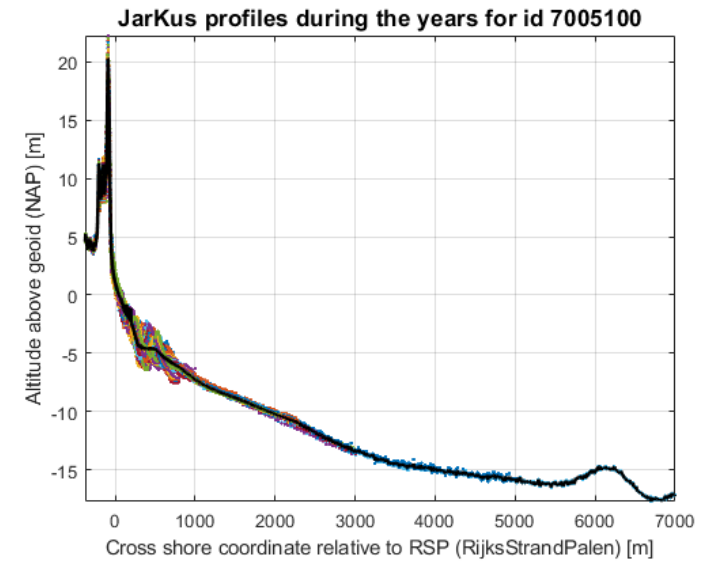

*Fig C.39: JarKus transect (measurements from 1965 up to present)*
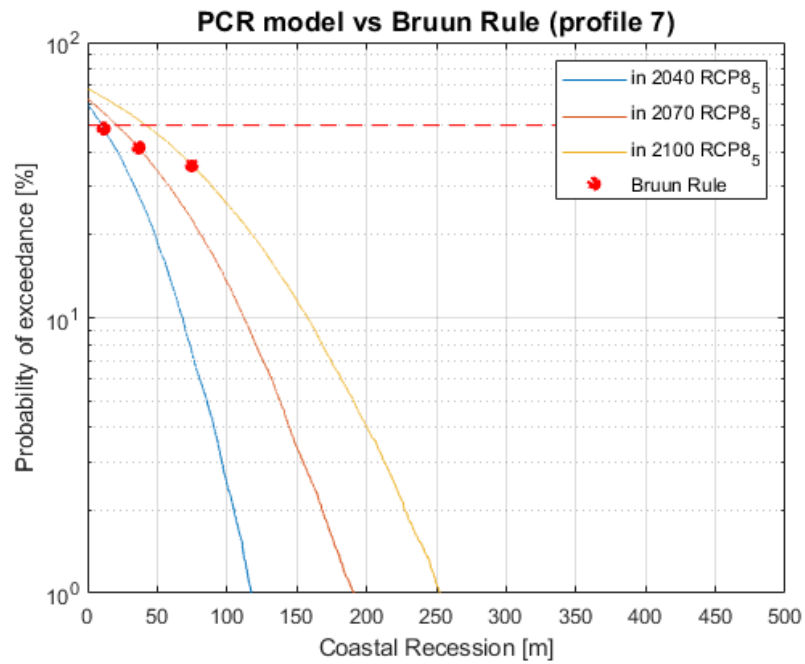
Fig C.40: PCR vs Bruun rule for Deltascenario
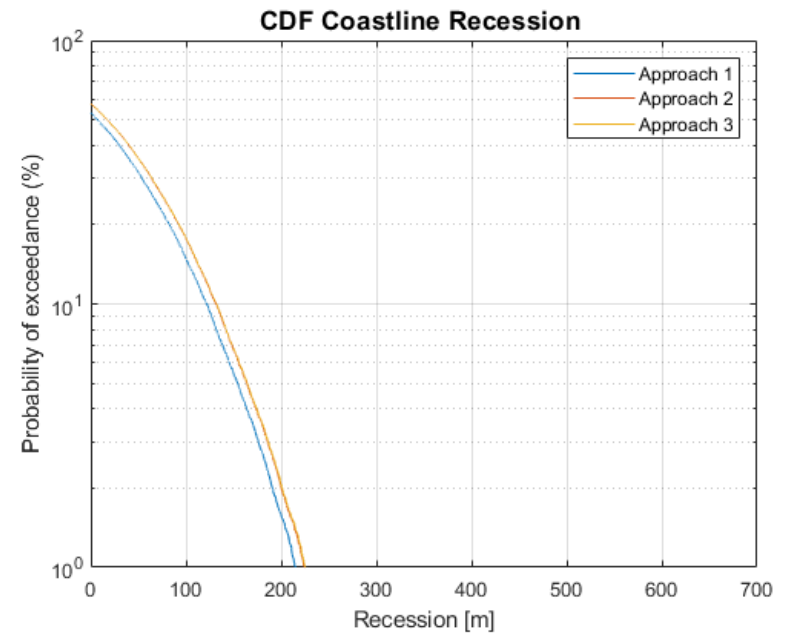
Fig C.42: Recession range for the profile 7, for the three RR
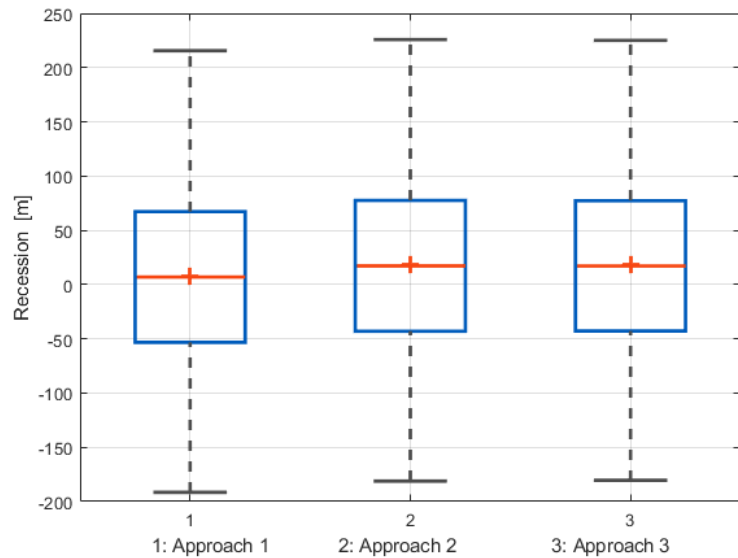
Fig C.41: Comparison among the three RR approaches

Profile 8

JarKus id	7004100
Dune crest level above NAP	21 m
Active height	36.58 m
Years of observations	1843-1960
Trend	Accretive ΔCL_rate = 0.15 m/year
UB Rays	70-71
S_1	0.0463 M m³/yr
S_2	0.0458 M m³/yr

Fig C.44: Dutch Beach Lines between 1843 and 1980
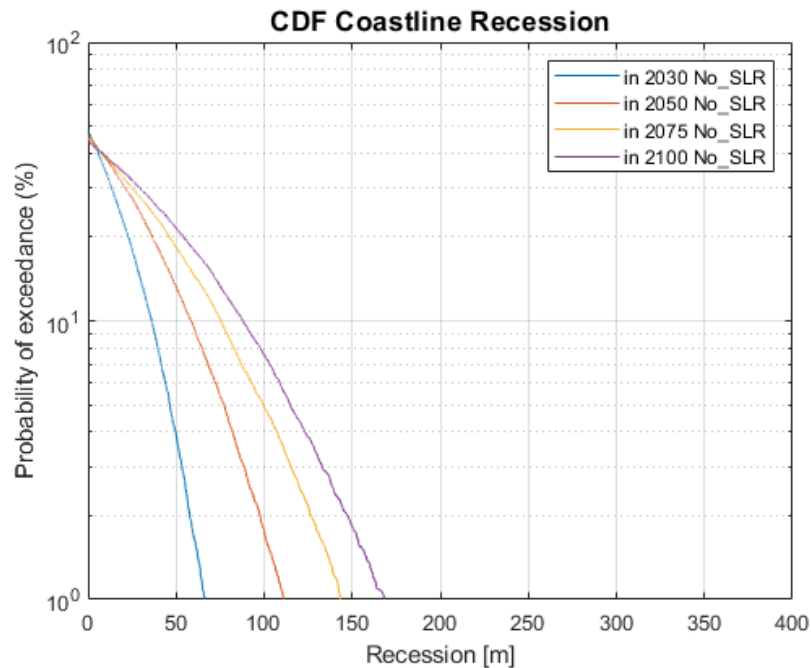
Fig C.43: Exceedance probability curves of coastal recession, under no SLR scenario
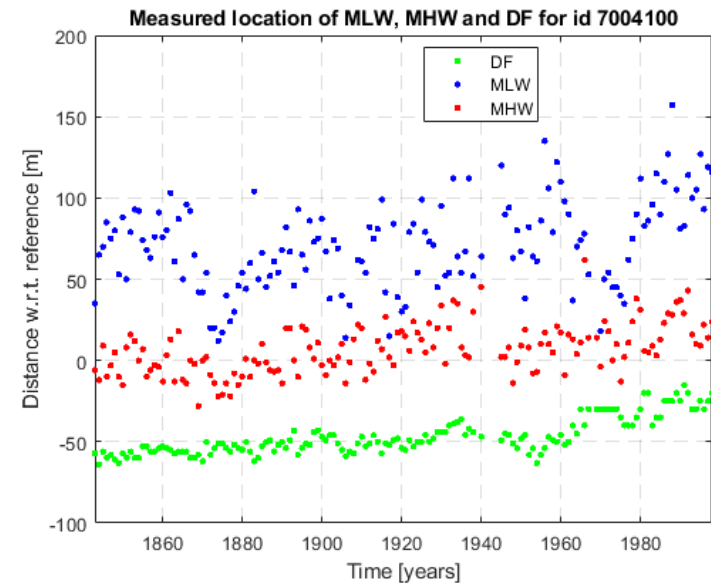
Fig C.45: JarKus transect (measurements from 1965 up to present)

Fig C.46: PCR vs Bruun rule for Deltascenario
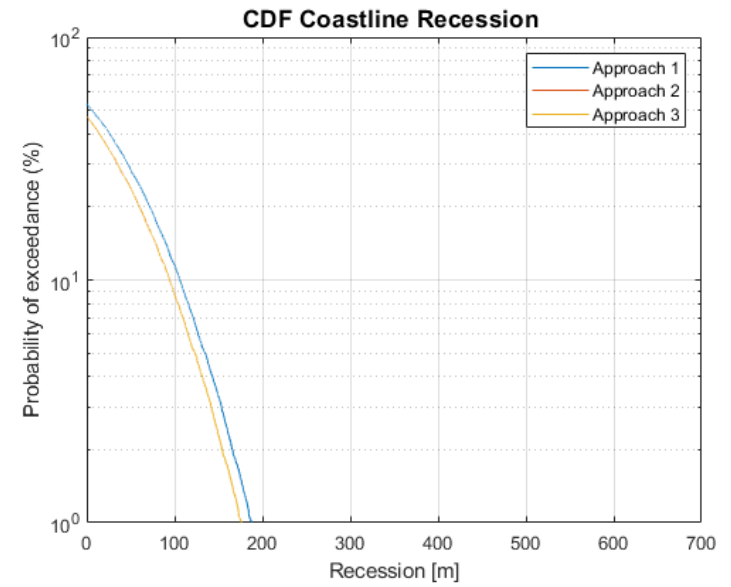
Fig C.48: Recession range for the profile 8, for the three RR
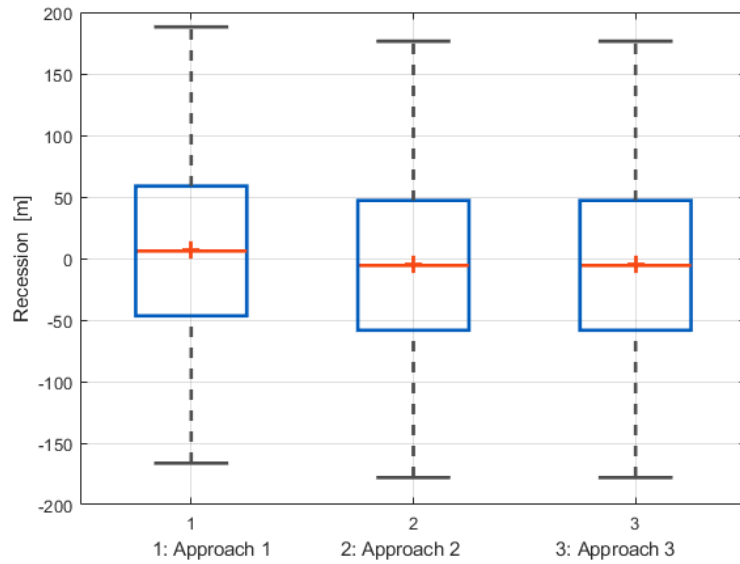
Fig C.47: Comparison among the three RR approaches

Profile 9

JarKus id	7003100
Dune crest level above NAP	14 m
Active height	30.04 m
Years of observations	1843-1952
Trend	Erosive ΔCL_rate = -0.77 m/year
UB Rays	80-81
S_1	0.06 M m³/yr
S_2	0.02 M m³/yr
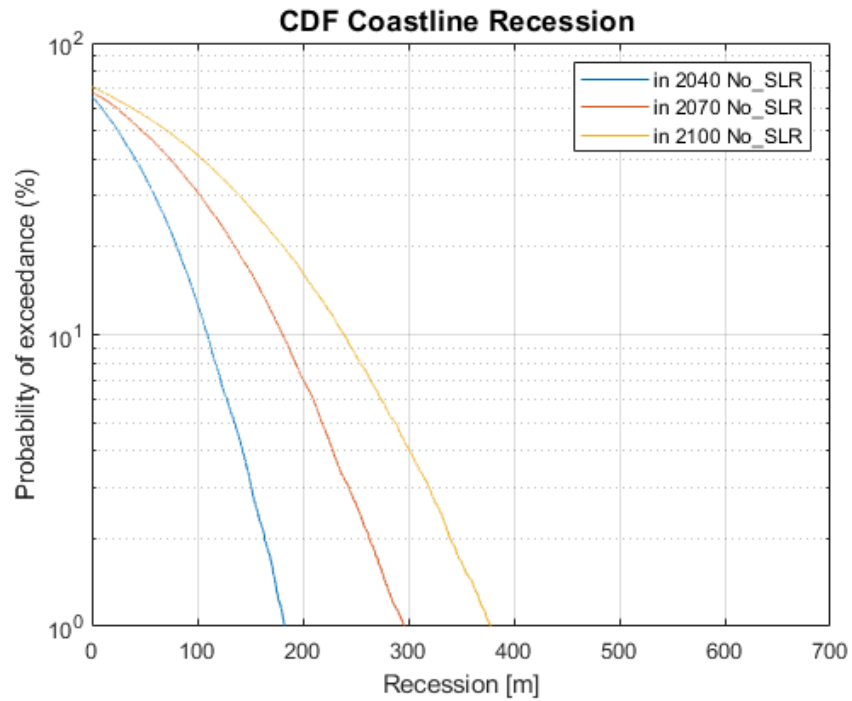
Fig C.50: Dutch Beach Lines between 1843 and 1980

Fig C.49: Exceedance probability curves of coastal recession, under no SLR scenario
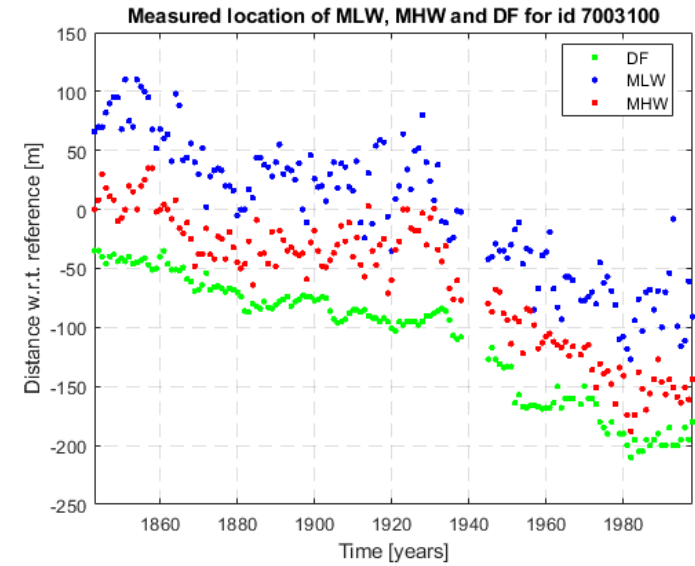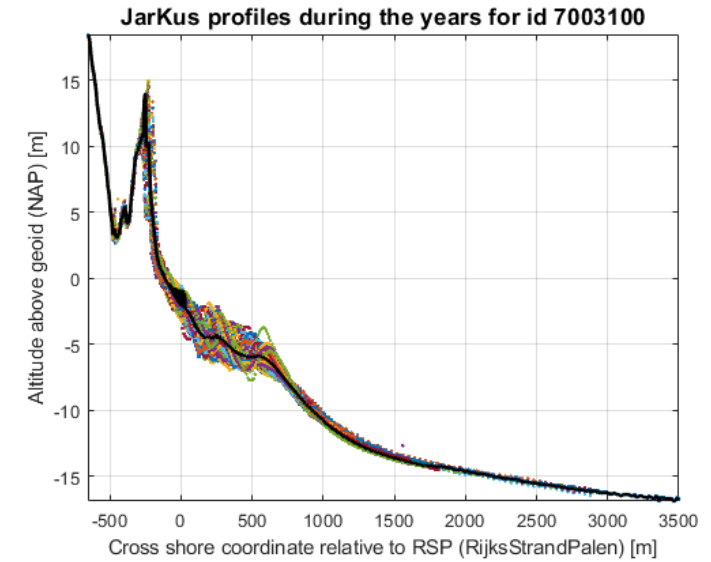
Fig C.51: JarKus transect (measurements from 1965 up to present)

Profile 10

JarKus id	7001990
Dune crest level above NAP	11.75 m
Active height	26.99 m
Years of observations	1843-1950
Trend	Erosive ΔCL_rate = -0.83 m/year
UB Rays	91-92
S_1	-0.70 M m³/yr
S_2	-0.37 M m³/yr

Fig C.53: Dutch Beach Lines between 1843 and 1980

*Fig C.52: Exceedance probability curves of coastal recession, under no SLR scenario*
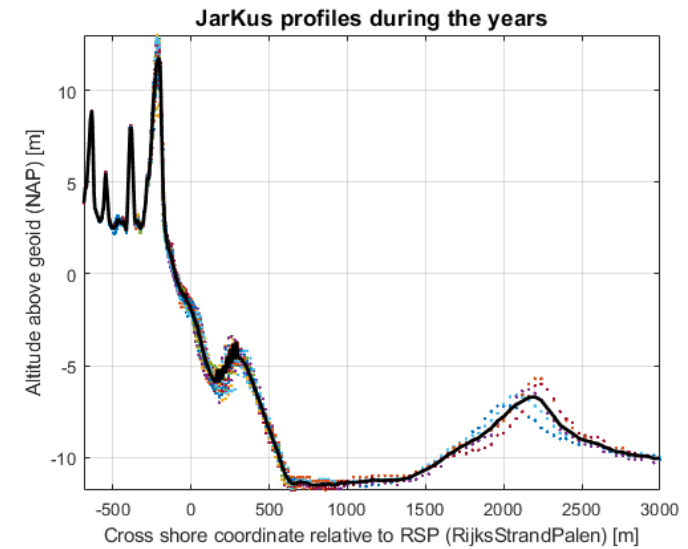
*Fig C.54: JarKus transect (measurements from 1965 up to present)*
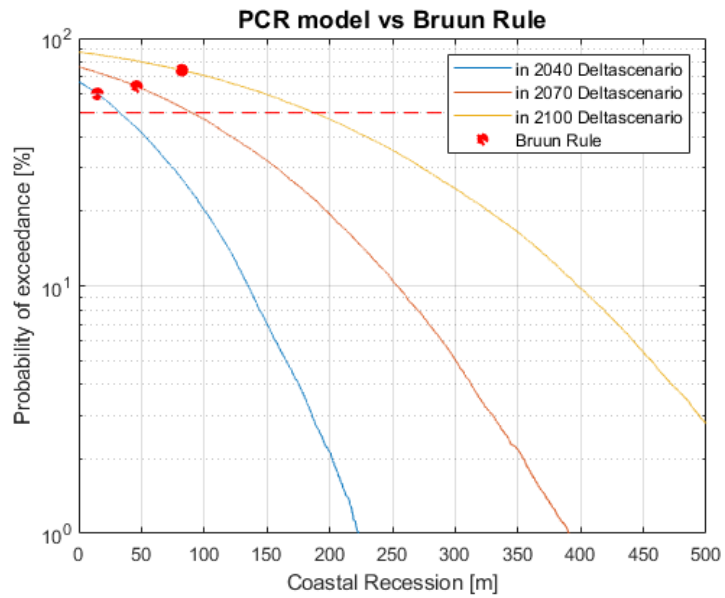
Fig C.55: PCR vs Bruun rule for Deltascenario
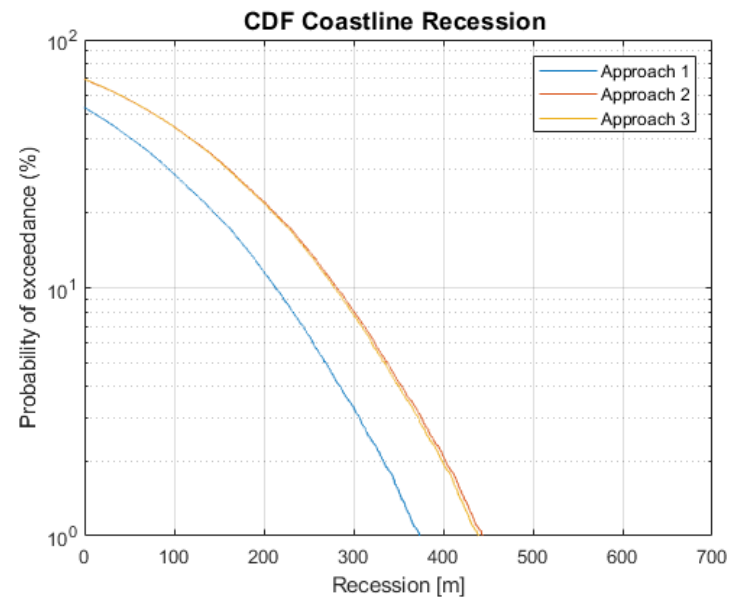
Fig C.57: Recession range for the profile 10, for the three RR
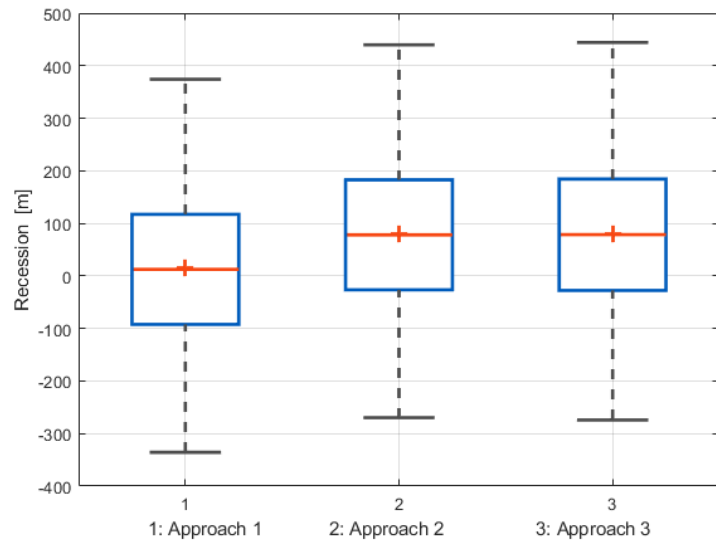
Fig C.56: Comparison among the three RR approaches

Profile 11

JarKus id	7000508
Dune crest level above NAP	17.42m
Active height	31.60 m
Years of observations	1843-1958
Trend	Erosive ΔCL_rate = -0.92 m/year
UB Rays	106-107
S_1	-0.54 M m³/yr
S_2	-0.51 M m³/yr

Fig C.59: Dutch Beach Lines between 1843 and 1980

Fig C.58: Exceedance probability curves of coastal recession, under no SLR scenario
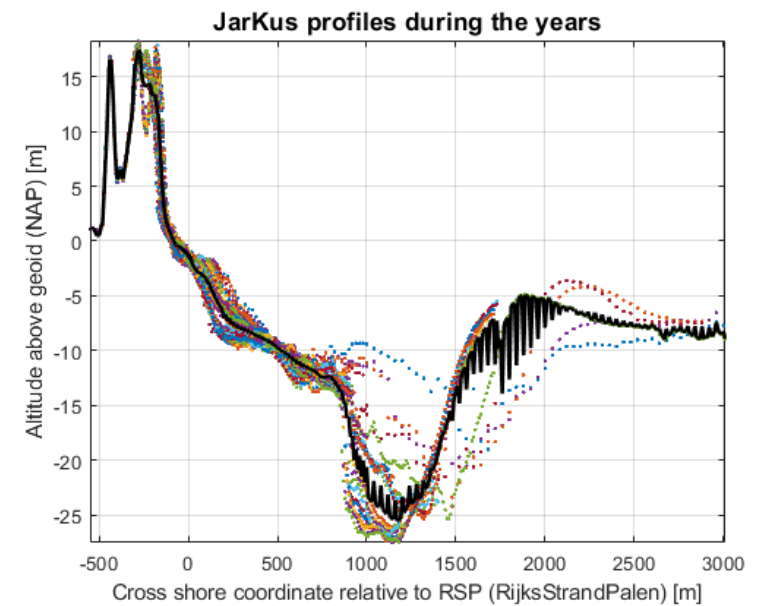
Fig C.60: JarKus transect (measurements from 1965 up to present)
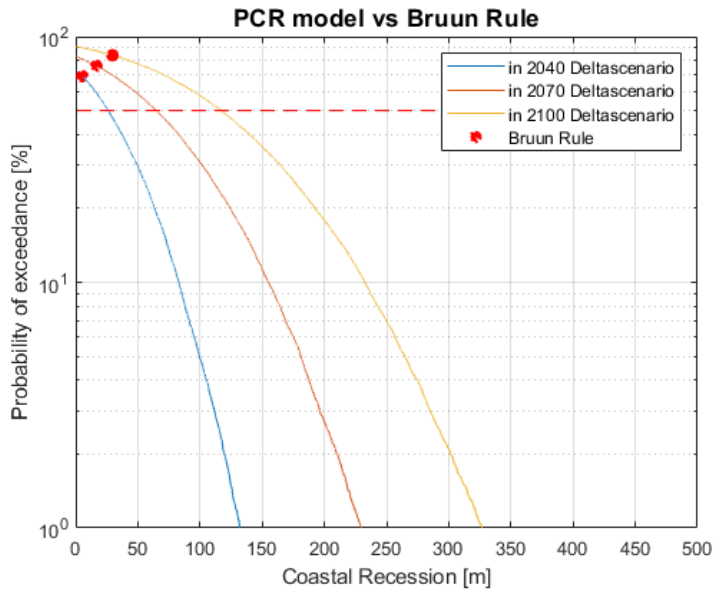
Fig C.61: PCR vs Bruun rule for Deltascenario
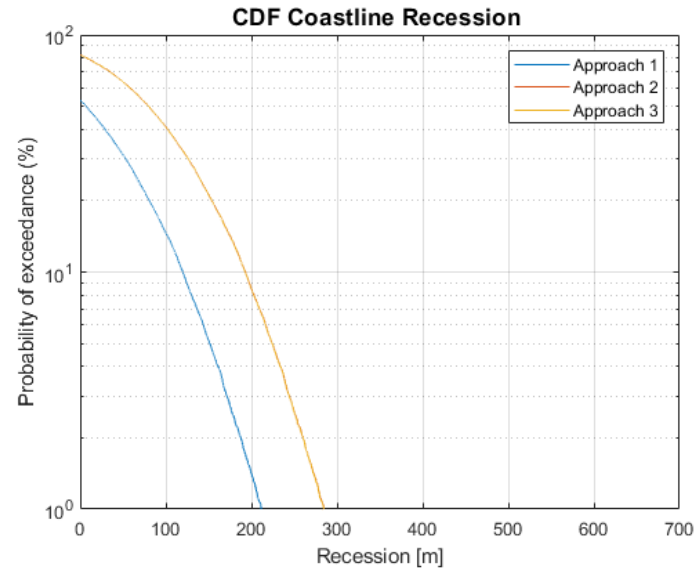
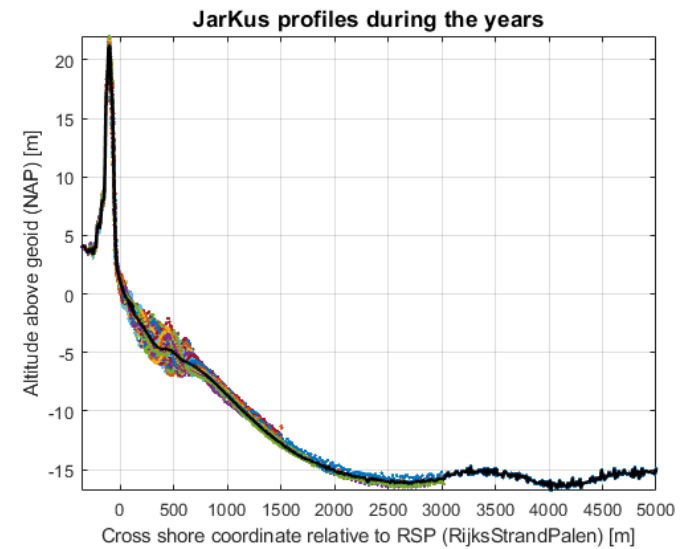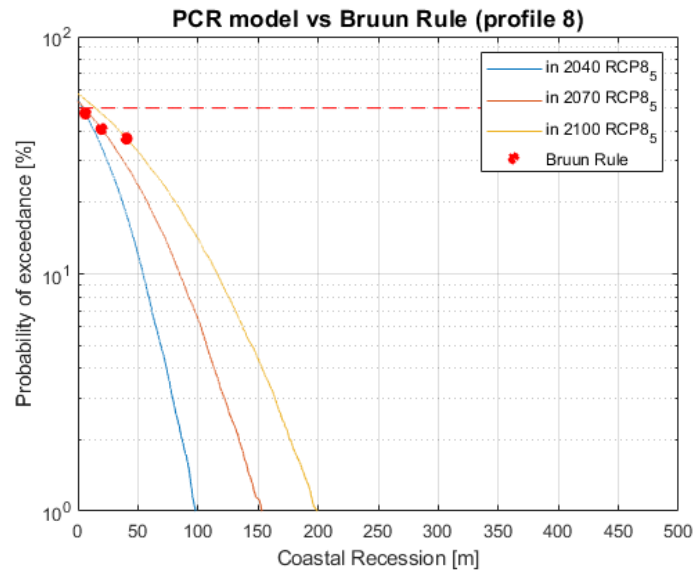Fig C.63: Recession range for the profile 11, for the three RR
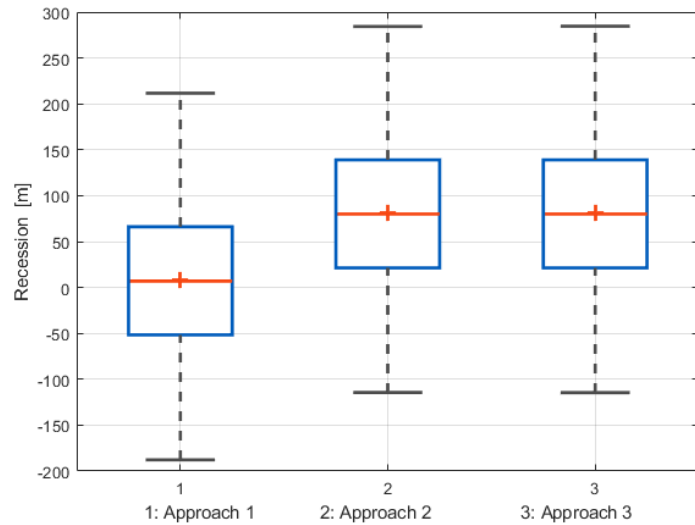
Fig C.62: Comparison among the three RR approaches

Appendix C

Table_ C.1: Recovery rate in cross-shore direction along the Holland coast

Profile	Approach 1		Approach 2		Approach 3	
	(m/day)	(m³/m/day)	(m/day)	(m³/m/day)	(m/day)	(m³/m/day)
1	0.1014	2.6319	0.1032	2.6798	0.1028	2.6684
2	0.1174	2.9644	0.1159	2.9274	0.1084	2.7372
3	0.0734	2.3139	0.0747	2.3527	0.0751	2.3667
4	0.1648	3.8351	0.1648	3.8353	0.1657	3.8561
5	0.0659	2.1992	0.0669	2.2345	0.0669	2.2327
6	0.0596	2.1044	0.0614	2.1679	0.0578	2.0424
7	0.0625	2.1897	0.0622	2.1767	0.0567	1.9873
8	0.0540	1.9760	0.0544	1.9914	0.0544	1.9901
9	0.0920	2.7645	0.0898	2.6985	0.0863	2.5929
10	0.1066	2.8774	0.1042	2.8135	0.1368	3.6921
11	0.0574	1.8135	0.0548	1.7303	0.0564	1.7831

Table_ C.2: Length of each cell in km

Cell 1	Cell 2	Cell 3	Cell 4	Cell 5	Cell 6	Cell 7	Cell 8	Cell 9	Cell 10	Cell 11
4.4	10.1	12	10.4	12.1	14.1	8.8	10.2	10.9	13.4	13.1

Appendix D

P50, p10 and p1% values for the coastal profiles, under different SLR scenarios

Profile 1

Profile 1 Recession [m]	Year		
Prob. of exceedance	2040	2070	2100
No SLR			
P50%	-1	-20	-40
P10%	87	120	136
P1%	164	244	287
RCP4.5			
P50%	1	1	14
P10%	91	141	193
P1%	168	266	347
RCP8.5			
P50%	2	2	28
P10%	91	114	209
P1%	167	269	363
Deltascenario			
P50%	3	12	57
P10%	93	1 55	240
P1%	170	282	396

Profile 1 Erosion volume [m³/m]	Year		
Prob. of exceedance	2040	2070	2100
No SLR			
P50%	-32	-532	-1043
P10%	2276	3117	3535
P1%	4263	6342	7448
RCP4.5			
P50%	36	36	352
P10%	2356	3653	5019
P1%	4351	6910	8999
RCP8.5			
P50%	42	42	736
P10%	2362	3735	5431
P1%	4358	6992	9427
Deltascenario			
P50%	76	317	1484
P10%	2402	4033	6220
P1%	4404	7309	10270

Profile 2

Profile 2 Recession [m]	Year		
Prob. of exceedance	2040	2070	2100
No SLR			
P50%	22	36	54
P10%	125	202	261
P1%	215	339	437
RCP4.5			
P50%	25	62	126
P10%	129	230	338
P1%	219	369	516
RCP8.5			
P50%	25	65	146
P10%	129	234	359
P1%	220	373	538
Deltascenario			
P50%	27	80	185
P10%	131	249	401
P1%	222	390	583

Profile 2 Erosion volume [m³/m]	Year		
Prob. of exceedance	2040	2070	2100
No SLR			
P50%	548	907	1359
P10%	3153	5097	6589
P1%	5430	8560	11045
RCP4.5			
P50%	637	1556	3187
P10%	3255	5801	8530
P1%	5540	9316	13028
RCP8.5			
P50%	644	1653	3700
P10%	3263	5904	9085
P1%	5548	9425	13582
Deltascenario			
P50%	690	2016	4682
P10%	3314	6298	10134
P1%	5605	9842	14716

Profile 3

Profile 3 Recession [m]	Year		
Prob. of exceedance	2040	2070	2100
No SLR			
P50%	-1	-14	-27
P10%	65	92	106
P1%	122	178	217
RCP4.5			
P50%	0.2	-4.5	0.8
P10%	66	102	135
P1%	124	190	248
RCP8.5			
P50%	-3	0.3	8
P10%	66	104	143
P1%	123	192	256
Deltascenario			
P50%	1	2	23
P10%	67	110	158
P1%	125	198	272

Profile 3 Erosion volume [m³/m]	Year		
Prob. of exceedance	2040	2070	2100
No SLR			
P50%	-37	-452	-836
P10%	2040	2891	3332
P1%	3840	5630	6851
RCP4.5			
P50%	-142	7	26
P10%	2087	3225	4248
P1%	3894	5989	7811
RCP8.5			
P50%	-98	10	259
P10%	2091	3277	4497
P1%	3898	6040	8077
Deltascenario			
P50%	31	70	716
P10%	2116	3459	4975
P1%	3926	6233	8573

Profile 4

Profile 4 Recession [m]	Year		
Prob. of exceedance	2040	2070	2100
No SLR			
P50%	16	15	16
P10%	166	255	317
P1%	295	452	566
RCP4.5			
P50%	23	64	155
P10%	174	308	464
P1%	303	509	720
RCP8.5			
P50%	24	71	194
P10%	174	316	506
P1%	304	517	763
Deltascenario			
P50%	27	99	272
P10%	178	347	588
P1%	309	548	848

Profile 4 Erosion volume [m³/m]	Year		
Prob. of exceedance	2040	2070	2100
No SLR			
P50%	384	353	378
P10%	3864	5940	7366
P1%	6873	10523	13180
RCP4.5			
P50%	542	1495	3604
P10%	4040	7178	10796
P1%	7072	11842	16764
RCP8.5			
P50%	554	1661	4520
P10%	4052	7364	11775
P1%	7089	12035	17758
Deltascenario			
P50%	635	2315	6320
P10%	4148	8070	13679
P1%	7194	12760	19740

Profile 5

Profile 5 Recession [m]	Year		
Prob. of exceedance	2040	2070	2100
No SLR			
P50%	-0.1	-11	-22
P10%	60	85	99
P1%	112	165	196
RCP4.5			
P50%	1	0.2	0.3
P10%	62	94	122
P1%	113	174	221
RCP8.5			
P50%	1	2	6
P10%	62	95	129
P1%	113	175	228
Deltascenario			
P50%	2	3	18
P10%	62	99	142
P1%	114	180	241

Profile 5 Erosion volume [m³/m]	Year		
Prob. of exceedance	2040	2070	2100
No SLR			
P50%	-3	-362	-725
P10%	2020	2834	3295
P1%	3738	5497	6543
RCP4.5			
P50%	34	22	11
P10%	2060	3125	4087
P1%	3784	5803	7380
RCP8.5			
P50%	37	54	216
P10%	2064	3165	4304
P1%	3788	5848	7602
Deltascenario			
P50%	56	93	608
P10%	2086	3322	4725
P1%	3812	6018	8041

Profile 6

Profile 6 Recession [m]	Year		
Prob. of exceedance	2040	2070	2100
No SLR			
P50%	-6	-25	-43
P10%	49	61	66
P1%	96	137	156
RCP4.5			
P50%	-5	-18	-25
P10%	50	68	85
P1%	97	144	177
RCP8.5			
P50%	-5	-17	-20
P10%	50	69	90
P1%	97	145	182
Deltascenario			
P50%	-4	-14	-14
P10%	51	73	100
P1%	98	149	192

Profile 6 Erosion volume [m³/m]	Year		
Prob. of exceedance	2040	2070	2100
No SLR			
P50%	-209	-868	-1508
P10%	1727	2167	2315
P1%	3384	4828	5505
RCP4.5			
P50%	-177	-640	-874
P10%	1762	2415	2996
P1%	3423	5091	6236
RCP8.5			
P50%	-174	-607	-701
P10%	1766	2451	3183
P1%	3426	5129	6430
Deltascenario			
P50%	-158	-481	-489
P10%	1785	2586	3535
P1%	3447	5272	6796

Profile 7

Profile 7 Recession [m]	Year		
Prob. of exceedance	2040	2070	2100
No SLR			
P50%	9	13	17
P10%	67	104	132
P1%	116	182	225
RCP4.5			
P50%	10	20	37
P10%	68	111	152
P1%	117	190	247
RCP8.5			
P50%	10	21	42
P10%	68	112	158
P1%	117	191	253
Deltascenario			
P50%	11	25	52
P10%	69	117	168
P1%	118	196	265

Profile 7 Erosion volume [m³/m]	Year		
Prob. of exceedance	2040	2070	2100
No SLR			
P50%	319	454	601
P10%	2340	3628	4610
P1%	4066	6377	7884
RCP4.5			
P50%	352	698	1282
P10%	2378	3893	5327
P1%	4110	6658	8640
RCP8.5			
P50%	355	733	1467
P10%	2382	3935	5520
P1%	4114	6700	8858
Deltascenario			
P50%	372	866	1824
P10%	2402	4080	5899
P1%	4136	6857	9267

Profile 8

Profile 8 Recession [m]	Year		
Prob. of exceedance	2040	2070	2100
No SLR			
P50%	3	-1	-6
P10%	53	78	94
P1%	97	145	176
RCP4.5			
P50%	4	4	10
P10%	54	84	111
P1%	98	152	194
RCP8.5			
P50%	4	5	15
P10%	54	85	116
P1%	98	153	199
Deltascenario			
P50%	4	8	23
P10%	55	88	125
P1%	99	157	209

Profile 8 Erosion volume [m³/m]	Year		
Prob. of exceedance	2040	2070	2100
No SLR			
P50%	114	-46	-207
P10%	1948	2839	3453
P1%	3551	5338	6455
RCP4.5			
P50%	143	162	378
P10%	1982	3064	4072
P1%	3585	5574	7109
RCP8.5			
P50%	146	192	533
P10%	1984	3096	4241
P1%	3587	5610	7295
Deltascenario			
P50%	160	307	835
P10%	2002	3221	4570
P1%	3605	5742	7644

Profile 9

Profile 9 Recession [m]	Year		
Prob. of exceedance	**2040**	**2070**	**2100**
No SLR			
P50%	25	47	71
P10%	110	181	239
P1%	183	297	378
RCP4.5			
P50%	27	62	114
P10%	112	197	284
P1%	185	314	425
RCP8.5			
P50%	27	65	125
P10%	112	200	297
P1%	186	317	439
Deltascenario			
P50%	28	73	148
P10%	113	209	320
P1%	187	327	465

Profile 9 Erosion volume [m³/m]	Year		
Prob. of exceedance	**2040**	**2070**	**2100**
No SLR			
P50%	742	1421	2140
P10%	3292	5438	7181
P1%	5490	8915	11355
RCP4.5			
P50%	803	1881	3419
P10%	3363	5928	8541
P1%	5571	9444	12766
RCP8.5			
P50%	808	1949	3770
P10%	3369	6002	8911
P1%	5577	9522	13192
Deltascenario			
P50%	841	2202	4452
P10%	3406	6274	9626
P1%	5618	9814	13967

Profile 10

Profile 10 Recession [m]	Year		
Prob. of exceedance	**2040**	**2070**	**2100**
No SLR			
P50%	28	53	79
P10%	130	214	281
P1%	217	349	444
RCP4.5			
P50%	31	75	138
P10%	133	237	344
P1%	220	374	512
RCP8.5			
P50%	31	78	155
P10%	133	241	363
P1%	221	377	531
Deltascenario			
P50%	33	90	188
P10%	135	254	397
P1%	223	391	567

Profile 10 Erosion volume [m³/m]	Year		
Prob. of exceedance	**2040**	**2070**	**2100**
No SLR			
P50%	751	1436	2119
P10%	3502	5770	7592
P1%	5853	9428	11993
RCP4.5			
P50%	831	2014	3738
P10%	3592	6404	9303
P1%	5952	10084	13811
RCP8.5			
P50%	837	2099	4191
P10%	3600	6493	9787
P1%	5960	10184	14332
Deltascenario			
P50%	878	2425	5063
P10%	3646	6846	10727
P1%	6013	10542	15314

Profile 11

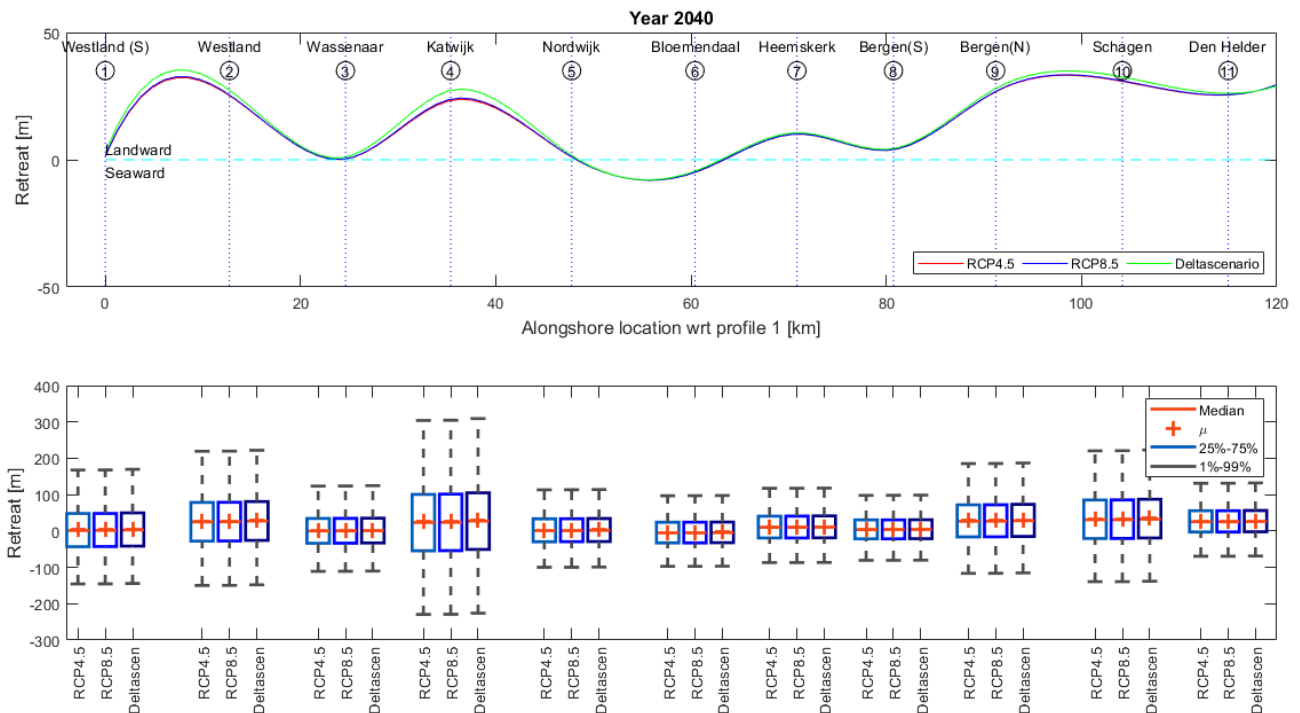| Profile 11 Recession [m]	Year			Profile 11 Erosion volume [m³/m]	Year		
Prob. of exceedance	2040	2070	2100	Prob. of exceedance	2040	2070	2100
No SLR				No SLR			
P50%	24	52	80	P50%	772	1651	2527
P10%	81	141	193	P10%	2563	4458	6097
P1%	130	215	285	P1%	4103	6799	8991
RCP4.5				RCP4.5			
P50%	25	60	101	P50%	804	1881	3180
P10%	82	149	215	P10%	2599	4713	6790
P1%	131	224	308	P1%	4146	7071	9728
RCP8.5				RCP8.5			
P50%	26	61	106	P50%	807	1914	3360
P10%	82	150	221	P10%	2602	4750	6985
P1%	131	225	315	P1%	4150	7112	9939
Deltascenario				Deltascenario			
P50%	26	65	117	P50%	823	2043	3700
P10%	83	155	233	P10%	2620	4892	7348
P1%	132	230	327	P1%	4173	7263	10328

Fig D.1: Estimates of coastal retreat along the Holland coast for the different SLR scenarios for 2040 (relevant to 2020)
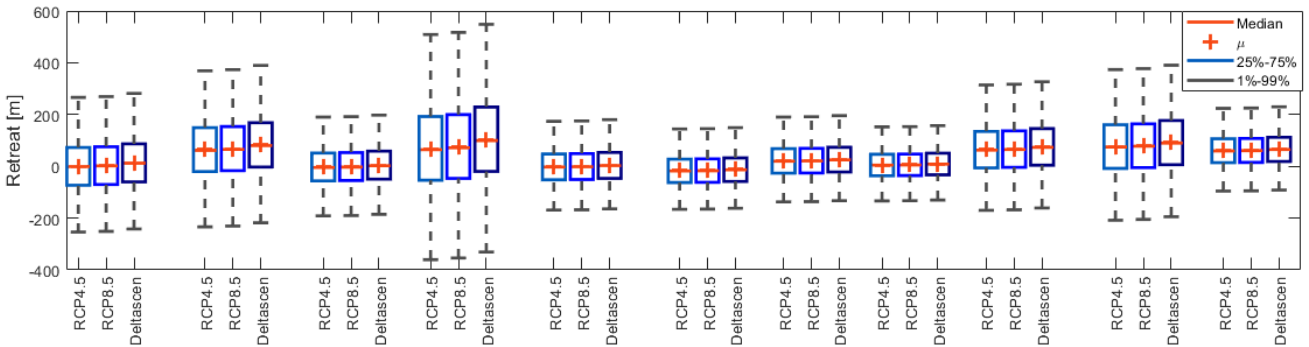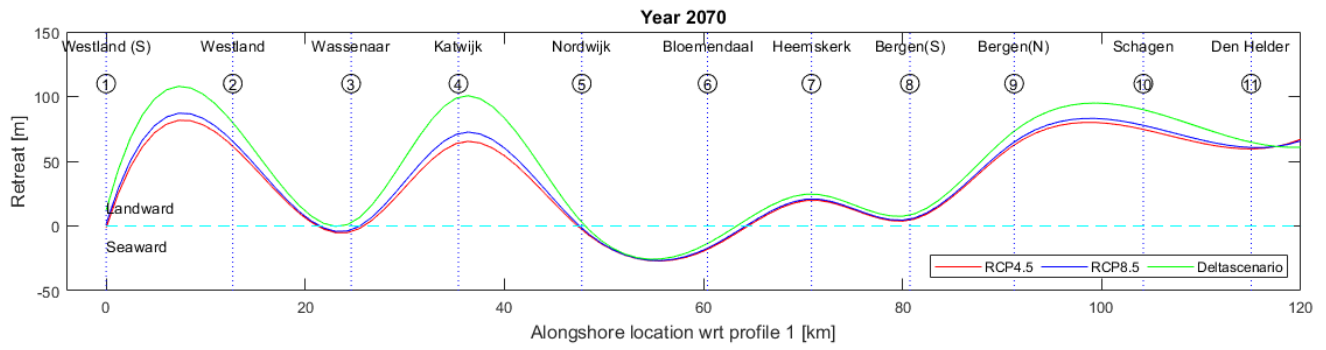
Fig D.2: Estimates of coastal retreat along the Holland coast for the different SLR scenarios for 2070 (relevant to 2020)
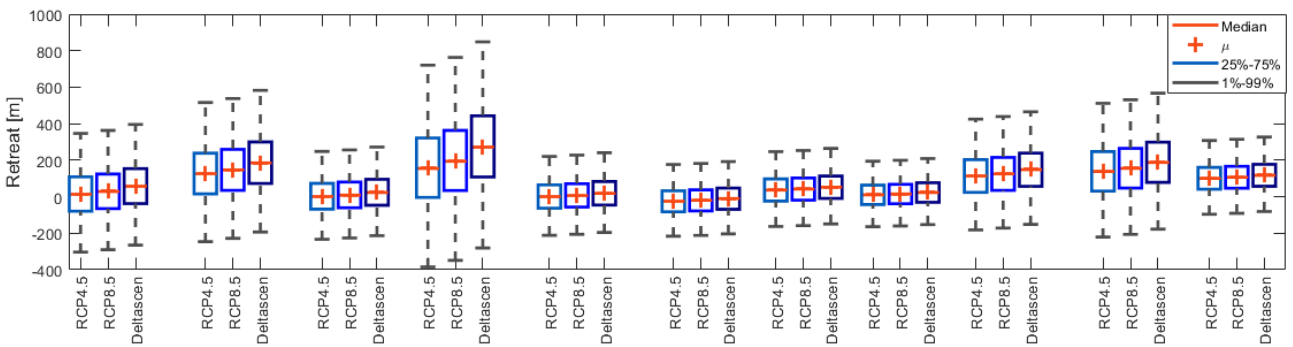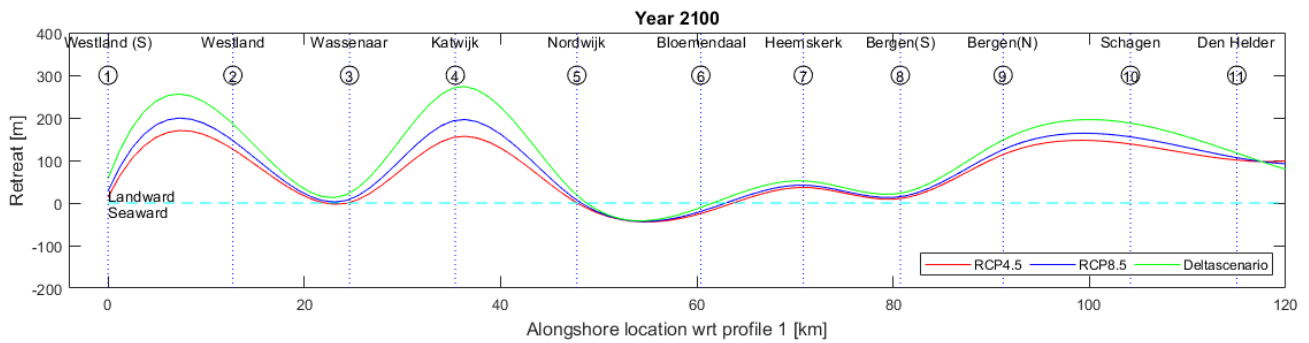

Fig D.3: Estimates of coastal retreat along the Holland coast for the different SLR scenarios for 2100 (relevant to 2020)